Master of Science in Omics Data Analysis

Master Thesis

Association between polymorphic inversions and miRNA in cancer data

by

Patricia Ramírez Priego

Supervisor: Dr. Juan Ramón González, Bioinformatics Research Group in Epidemiology, Barcelona Institute for Global Health (ISGlobal)

Co-supervisor: Dr. Josep Maria Serrat Jurado, Research Group in Bioinformatics and Medical Statistics, University of Vic – Central University of Catalonia (UVic – UCC)

Department of Systems Biology

University of Vic – Central University of Catalonia

September 2016

Association between polymorphic inversions and miRNA in cancer data

Patricia Ramirez[1,2] and Juan R. González[1,2]

[1] University of Vic – Central University of Catalonia (UVic – UCC), Vic, Spain.
[2] ISGlobal, Center for Research in Environmental Epidemiology (CREAL), Barcelona, Spain.

Abstract—Inversion polymorphisms is a mechanism that involves a change in the orientation of a DNA segment within a chromosome, but there is still a lack of their association with disease. However, recently developed computational methods have enabled to discover new human inversion polymorphisms and their association with complex diseases. To overcome this lack of knowledge, we aimed to investigate the effect of four well characterized inversions (8p23, 15q24.2, 16p11.2 and 17q23.31) on miRNA expression in cancer samples. We perform an association analysis between inversion and miRNA expression and Gene Ontology enrichment analysis using different R packages. Our preliminary findings show that there are an association between miRNA expression and cancer, and that it affects important pathways related to cancer.

***Index Terms*—Bioinformatics, cancer, polymorphic inversions, miRNA**

I. Introduction

INVERSION polymorphisms is a mechanism that involves a change in the orientation of a DNA segment within a chromosome. These types of variants have long been playing an important role in chromosomal evolution [1] and also been extensively studied in model organisms like *Drosophila* [2–6]. More recently, many polymorphic inversions have also been described in humans. However, there is still a lack of a complete understanding of how many inversions exist in the human genome and their association with changes in gene expression, adaptation and disease.

Inversions are often generated by non-allelic homologous recombination (NAHR) [7] between inverted sequence repeats, but they can also be originated by double-strand break repair mechanisms, as in non-homologous end joining (NHEJ) [8]; or by errors in replication, such as fork stalling and template switching (FoSTeS) [9] (for detailed explanation of each mechanism see the review by Escaramís et. al. [10]).

Human chromosomes 1, 2, 3, 5, 9, 10 and 16 present several pericentric inversions (i.e. inverted sequences including the centromere). However, up to the present, no related phenotypic effect of clinical significance has been described [11]. Nevertheless, not all inversions are harmless and several diseases have been described to be occasionally caused by inversions, mostly by direct disruption of one gene [12,13] or by alteration on its gene expression [14,15]. To date, associations between inversion alleles and gene expression have been described only for a few of the most studied human inversions (8p23, 15q24.2, 16p11-2 and 17q23.31) [16–20]. Differences in gene expression could be caused either by inversion breakpoint separating coding regions from regulatory elements, or by functional SNPs fixed in one of the divergent haplotypes maintained by the inversion [16–18]. Moreover, a recent study has found a strong association between hypomethylation and genomic instability, describing that DNA methylation deserts are highly enriched for structural rearrangements [21].

In addition, the recently developed computational methods for predicting inversions based in nucleotide variation data have enabled to discover new human inversion polymorphisms [22]. These methods have also made possible to discover few inversions associated with complex diseases (Table I). Inversions can also disrupt coding regions [23] or cancer onset and their study can contribute to a more accurate prognosis of the patient.

MicroRNAs (miRNAs) are short non-coding RNA molecules of around 20 – 24 nucleotides [24,25] that play essential roles in gene expression regulation at post-transcriptional levels [26]. Accordingly, several studies have demonstrated the importance of miRNAs in cancer biology by controlling expression of their target mRNAs facilitating

TABLE I
Human inversions associated with diseases

Cytogenetic band	Inversion length	Disorder	Reference
8p23	4.5 Mb	Brain problems and neuroticism	[16,20]
15q24.2	1.2 Mb	Autism and cognitive impairment	[19]
16p11.2	0.45 Mb	Asthma and obesity	[17]
17q21.31	900 Kb	Neurodegenerative diseases and neuroticism	[18,20]

the appearance of fusion genes [27,28] that can be directly related to the tumor growth, invasion, angiogenesis, and immune evasion mechanisms [24,26,29]. Although there is no proved evidence of a relationship between miRNA expression and inversion polymorphism, it would not be surprising their direct contribution to such mechanism.

Polymorphic inversions are a promising source of genetic variability poorly studied. In particular, its role in miRNA machinery is still unknown. To contribute to this knowledge, in this work we aimed to investigate the effect of four well characterized inversions (8p23, 15q24.2, 16p11.2 and 17q23.31) on miRNA expression in cancer samples.

II. Materials and Methods

A. TCGA Datasets

The Cancer Genome Atlas represents a comprehensive and coordinated effort to accelerate our understanding of the molecular basis of cancer through the application of genome analysis [30]. The data used in this study were downloaded using the R package *TCGAbiolinks* [31], comprised by miRNA expression data collected of TCGA for 15 different types of cancer (see Table II). Sequencing was obtained at an Illumina HiSeq 2000 miRNA platform. Data processing followed the procedures as described in TCGA. Briefly, the raw reads were subjected to the Illumina pipeline filter, and then dataset was further processed to remove adapter dimers, junk, low complexity and repeats. Subsequently, any processed read under 15 base pairs (bp) is discarded, the remaining data is sent to alignment. 15 bp is chosen as a threshold value, because it is the shortest length of a mature miRNA in miRBase [32]. Currently, only perfect alignments with no mismatches are used. After alignment miRNASeq read sequence to target sequences, the expression level of each miRNA was measured as the number of clean reads mapped to its sequence. Mapped clean read number alone is not sufficient to compare expression levels among samples, as these values are affected by factors such as transcript length, total number of reads, and sequencing biases. For this reason, mapped clean read was normalized to RPM (reads per million mapped reads). For detailed information of miRNASeq see the DESCRIPTION.txt of one of the TCGA files in GDC Data Portal [33]. miRNAs having less than 80% of samples with more than 0.5 counts per million reads were removed from the analyses. This filtering was performed using *tweeDEseq* R package [34].

B. Inversion Classification and Detection

SNP data of TCGA samples were downloaded from dbGAP (phs000178.v9.p8). Data were processed using two different algorithms that allow us to get inversion genotypes for each of the 4 inversions analyzed: *inveRsion* and *invClust*.

The first algorithm, *inveRsion* [22], is based on detecting differences in linkage disequilibrium (LD) between SNP blocks across inversion breakpoints [22]. Scanning the genome with predefined window sizes allow the search for inversion signals without previous knowledge of the breakpoints. A positive signal between two is given by the difference of Bayes Information Criterion (BIC), which, if greater than zero, indicates that the chromosomes of some individuals considering the breakpoints tested are more likely to be inverted [22].

The second algorithm, *invClust* [6], detects extended haplotype-genotypes that satisfy the Hardy-Weinberg Equilibrium. It is based on the multivariate analysis of the SNPs within the interrogated region. The algorithm clusters individuals into inversion homozygotes (I/I), standard homozygotes (NI/NI) and heterozygotes (I/NI) using the first two component of a multidimensional scaling (MDS) analysis of SNPs in regions with positive signals given by inveRsion. For clarity, N (noninverted) refers to the orientation represented in the human genome reference (hg19) and I, to the inverted state. As well as, algorithm clusters a few inversions into six inverted states show to correspond to three haplotypes supported by the inversion.

C. miRNA Annotation

We used miRDB (v5.0) [35] to predict miRNAs from sequenced small RNAs. This database is useful for miRNA target prediction and functional annotation. All targets in miRDB was obtained by a bioinformatics tool, mirTarget, which was developed by analyzing thousands of miRNA-target interactions from throughput sequencing, and using miRBase as miRNA source [35].

To obtain the related information about the target gene, as chromosome, start and end position, etc, we used biomaRt [36,37].

D. Association Analysis

Association analyses between miRNA expression and inversion genotypes were performed by using the *DESeq2* package [38]. Each inversion was properly coded using functions in *SNPassoc* package [39] to model association between miRNAs and inversion under three different genetic models (dominant, recessive and additive). The inversion 15q24.2 has three haplotypes, and hence, 6 different genotypes are obtained. In that case, we compare haplotype 1, 3 and 6 with the remaining ones as performed in [19]. miRNA quantification may be affected by hidden and unwanted variation. In order to overcome this issue, we used a statistical method based on surrogate variables analyses that is implemented in the *sva* package [40].

An easy way to represent this p-values obtained with *DESeq2* package [38] is a Quantile-Quantile (QQ) plot. This plot represents the deviation of the observed p-values from the null hypothesis: the observed p-values for each miRNA are sorted from largest to smallest and plotted against expected values from a theoretical distribution. The middle red line between the x-axis and the y-axis represents the null hypothesis. Moreover, those miRNAs with an adjusted p-value lower than 0.05 are color-filled in QQ plot.

E. Gene Ontology Annotation and Enrichment Analysis

The annotation of the Gene Ontology (GO) pathways that are related with targets genes were performed by using *biomaRt* package [36,37]. Pathway enrichment analysis identifies significantly enriched metabolic pathways or signal transduction pathways using the corrected P-value < 0.05 as a threshold to find significantly enriched Gene Ontology (GO) terms in the input list of significant miRNA between different inversions, comparing them to whole genome background. This kind of analysis is implemented in *miRNApath* package [41].

In this work, we used hg19 build as the reference, as it was the most common annotation over all datasets. In all the analyses, false discovery rate (FDR) correction was applied to account for the analysis of several miRNAs. An additional factor of correction of 2.2 was applied to account for the use of 3 different genetic models [42] and another factor of 4 was used to correct for the use of four different inversions. A FDR < 0.05 was considered to indicate a statistically significant association between miRNA expression or pathway and a given inversion.

III. RESULTS

Association studies

To perform the association studies we first analyzed expression data of the fifteen different tumors from the TCGA for each specific inversion and inheritance model. The obtained p-values with *DESeq2* package were represented in a QQ plot for each tumor, inversion and genetic model (Supplementary Information Figs. 1 – 15). We observed 167 significant associations between miRNA expression and inversions in 136 different miRNAs (Supplementary Information Tables 1 – 31). There are tumors showing more associations than others (Supplementary Information Figs. 1 – 15 and Tables 1 – 31). For example, it was noticed that BLCA and UCEC tumors present at least one significant miRNA in the four studied inversions. On the other hand, the remain tumors have at least one significant miRNA in one of the inversions. Only PRAD tumor did not show any association between miRNA expression and inversions. We also realized that these significant associations were also dependent on the genetic model. Figure 1 depicts differences in miRNA expression for different features and inversions. The figure also illustrates how the association between polymorphic inversions and miRNA quantification is different with regard to inversion genotypes. For instance, inversion 8p23 is associated with hsa-miR-205 under dominant model indicating that individuals having the inverted allele (I) show less miRNA expression (Fig. 1B).

TABLE II
List of tumors

Tumor	Abbreviation
BLCA	Bladder Urothelial Carcinoma
BRCA	Breast Invasive Carcinoma
COAD	Colon Adenocarcinoma
KICH	Kidney Chromophobe
KIRC	Kidney Renal Papillary Cell Carcinoma
KIRP	Kidney Renal Clear Cell Carcinoma
LGG	Brain Lower Grade Glioma
LIHC	Liver Hepatocellular Carcinoma
LUAD	Lung Adenocarcinoma
PRAD	Prostate Adenocarcinoma
READ	Rectum Adenocarcinoma
SKCM	Skin Cutaneous Melanoma
STAD	Stomach Adenocarcinoma
THCA	Thyroid Carcinoma
UCEC	Uterine Corpus Endometrial Carcinoma

As can be observed in Figure 1, miRNA expression varied depending on the type of cancer, genotype and inversion. For example, in the case of inversion 8p23 (Figs. 1A – B), in Figure 1A (P-value Dominant: 0.374; P-value Recessive: 4.680×10^{-5} and P-value Additive: 3.179×10^{-8}) only one inversion allele produced an increase of miRNA expression. In fact, there was an increase in miRNA expression in homozygote patients, but with higher effect in NI/NI genotype (Fig. 1B; P-value Dominant: 1.000; P-value Recessive: 1.540×10^{-2} and P-value Additive: 5.963×10^{-3}). On the other hand, for the inversion 15q24.3 (Figs. 1C – D) with six genotypes, a relation between genotype 1 and 6, was observed: when one of them increases, the other genotype decreases its expression, and vice-versa. In inversion 16p11.2 there was a positive tendency, which suggested that expression increased with the number of I alleles (Fig. 1F; P-value Dominant: 0.343; P-value Recessive: 0.012 and P-value Additive: 0.025). However, in the case of hsa-miR-337 (Fig. 1E; P-value Dominant: 1.000; P-value Recessive: 1.072×10^{-3} and P-value Additive: 0.107), we observed the same pattern as in hsa-miR-205 (Fig. 1B). Finally, in inversion 17q21.31 (Figs. 1G – H), there was either an increase (Fig. 1G) or a decrease (Fig. 1H) in miRNAs respect to I/I patients.

Following, we evaluated the effects between every inversion and miRNAs (Fig. 2) dividing those significant miRNAs in two main groups: *cis* and *trans*. miRNAs in *cis* are those which have at least one target in the cytogenetic band of the inversion, while the remaining miRNAs are considered *trans*. We can observe that depending on the inversion there are more miRNAs in *cis* than in *trans*, i.e. in inversion 17q21.31 more miRNAs were found in *cis* than in

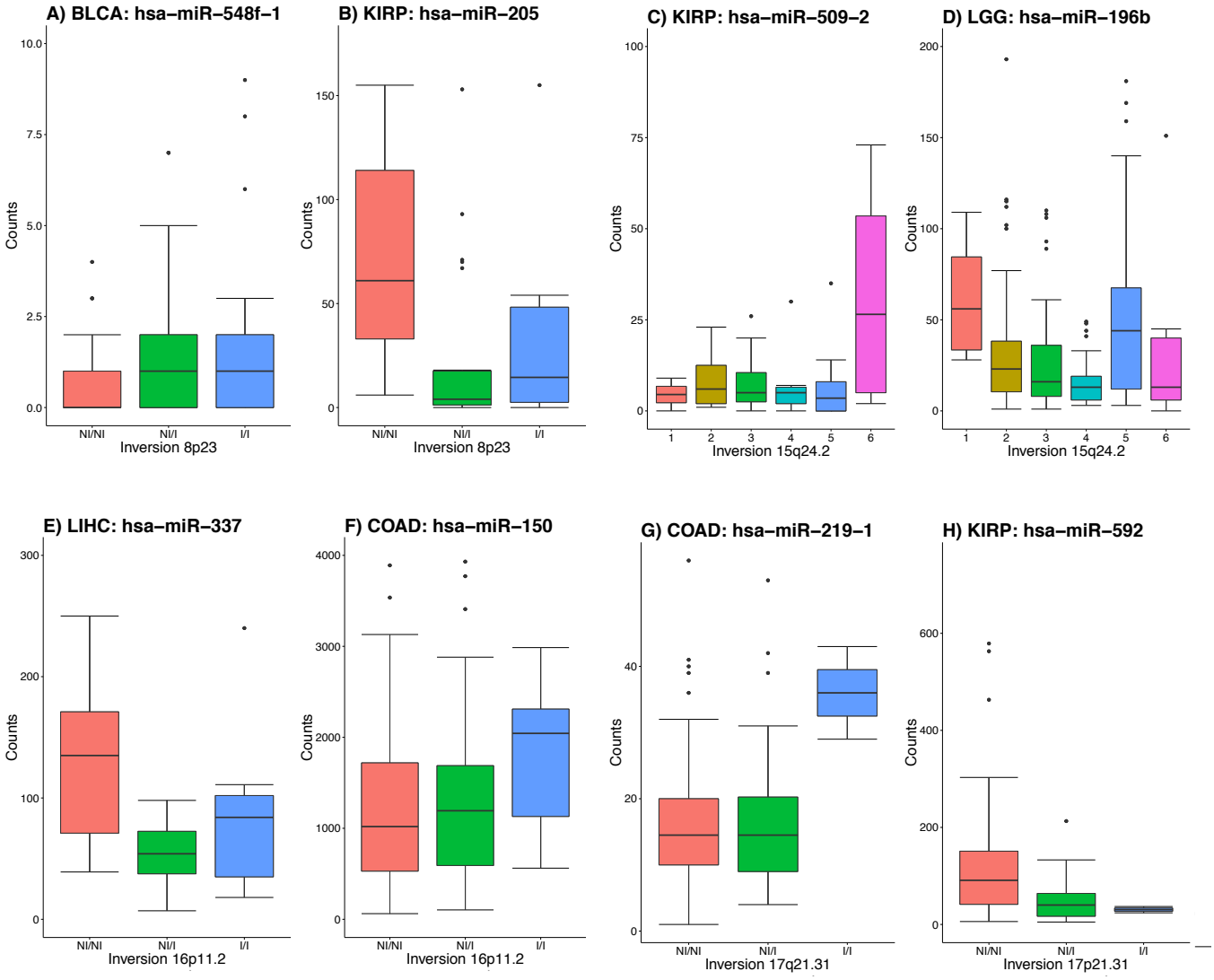

Figure 1. Association between inversion genotypes and miRNA expression of cancer samples. Boxplots for miRNA expression with respect to inversions in different tumor samples, interquartile (box) and median (line). Genotype names are coded as: N (noninverted) refers to the orientation represented in the human genome reference (hg19) and I, to the inverted state, and six inverted haplotypes.

the other inversion types. Also this inversion was the one with higher miRNA expression differences between genotypes. Generally, there are more miRNAs close to or far from the cytogenetic band of the inversion than in the inversion region.

To check if there were significant miRNAs in common between different tumors, we performed Venn Diagrams with the top 5 tumors showing more significant miRNAs (Fig. 3). Interestingly, for inversion 16p11.2 and 17q21.31, all tumors had their unique miRNA. However, in inversion 8p23 there were two miRNAs (hsa-miR-9-1 and hsa-miR-9-2) present in both KIRC and LUAD cancers, and hsa-miR-215 between BLCA and LUAD tumors. In the other inversion, 17q21.31, miRNAs hsa-miR-1269 and hsa-miR-514-3 were in common between BLCA-UCEC and STAD-UCEC, respectively.

Enrichment Analysis

In order to define globally the miRNA transcriptomic effects of the four studied inversions, gene ontology (GO) enrichment analysis was performed including all significant miRNA in all data sets with respect to the inversion (p-value < 0.05). When we evaluated the *miRNApath* function, it did not work for all tumors and inversions. This problem could be related either to the sample size or to the p-values. For this reason, we performed only enrichment analysis with BRCA cancer and inversion 8p23, and compared the results obtained in each case.

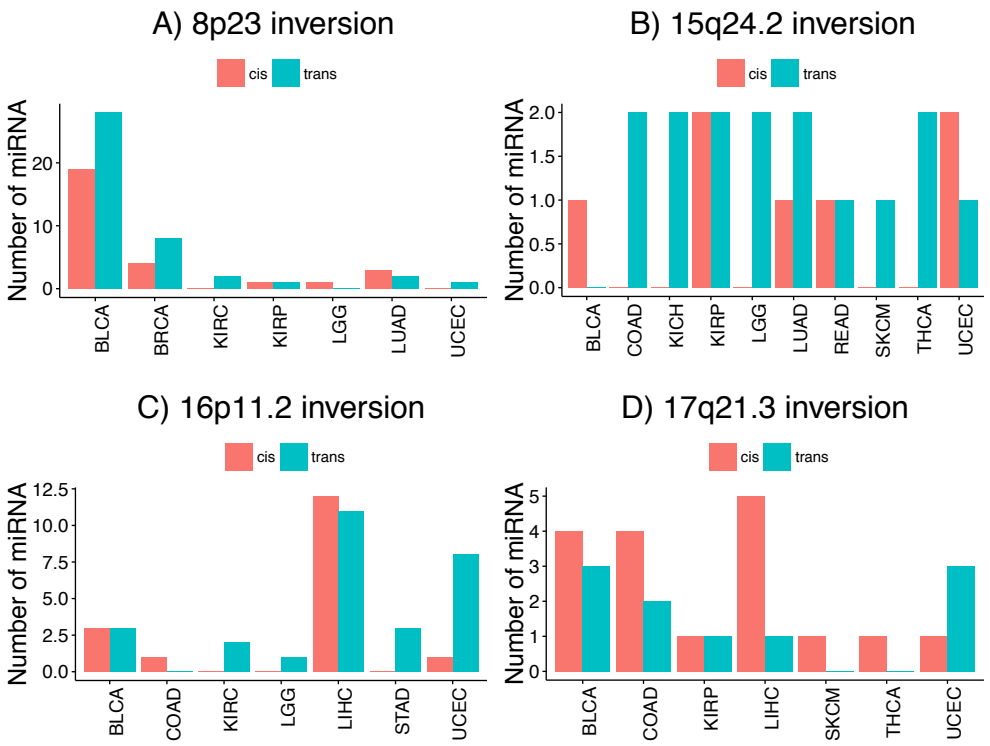

Figure 2. *Cis* and *trans* inversion effect on miRNA expression. Barplots depict the number of significant miRNA (at 5% FDR level) with target genes in the inversion region (red color) and outside the inversion region (blue color).

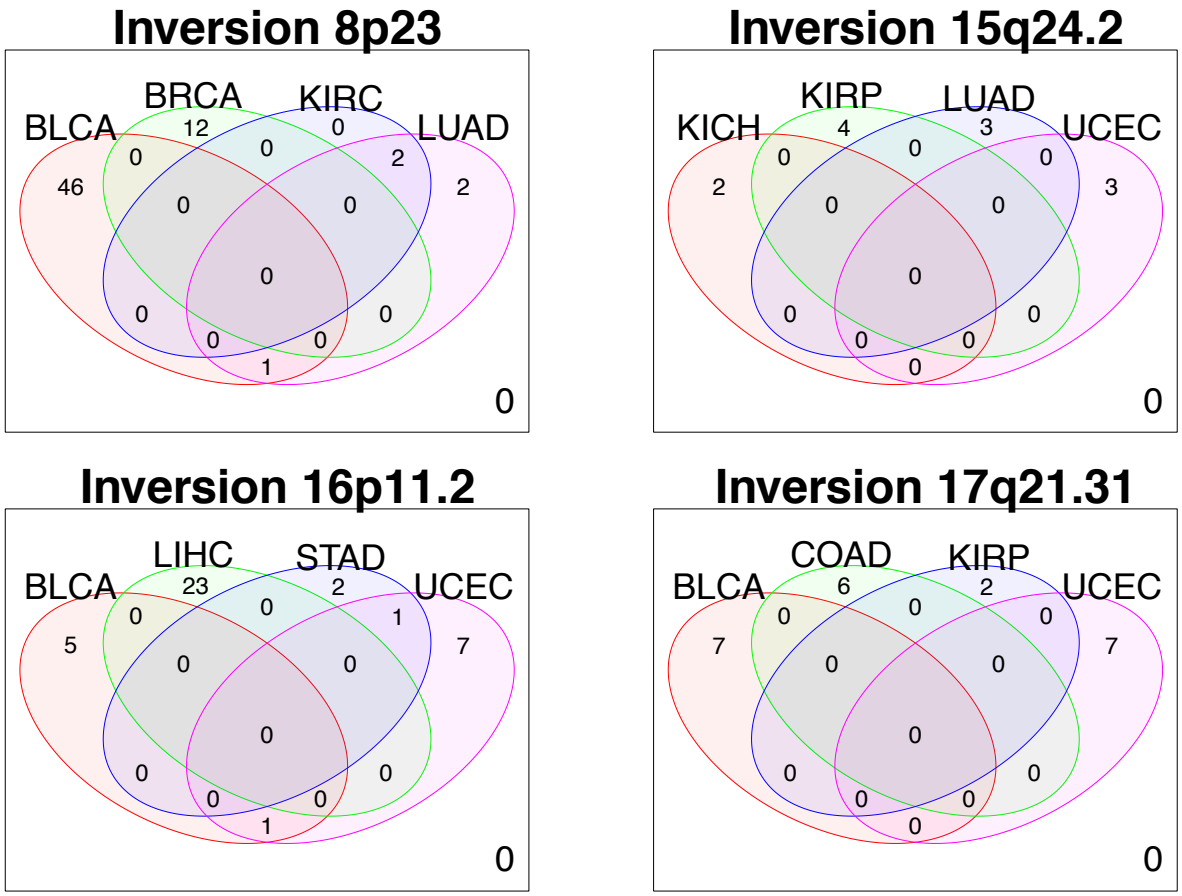

Figure 3. Venn Diagrams representing significant miRNAs. Venn Diagrams illustrating, for each polymorphic inversion, the number of common miRNAs between the top five tumor samples (e.g those having more miRNAs significantly associated at 5 % FDR level).

Considering the enriched GO pathways with significant miRNA, a concept-network was obtained (Fig. 4A and Table III) showing a remarkable enrichment of terms related to DNA damage detection, regulation of region RNA binding, changes in cellular activity and several changes in regulation of cellular components and molecular functions (i.e. response to stress, regulation and activation of immune response, etc.). This DNA damage results in the stop or reduction in the rate of vital processes such as the cell cycle. Regulation of region RNA binding includes transcription, DNA replication and DNA repair. The analysis of the top 50 miRNA with respect to the inversion 8p23 (Fig. 4B and Table IV) also revealed a remarkable enrichment of terms related to regulation and activation of immune response, mostly presenting a relation with Major histocompatibility complex (MHC) and T cells.

In addition, generally GO terms are significant for the Additive model instead of the other two inheritance models, but there are some GO terms that are in common in the three models (i.e. GO: 0006334 – cellular iron ion homeostasis).

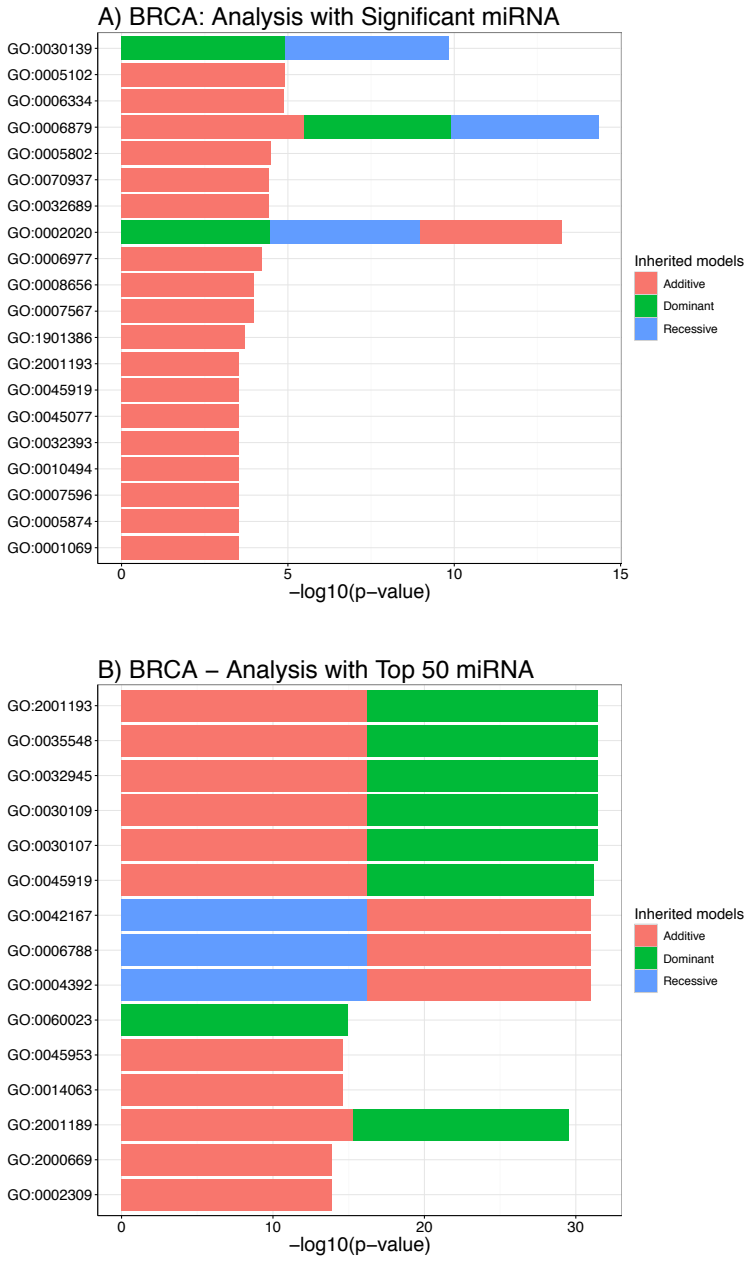

Figure 4. Functional correlations of the 8p23 inversion in BRCA samples. Barplot showing the top twenty-five obtained with (A) significant miRNAs and (B) top fifty miRNAs GO terms both at FDR < 0.05.

IV. Discussion

Transcription factors regulate miRNA transcription in cancer, and there are several miRNAs that can be regulating other miRNAs [43,44]. In addition, several miRNAs have the function of enhancing the tumor-suppressor function, while others result in increased miRNA expression and consequent oncogenic activity [43]. Inversions also have an effect at transcriptional level, mostly caused by inversion breakpoint separating coding regions from regulatory elements [16–18] or cancer onset. This transcriptional dysregulation is an important mechanism for altered miRNA expression in cancer [43].

In this work, we hypothesize that there is an association between inversions and miRNA expression that can be due to the localization of a considerable number of miRNA sequences at fragile sites or genomic regions that are deleted, amplified or translocated, most of them related to the onset of cancer [43].

After performing association analysis between miRNA expression and inversions, we obtained several miRNAs with a significant change in their expression. From those significant miRNAs that we found, there are several ones well studied that play an important role in cancer. For example, expression of the hsa-miR-200 family is frequently suppressed in human tumors. These miRNAs are known to directly target the mRNAs encoding the zinc-finger E-box-binding homeobox (ZEB) transcription factors, which suppress the expression of epithelial genes to promote the epithelial-mesenchymal transition (EMT) [45]. Interestingly, ZEB directly binds to a regulatory element at the miR-200 promoter to repress transcription of miR-200 as part of a negative regulatory feedback loop that promotes EMT [46]. In agreement with our data, hsa-miR-200c is significant in LIHC tumor and presents high expression in patients with homozygote I genotype for inversion 17q21.31.

The oncogenic transcription factor Myc binds to the promoter region of many miRNAs, and generally acts as a negative regulator of miRNA expression. It also has indirect effects on miRNA activity through the activation of secondary factors that, downregulate antiproliferative, tumor-supressive and proapoptotic activities of hsa-let7 and hsa-miR-34c [47,48], two significant miRNAs in our data. Nowadays, these two miRNAs are being used as a therapeutic approach in lung cancer and pancreatic cancer [49,50].

TABLE III

Top 25 significant (FDR < 0.05) enriched GO terms obtained by using those miRNAs that were significantly associated between inversion 8p23 and BRCA at 5% FDR level.

GO ID	GO Name	Inherited Model	Adjusted P-values
GO:0006879	cellular iron ion homeostasis	Additive	3.288e-06
GO:0030139	endocytic vesicle	Dominant	1.192e-05
GO:0030139	endocytic vesicle	Recessive	1.192e-05
GO:0005102	receptor binding	Additive	1.192e-05
GO:0006334	nucleosome assembly	Additive	1.321e-05
GO:0005802	trans-Golgi network	Additive	3.292e-05
GO:0002020	protease binding	Dominant	3.292e-05
GO:0002020	protease binding	Recessive	3.292e-05
GO:0070937	CRD-mediated mRNA stability complex	Additive	3.801e-05
GO:0032689	negative regulation of interferon-gamma production	Additive	3.801e-05
GO:0006879	cellular iron ion homeostasis	Dominant	3.801e-05
GO:0006879	cellular iron ion homeostasis	Recessive	3.801e-05
GO:0002020	protease binding	Additive	5.396e-05
GO:0006977	DNA damage response, signal transduction by p53 class mediator resulting in cell cycle arrest	Additive	5.905e-05
GO:0008656	cysteine-type endopeptidase activator activity involved in apoptotic process	Additive	1.056e-04
GO:0007567	parturition	Additive	1.056e-04
GO:1901386	negative regulation of voltage-gated calcium channel activity	Additive	1.927e-04
GO:0045919	positive regulation of cytolysis	Additive	3.037e-04
GO:0001069	regulatory region RNA binding	Additive	3.037e-04
GO:0032393	MHC class I receptor activity	Additive	3.037e-04
GO:0045077	negative regulation of interferon-gamma biosynthetic process	Additive	3.037e-04
GO:0005874	microtubule	Additive	3.037e-04
GO:0010494	cytoplasmic stress granule	Additive	3.037e-04
GO:0007596	blood coagulation	Additive	3.037e-04
GO:2001193	positive regulation of gamma-delta T cell activation involved in immune response	Additive	3.037e-04

TABLE IV

Top 25 significant (FDR < 0.05) enriched GO terms obtained by using the top-50 miRNAs that were significantly associated between inversion 8p23 and BRCA

GO ID	GO Name	Inherited Model	Adjusted P-values
GO:2001193	positive regulation of gamma-delta T cell activation involved in immune response	Additive	5.847e-17
GO:0030107	HLA-A specific inhibitory MHC class I receptor activity	Additive	5.847e-17
GO:0030109	HLA-B specific inhibitory MHC class I receptor activity	Additive	5.847e-17
GO:0035548	negative regulation of interferon-beta secretion	Additive	5.847e-17
GO:0032945	negative regulation of mononuclear cell proliferation	Additive	5.847e-17
GO:0042167	heme catabolic process	Recessive	5.847e-17
GO:0006788	heme oxidation	Recessive	5.847e-17
GO:0004392	heme oxygenase (decyclizing) activity	Recessive	5.847e-17
GO:0045919	positive regulation of cytolysis	Additive	5.986e-17
GO:2001189	negative regulation of T cell activation via T cell receptor	Additive	5.446e-16
GO:2001193	positive regulation of gamma-delta T cell activation involved in immune response	Dominant	5.784e-16
GO:0030107	HLA-A specific inhibitory MHC class I receptor activity	Dominant	5.784e-16
GO:0030109	HLA-B specific inhibitory MHC class I receptor activity	Dominant	5.784e-16
GO:0035548	negative regulation of interferon-beta secretion	Dominant	5.784e-16
GO:0032945	negative regulation of mononuclear cell proliferation	Dominant	5.784e-16
GO:0045919	positive regulation of cytolysis	Dominant	1.087e-15
GO:0060023	soft palate development	Dominant	1.151e-15
GO:0042167	heme catabolic process	Additive	1.617e-15
GO:0006788	heme oxidation	Additive	1.617e-15
GO:0004392	heme oxygenase (decyclizing) activity	Additive	1.617e-15
GO:0045953	negative regulation of natural killer cell mediated cytotoxicity	Additive	2.302e-15
GO:0014063	negative regulation of serotonin secretion	Additive	2.302e-15
GO:2001189	negative regulation of T cell activation via T cell receptor	Dominant	5.448e-15
GO:0002309	T cell proliferation involved in immune response	Additive	1.330e-14
GO:2000669	negative regulation of dendritic cell apoptotic process	Additive	1.330e-14

Briefly, there are also several miRNAs that inhibits cell invasion and migration, as hsa-miR-345 [51], has-miR-372 [52], hsa-miR-196b [53], hsa-miR-493 [54], etc. There are others that promote metastasis (i.e. hsa-miR-1269 [55]), suppress metastasis (hsa-miR-206 [56], hsa-miR-382 [57]). Here we present, for the first time, sixty novel miRNAs (Table V) that their effects are not known in cancer. Interestingly, these miRNAs can be used as biomarkers to cancer diagnosis. As some of them are unique for each type of cancer, if we realized the same study with different populations we could determine which ones are the common significant miRNAs and create a new approach to detect and determine the type of cancer.

We observed a strong correlation of inversion genotypes with miRNA expression effects. These expression effects could be because *cis*-miRNAs are disrupting directly coding

TABLE V
Novel miRNAs associated with inversions

hsa-miR-518e	hsa-miR-3200
hsa-miR-520f	hsa-miR-129-2
hsa-miR-527	hsa-miR-521-1
hsa-miR-518a-1	hsa-miR-1180
hsa-miR-3074	hsa-miR-224
hsa-miR-548f-1	hsa-miR-509-3
hsa-miR-512-2	hsa-miR-509-2
hsa-miR-520c	hsa-miR-514-1
hsa-miR-512-1	hsa-miR-514-2
hsa-miR-517b	hsa-miR-133a-1
hsa-miR-520a	hsa-miR-133b
hsa-miR-520f	hsa-miR-219-1
hsa-miR-624	hsa-miR-193b
hsa-miR-517c	hsa-miR-891b
hsa-miR-518c	hsa-miR-889
hsa-miR-3691	hsa-miR-329-2
hsa-miR-129-1	hsa-miR-376c
hsa-miR-518b	hsa-miR-370
hsa-miR-1323	hsa-miR-654
hsa-miR-518a-1	hsa-miR-539
hsa-miR-520d	hsa-miR-541
hsa-miR-520g	hsa-miR-514-3
hsa-miR-615	hsa-miR-598
hsa-miR-451	hsa-miR-138-1
hsa-miR-498	hsa-miR-196a-1
hsa-miR-515-2	hsa-miR-323b
hsa-miR-518f	hsa-miR-374a
hsa-miR-520b	hsa-miR-138-2
hsa-miR-181d	hsa-miR-551b
hsa-miR-194-1	hsa-miR-194-2

regions or one gene, creating fusion genes or epigenetic effect, with a direct transcriptomic effect. As well as, to have a miRNAs expression effect it is not necessary that miRNAs targets are in the cytogenetic band of the inversion. The influence of inversion is probably mediated by its strong effect on the expression of several neighboring genes with regulatory functions.

The analysis of all miRNA differentially expressed and the top-50 with respect to the inversion 8p23 in BRCA cancer also revealed a remarkable enrichment of terms related to DNA damage detection, regulation of RNA binding, regulation and activation of immune response and changes in cellular components and molecular functions. This pattern is consistent with a disturbance of regulatory elements and changes in cellular components, and further supports the observation that miRNA deregulated by the inversion polymorphism or associated genotypes may be responsible for the association with cancer.

V. Conclusion and future work

In this study, we evaluated the association and gene ontology enrichment analysis between miRNA expression and inversions in fifteen cancer types. Based on our statistical results, an association was observed in fourteen cancer types, and also a dependence on the patient genotype. Even though, there are already several significant miRNAs described in the literature, we here present for the first time sixty novel miRNAs that are inversion-related. From these miRNAs, fifty-three of them are uniquely related with a single cancer type. This observed specificity may represent a highly potential biomarker-based technique for cancer diagnosis. The gene ontology enrichment analysis also revealed a remarkable enrichment of terms related to cancer. These results will be validated with a Genome-wide association study (GWAS) of dbGAP.

In the near future, all this information will be correlated with gene expression data in order to check whether those significant miRNAs for inversions have some effect in the transcriptome or, on the contrary, inversions in the transcriptome modify miRNA expression.

Supplementary information

Supplementary Information includes forty-six figures, and thirty-one tables providing the same information as the one described in this manuscript for all tumors and polymorphic inversions.

Acknowledgment

I would like to thank to the ISGlobal - Center for Research in Environmental Epidemiology (CREAL) for give me the opportunity to carry out my final master thesis. Especially, I express my deep gratitude to Juan Ramón González for guide me in the realization of this work.

References

[1] A.A. Hoffmann, L.H. Rieseberg, Revisiting the Impact of Inversions in Evolution: From Population Genetic Markers to Drivers of Adaptive Shifts and Speciation?, Annu. Rev. Ecol. Evol. Syst. 39 (2008) 21–42. doi:10.1146/annurev.ecolsys.39.110707.173532.

[2] P. Biology, Inversion polymorphisms and nucleotide variability in Drosophila, (2001) 1–8.

[3] W.J. Kennington, L. Partridge, A.A. Hoffmann, Patterns of diversity and linkage disequilibrium within the cosmopolitan inversion In(3R)Payne in Drosophila melanogaster are indicative of coadaptation., Genetics. 172 (2006) 1655–63. doi:10.1534/genetics.105.053173.

[4] A. Navarro, A. Barbadilla, A. Ruiz, Effect of inversion polymorphism on the neutral nucleotide variability of linked chromosomal regions in drosophila, Genetics. 155 (2000) 685–698.

[5] L.R. Osborne, M. Li, B. Pober, D. Chitayat, J. Bodurtha, et. al, A 1.5 million-base pair inversion polymorphism in families with Williams-Beuren syndrome., Nat. Genet. 29 (2001) 321–5. doi:10.1038/ng753.

[6] A. Cáceres, J.R. González, Following the footprints of polymorphic inversions on SNP data: from detection to association tests., Nucleic Acids Res. 43 (2015) e53. doi:10.1093/nar/gkv073.

[7] J.R. Lupski, Genomic disorders: Structural features of the genome can lead to DNA rearrangements and human disease traits, Trends Genet. 14 (1998) 417–422. doi:10.1016/S0168-9525(98)01555-8.

[8] J.K. Moore, J.E. Haber, Cell cycle and genetic requirements of two pathways of nonhomologous end-joining repair of double-strand breaks in Saccharomyces cerevisiae., Mol. Cell. Biol. 16 (1996) 2164–2173. doi:10.1128/MCB.16.5.2164.

[9] J.A. Lee, C.M.B. Carvalho, J.R. Lupski, A DNA Replication Mechanism for Generating Nonrecurrent Rearrangements Associated with Genomic Disorders, Cell. 131 (2007) 1235–1247. doi:10.1016/j.cell.2007.11.037.

[10] G. Escaramís, E. Docampo, R. Rabionet, A decade of structural variants: description, history and methods to detect structural variation, Brief. Funct. Genomics. 14 (2015) 305–314. doi:10.1093/bfgp/elv014.

[11] N.S. Thomas, V. Bryant, V. Maloney, A.E. Cockwell, P.A. Jacobs, Investigation of the origins of human autosomal inversions, Hum. Genet. 123 (2008) 607–616. doi:10.1007/s00439-008-0510-z.

[12] M.L. Jones, S.L. Murden, C. Brooks, V. Maloney, R.A. Manning, , et. al, Disruption of AP3B1 by a chromosome 5 inversion: a new disease mechanism in Hermansky-Pudlak syndrome type 2., BMC Med. Genet. 14 (2013) 42. doi:10.1186/1471-2350-14-42.

[13] V. Cacheux, Detection of chromosomal breakpoints in patients with developmental delay and speech disorders, PLoS One. 9 (2014) e90852. doi:10.1371/journal.pone.0090852.

[14] G.J. Anger, S. Crocker, K. McKenzie, K.K. Brown, C.C. Morton, et. al, X-linked deafness-2 (DFNX2) phenotype associated with a paracentric inversion upstream of POU3F4., Am. J. Audiol. 23 (2014) 1–6. doi:10.1044/1059-0889(2013/13-0018).

[15] K.K. Brown, J.A. Reiss, K. Crow, H.L. Ferguson, C. Kelly, et. al, Deletion of an enhancer near DLX5 and DLX6 in a family with hearing loss, craniofacial defects, and an inv(7)(q21.3q35), Hum. Genet. 127 (2010) 19–31. doi:10.1007/s00439-009-0736-4.

[16] M.P.A. Salm, S.D. Horswell, C.E. Hutchison, H.E. Speedy, X. Yang, et. al, The origin, global distribution, and functional impact of the human 8p23 inversion polymorphism., Genome Res. 22 (2012) 1144–53. doi:10.1101/gr.126037.111.

[17] J.R. González, A. Cáceres, T. Esko, I. Cuscó, M. Puig, , et. al, L.A. Pérez-Jurado, A common 16p11.2 inversion underlies the joint susceptibility to asthma and obesity, Am. J. Hum. Genet. 94 (2014) 361–372. doi:10.1016/j.ajhg.2014.01.015.

[18] S. de Jong, I. Chepelev, E. Janson, E. Strengman, L.H. van den Berg, et. al, Common inversion polymorphism at 17q21.31 affects expression of multiple genes in tissue-specific manner, BMC Genomics. 13 (2012) 458. doi:10.1186/1471-2164-13-458.

[19] A. Cáceres, T. Esko, I. Pappa, A. Gutiérrez, M.-J. Lopez-Espinosa, et. al, Ancient Haplotypes at the 15q24.2 Microdeletion Region Are Linked to Brain Expression of MAN2C1 and Children's Intelligence, PLoS One. 11 (2016) e0157739. doi:10.1371/journal.pone.0157739.

[20] A. Okbay, B.M.L. Baselmans, J.-E. De Neve, P. Turley, M.G. Nivard, et. al, Genetic variants associated with subjective well-being, depressive symptoms, and neuroticism identified through genome-wide analyses., Nat. Genet. 48 (2016) 624–33. doi:10.1038/ng.3552.

[21] J. Li, R.A. Harris, S.W. Cheung, C. Coarfa, M. Jeong, et. al, Genomic hypomethylation in the human germline associates with selective structural mutability in the human genome, PLoS Genet. 8 (2012). doi:10.1371/journal.pgen.1002692.

[22] A. Cáceres, S.S. Sindi, B.J. Raphael, M. Cáceres, J.R. González, Identification of polymorphic inversions from genotypes, BMC Bioinformatics. 13 (2012) 28. doi:10.1186/1471-2105-13-28.

[23] J. Rhees, M. Arnold, C.R. Boland, Inversion of exons 1-7 of the MSH2 gene is a frequent cause of unexplained Lynch syndrome in one local population., Fam. Cancer. 13 (2014) 219–25. doi:10.1007/s10689-013-9688-x.

[24] M.D. Jansson, A.H. Lund, E. Alvarez-Saavedra, H.R. Horvitz, P. Anderson, et. al, MicroRNA and cancer, Mol. Oncol. 6 (2012) 590–610. doi:10.1016/j.molonc.2012.09.006.

[25] Y. Li, K. V. Kowdley, MicroRNAs in Common Human Diseases, Genomics. Proteomics Bioinformatics. 10 (2012) 246–253. doi:10.1016/j.gpb.2012.07.005.

[26] M.S. Ebert, P.A. Sharp, A.L. Abbott, E. Alvarez-Saavedra, E.A. Miska, et. al, Roles for MicroRNAs in Conferring Robustness to Biological Processes, Cell. 149 (2012) 515–524. doi:10.1016/j.cell.2012.04.005.

[27] M. Soda, Y.L. Choi, M. Enomoto, S. Takada, Y. Yamashita, et. al, Identification of the transforming EML4-ALK fusion gene in non-small-cell lung cancer., Nature. 448 (2007) 561–6. doi:10.1038/nature05945.

[28] T.A. Gruber, A. Larson Gedman, J. Zhang, C.S. Koss, S. Marada, et. al, An Inv(16)(p13.3q24.3)-encoded CBFA2T3-GLIS2 fusion protein defines an aggressive subtype of pediatric acute megakaryoblastic leukemia., Cancer Cell. 22 (2012) 683–97. doi:10.1016/j.ccr.2012.10.007.

[29] J. Hayes, P.P. Peruzzi, S. Lawler, MicroRNAs in cancer: biomarkers, functions and therapy, Trends Mol. Med. 20 (2014) 460–469. doi:10.1016/j.molmed.2014.06.005.

[30] Home - The Cancer Genome Atlas - Cancer Genome - TCGA, (n.d.). http://cancergenome.nih.gov/.

[31] A. Colaprico, T.C. Silva, C. Olsen, L. Garofano, C. Cava, et. al, *TCGAbiolinks*: an R/Bioconductor package for integrative analysis of TCGA data, Nucleic Acids Res. 44 (2016) e71–e71. doi:10.1093/nar/gkv1507.

[32] A. Kozomara, S. Griffiths-Jones, miRBase:

annotating high confidence microRNAs using deep sequencing data, Nucleic Acids Res. 42 (2014) D68–D73. doi:10.1093/nar/gkt1181.

[33] Welcome to The Genomics Data Commons Data Portal | GDC, (n.d.). https://gdc-portal.nci.nih.gov/.

[34] M. Esnaola, P. Puig, D. Gonzalez, R. Castelo, J.R. Gonzalez, A flexible count data model to fit the wide diversity of expression profiles arising from extensively replicated RNA-seq experiments., BMC Bioinformatics. 14 (2013) 254. doi:10.1186/1471-2105-14-254.

[35] miRDB - MicroRNA Target Prediction And Functional Study Database, (n.d.). http://mirdb.org/miRDB/.

[36] S. Durinck, Y. Moreau, A. Kasprzyk, S. Davis, B. De Moor, et. al, BioMart and Bioconductor: a powerful link between biological databases and microarray data analysis., Bioinformatics. 21 (2005) 3439–40. doi:10.1093/bioinformatics/bti525.

[37] S. Durinck, P.T. Spellman, E. Birney, W. Huber, Mapping identifiers for the integration of genomic datasets with the R/Bioconductor package biomaRt., Nat. Protoc. 4 (2009) 1184–91. doi:10.1038/nprot.2009.97.

[38] M.I. Love, W. Huber, S. Anders, Moderated estimation of fold change and dispersion for RNA-seq data with DESeq2., Genome Biol. 15 (2014) 550. doi:10.1186/s13059-014-0550-8.

[39] J.R. González, L. Armengol, X. Solé, E. Guinó, J.M. Mercader, et. al, SNPassoc: an R package to perform whole genome association studies., Bioinformatics. 23 (2007) 644–5. doi:10.1093/bioinformatics/btm025.

[40] J. Leek, W.E. Johnson, A. Jaffe, H. Parker, J. Storey, The SVA package for removing batch effects and other unwanted variation in high-throughput experiments, (n.d.).

[41] J.P. Cogswell, J. Ward, I.A. Taylor, M. Waters, Y. Shi, et. al, Identification of miRNA changes in Alzheimer's disease brain and CSF yields putative biomarkers and insights into disease pathways., J. Alzheimers. Dis. 14 (2008) 27–41. http://www.ncbi.nlm.nih.gov/pubmed/18525125 (accessed September 5, 2016).

[42] J.R. González, J.L. Carrasco, F. Dudbridge, L. Armengol, X. Estivill, V. Moreno, Maximizing association statistics over genetic models., Genet. Epidemiol. 32 (2008) 246–54. doi:10.1002/gepi.20299.

[43] S. Lin, R.I. Gregory, MicroRNA biogenesis pathways in cancer, Nat. Rev. Cancer. 15 (2015) 321–333. doi:10.1038/nrc3932.

[44] MicroRNA in Cancer An Overview, (n.d.). https://www.promega.es/resources/pubhub/features/microrna-in-cancer-an-overview/.

[45] P.A. Gregory, The miR-200 family and miR-205 regulate epithelial to mesenchymal transition by targeting ZEB1 and SIP1, Nat. Cell Biol. 10 (2008). doi:10.1038/ncb1722.

[46] C.P. Bracken, P.A. Gregory, N. Kolesnikoff, A.G. Bert, J. Wang, et. al, A double-negative feedback loop between ZEB1-SIP1 and the microRNA-200 family regulates epithelial-mesenchymal transition., Cancer Res. 68 (2008) 7846–54. doi:10.1158/0008-5472.CAN-08-1942.

[47] T.C. Chang, Widespread microRNA repression by Myc contributes to tumorigenesis, Nat. Genet. 40 (2008). doi:10.1038/ng.2007.30.

[48] T. V Bui, J.T. Mendell, Myc: Maestro of MicroRNAs., Genes Cancer. 1 (2010) 568–575. doi:10.1177/1947601910377491.

[49] P. Trang, J.F. Wiggins, C.L. Daige, C. Cho, M. Omotola, et. al, Systemic delivery of tumor suppressor microRNA mimics using a neutral lipid emulsion inhibits lung tumors in mice., Mol. Ther. 19 (2011) 1116–22. doi:10.1038/mt.2011.48.

[50] D. Pramanik, N.R. Campbell, C. Karikari, R. Chivukula, O.A. Kent, et. al, Restitution of tumor suppressor microRNAs using a systemic nanovector inhibits pancreatic cancer growth in mice., Mol. Cancer Ther. 10 (2011) 1470–80. doi:10.1158/1535-7163.MCT-11-0152.

[51] Q. Chen, W. Zhou, T. Han, S. Du, Z. Li, Z. Zhang, G. Shan, C. Kong, MiR-345 suppresses proliferation, migration and invasion by targeting Smad1 in human prostate cancer., J. Cancer Res. Clin. Oncol. 142 (2016) 213–24. doi:10.1007/s00432-015-2016-0.

[52] X. Huang, M. Huang, L. Kong, Y. Li, miR-372 suppresses tumour proliferation and invasion by targeting IGF2BP1 in renal cell carcinoma., Cell Prolif. 48 (2015) 593–9. doi:10.1111/cpr.12207.

[53] W. Abe, K. Nasu, C. Nakada, Y. Kawano, M. Moriyama, H. Narahara, miR-196b targets c-myc and Bcl-2 expression, inhibits proliferation and induces apoptosis in endometriotic stromal cells., Hum. Reprod. 28 (2013) 750–61. doi:10.1093/humrep/des446.

[54] Y. Gu, Y. Cheng, Y. Song, Z. Zhang, M. Deng, , et. al, MicroRNA-493 suppresses tumor growth, invasion and metastasis of lung cancer by regulating E2F1., PLoS One. 9 (2014) e102602. doi:10.1371/journal.pone.0102602.

[55] P. Bu, L. Wang, K.-Y. Chen, N. Rakhilin, J. Sun, et. al, miR-1269 promotes metastasis and forms a positive feedback loop with TGF-β., Nat. Commun. 6 (2015) 6879. doi:10.1038/ncomms7879.

[56] R. Samaeekia, V. Adorno-Cruz, J. Bockhorn, Y.-F. Chang, S. Huang, et. al, MicroRNA-206 inhibits stemness and metastasis of breast cancer by targeting MKL1/IL11 pathway., Clin. Cancer Res. (2016). doi:10.1158/1078-0432.CCR-16-0943.

[57] D. Hanniford, M.F. Segura, J. Zhong, E. Philips, X. Jirau-Serrano, et. al, Identification of metastasis-suppressive microRNAs in primary melanoma., J. Natl. Cancer Inst. 107 (2015). doi:10.1093/jnci/dju494.

Supplementary Information

Patricia Ramirez [1] and Juan Ramón González[1,2]
[1]University of Vic - Central University of Catalonia (UVIC-UCC), Vic, Spain
[2]IS Global, Center for Research in Environmental Epidemiology (CREAL), Barcelona, Spain

Contents

1. Association Analysis

1.1. Q-Q Plots

1.1.1. BLCA

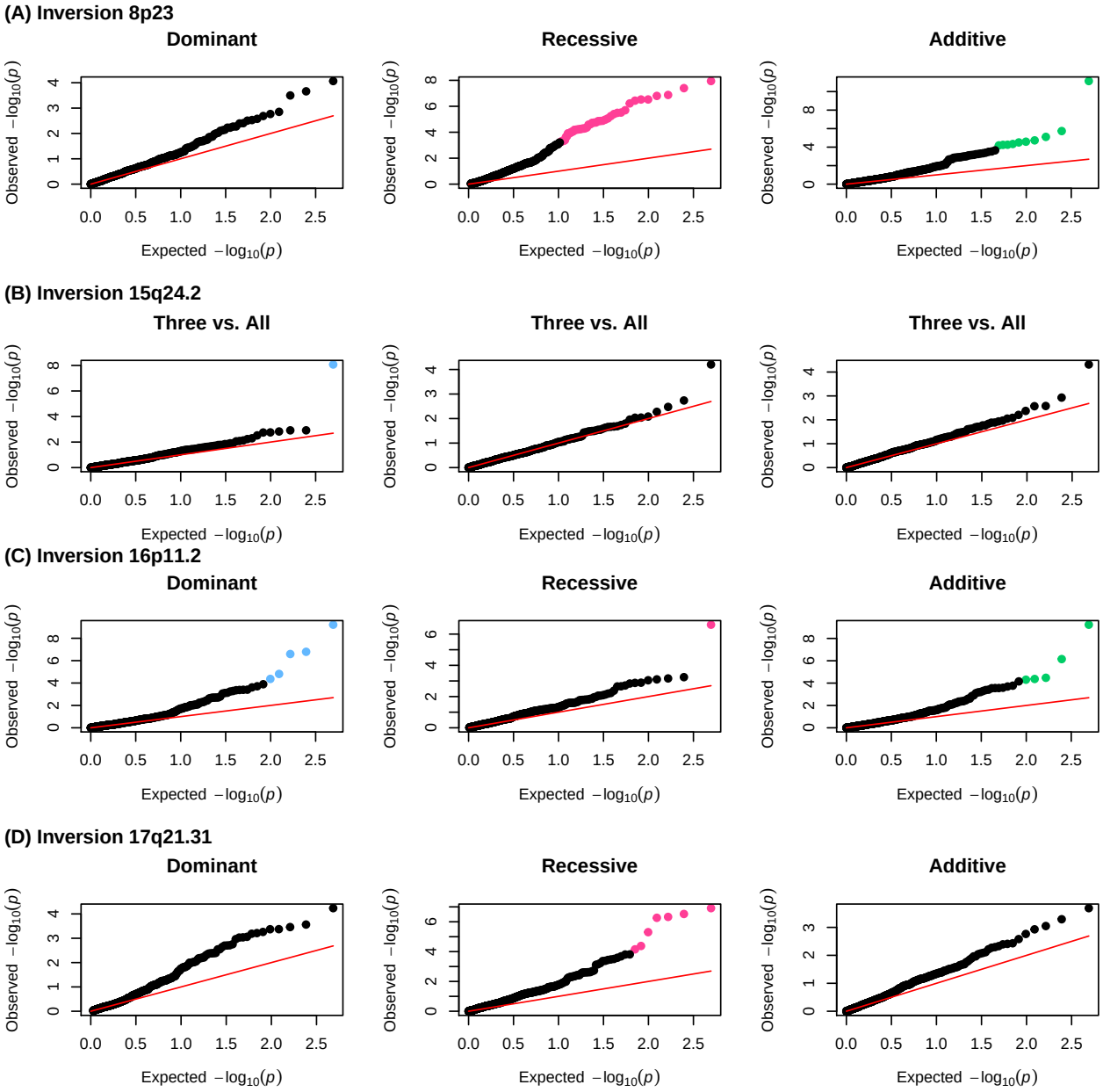

Figure 1. Quantile-Quantile (QQ) plot of observed vs. expected P-values of BLCA samples. The QQ plot of observed P-values shows whether they follow the expected null distribution (red line) apart from significant miRNA with an Adjusted P-value lower than 0.05 (colored points).

1.1.2. BRCA

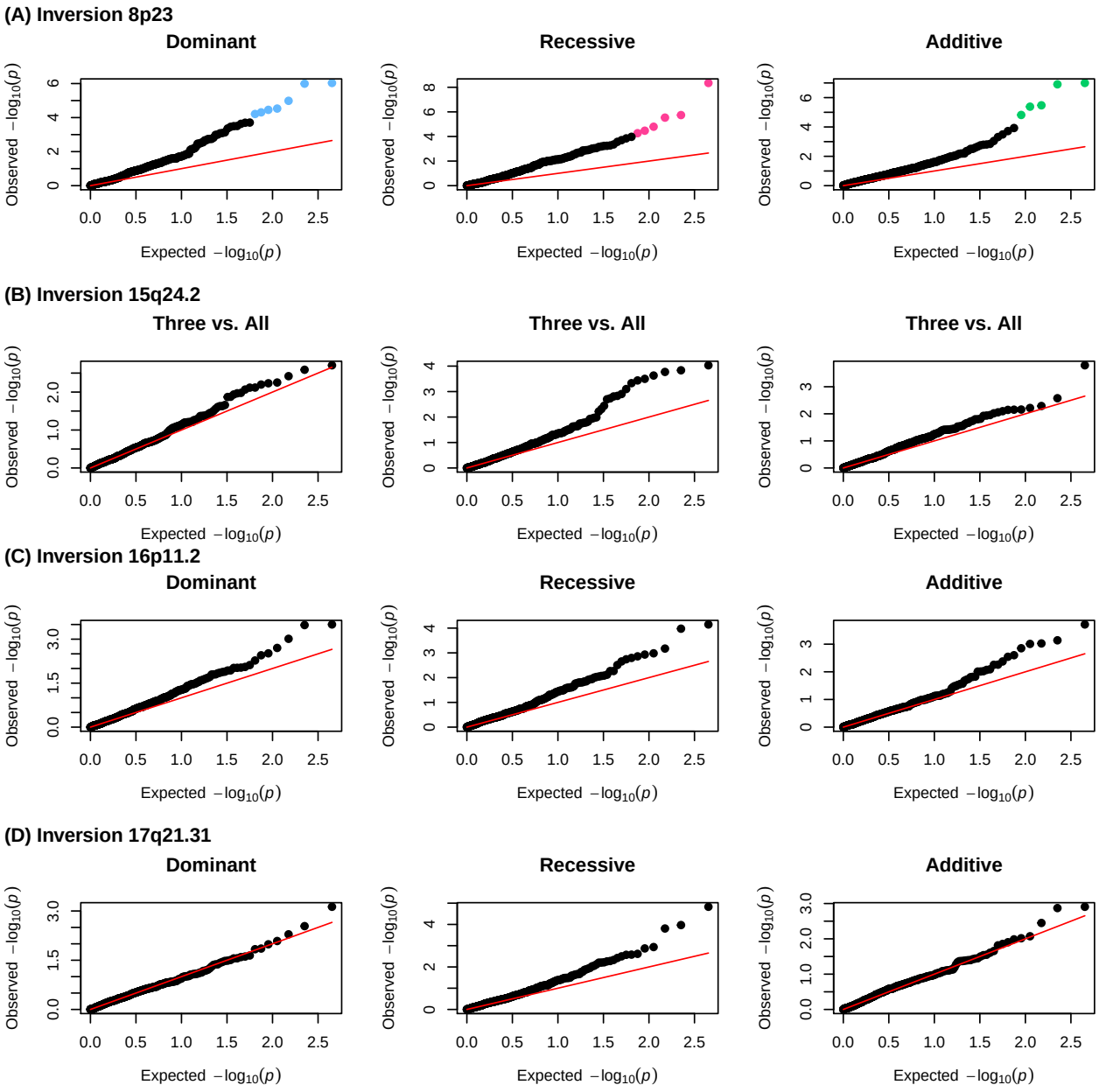

Figure 2. Quantile-Quantile (QQ) plot of observed vs. expected P-values of BRCA samples. The QQ plot of observed P-values shows whether they follow the expected null distribution (red line) apart from significant miRNA with an Adjusted P-value lower than 0.05 (colored points).

1.1.3. COAD

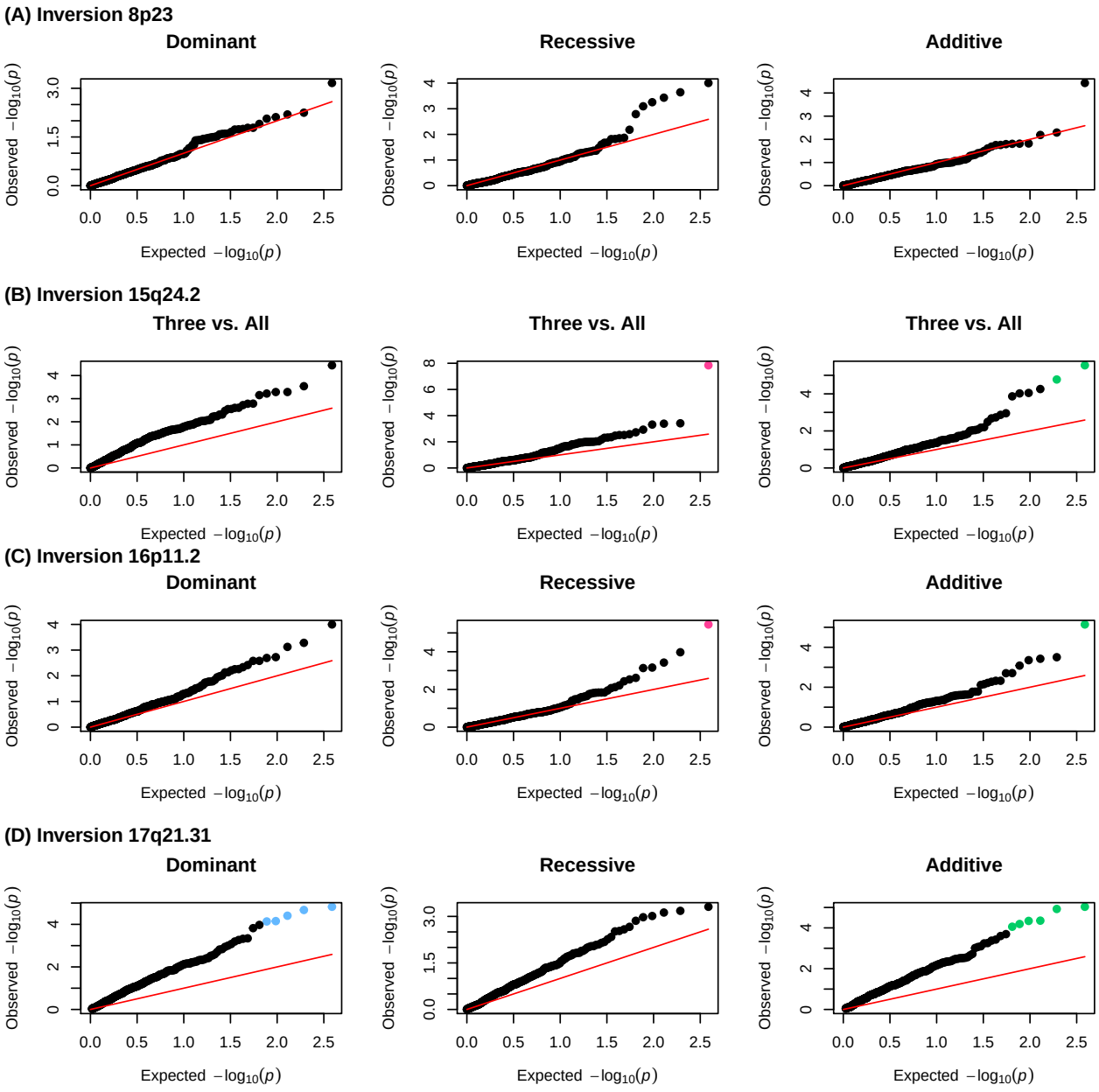

Figure 3. Quantile-Quantile (QQ) plot of observed vs. expected P-values of COAD samples. The QQ plot of observed P-values shows whether they follow the expected null distribution (red line) apart from significant miRNA with an Adjusted P-value lower than 0.05 (colored points).

1.1.4. KICH

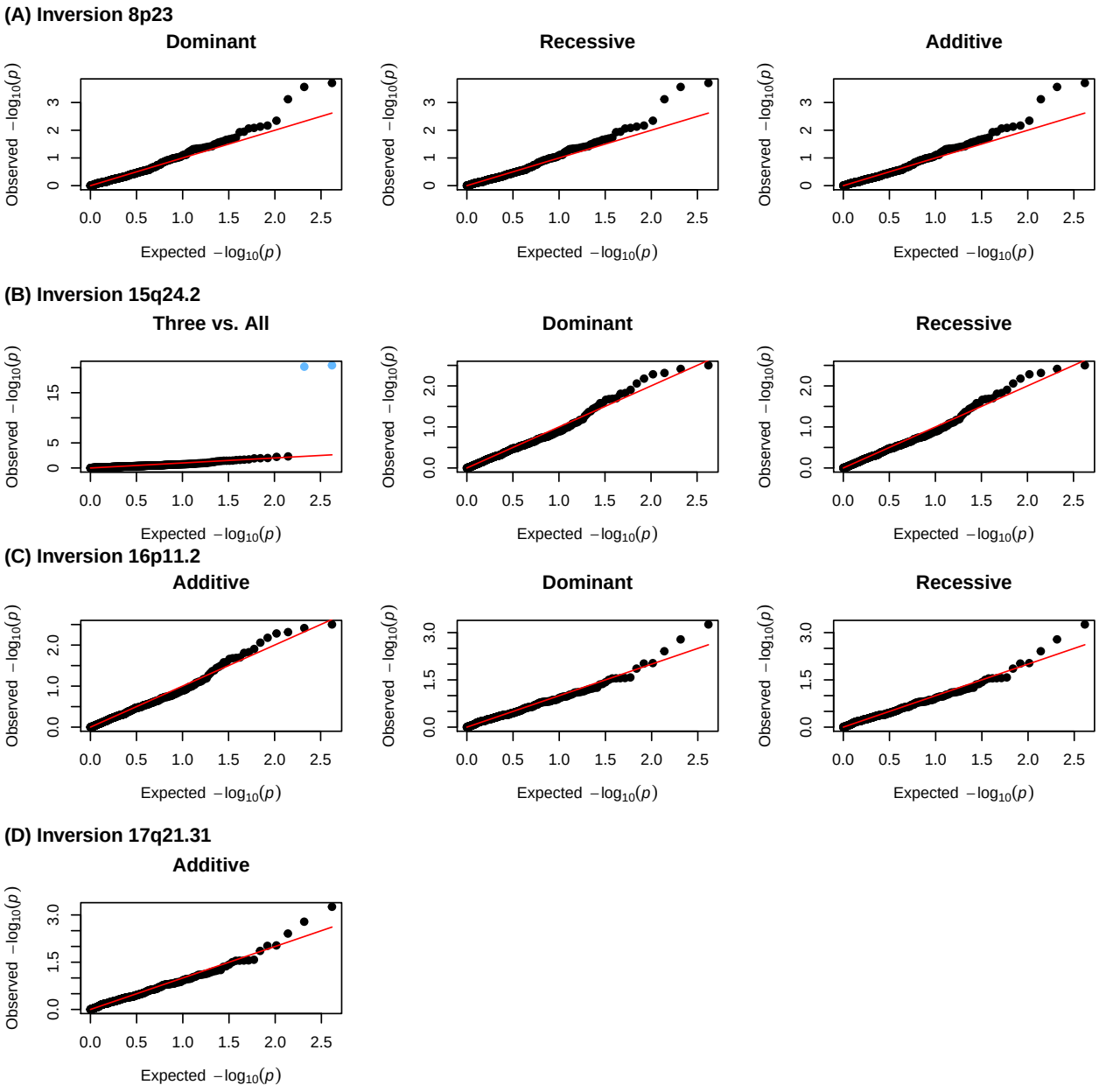

Figure 4. Quantile-Quantile (QQ) plot of observed vs. expected P-values of KICH samples. The QQ plot of observed P-values shows whether they follow the expected null distribution (red line) apart from significant miRNA with an Adjusted P-value lower than 0.05 (colored points).

1.1.5. KIRC

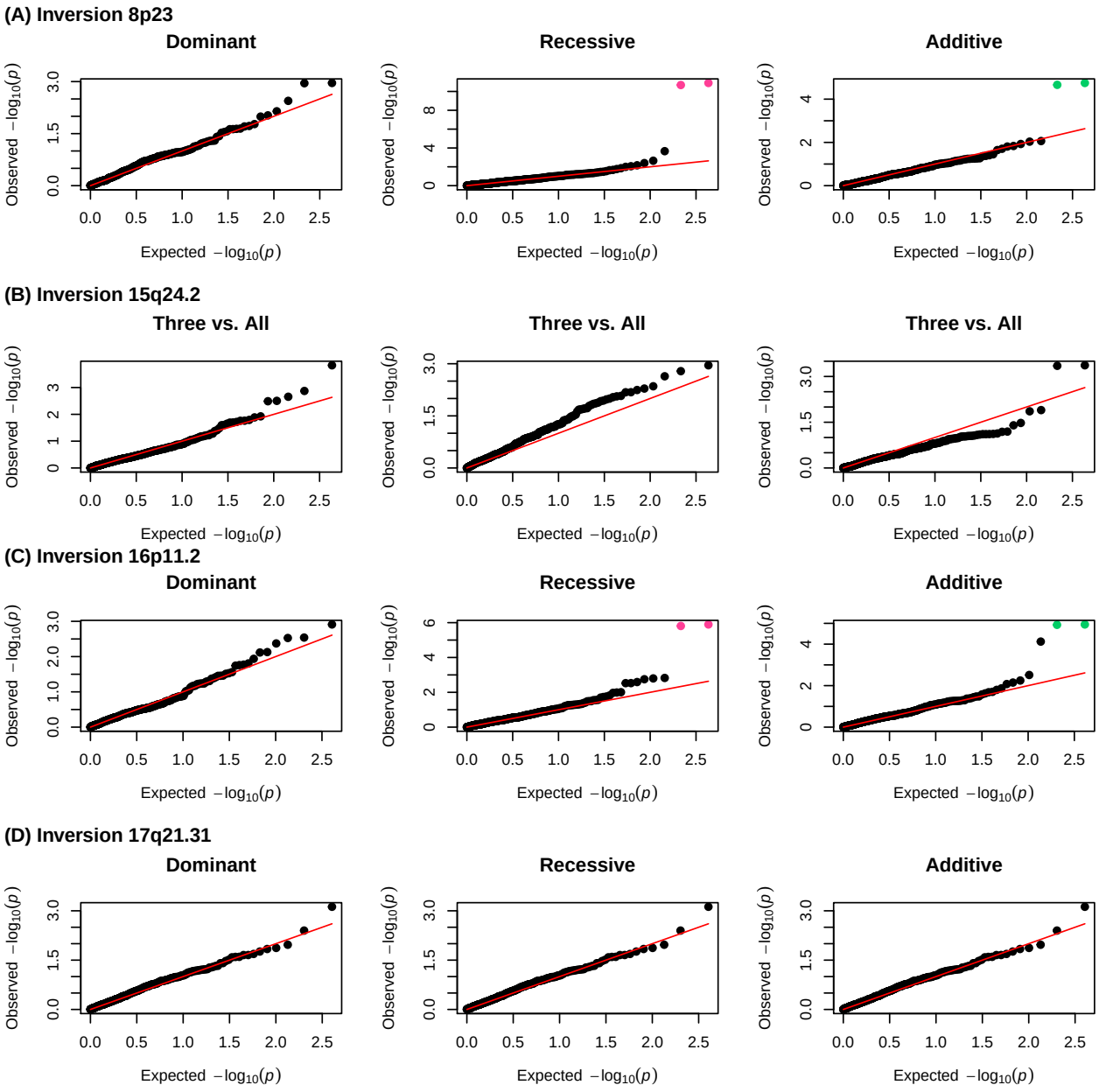

Figure 5. Quantile-Quantile (QQ) plot of observed vs. expected P-values of KIRC samples. The QQ plot of observed P-values shows whether they follow the expected null distribution (red line) apart from significant miRNA with an Adjusted P-value lower than 0.05 (colored points).

1.1.6. KIRP

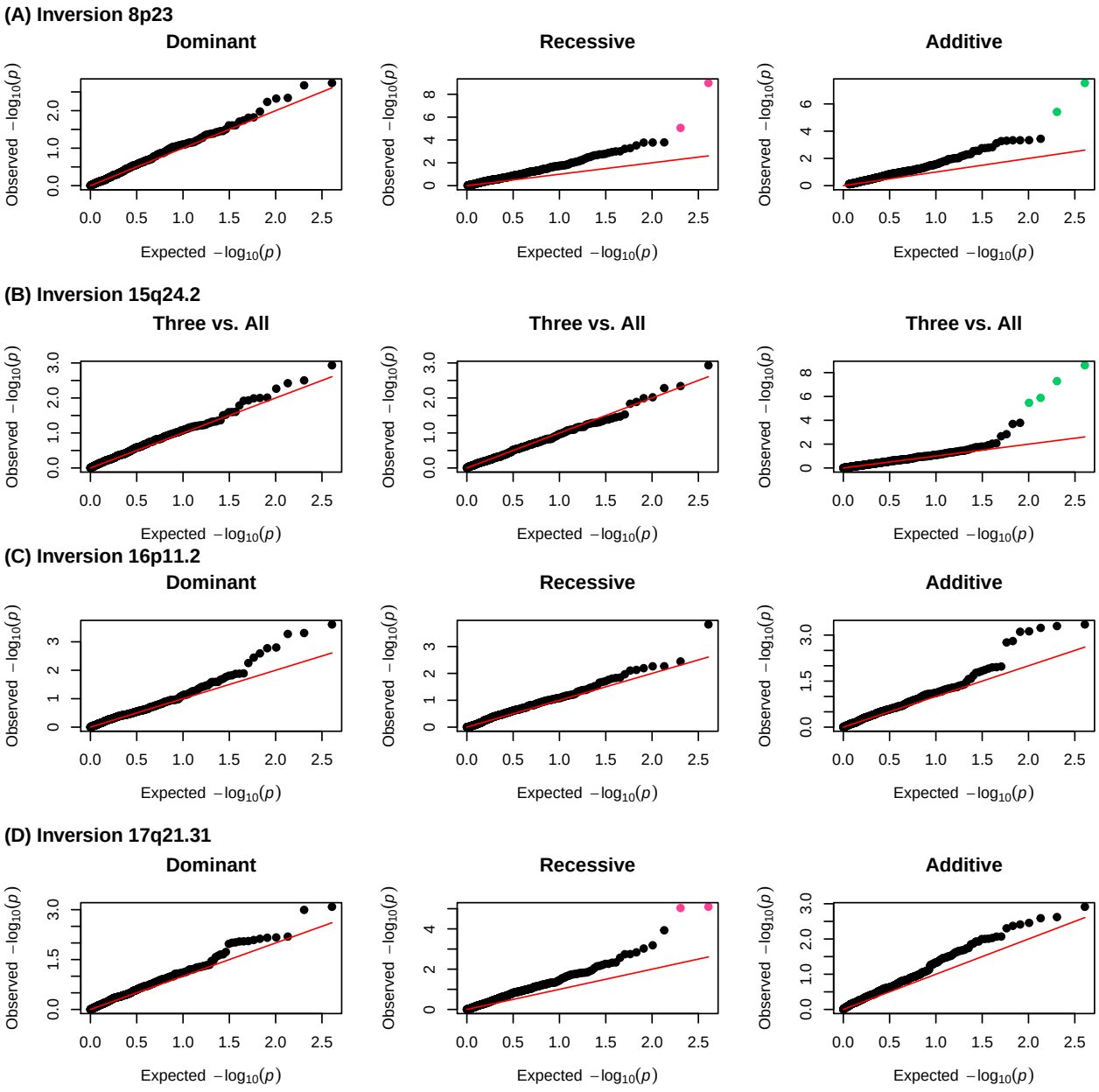

Figure 6. Quantile-Quantile (QQ) plot of observed vs. expected P-values of KIRP samples. The QQ plot of observed P-values shows whether they follow the expected null distribution (red line) apart from significant miRNA with an Adjusted P-value lower than 0.05 (colored points).

1.1.7. LGG

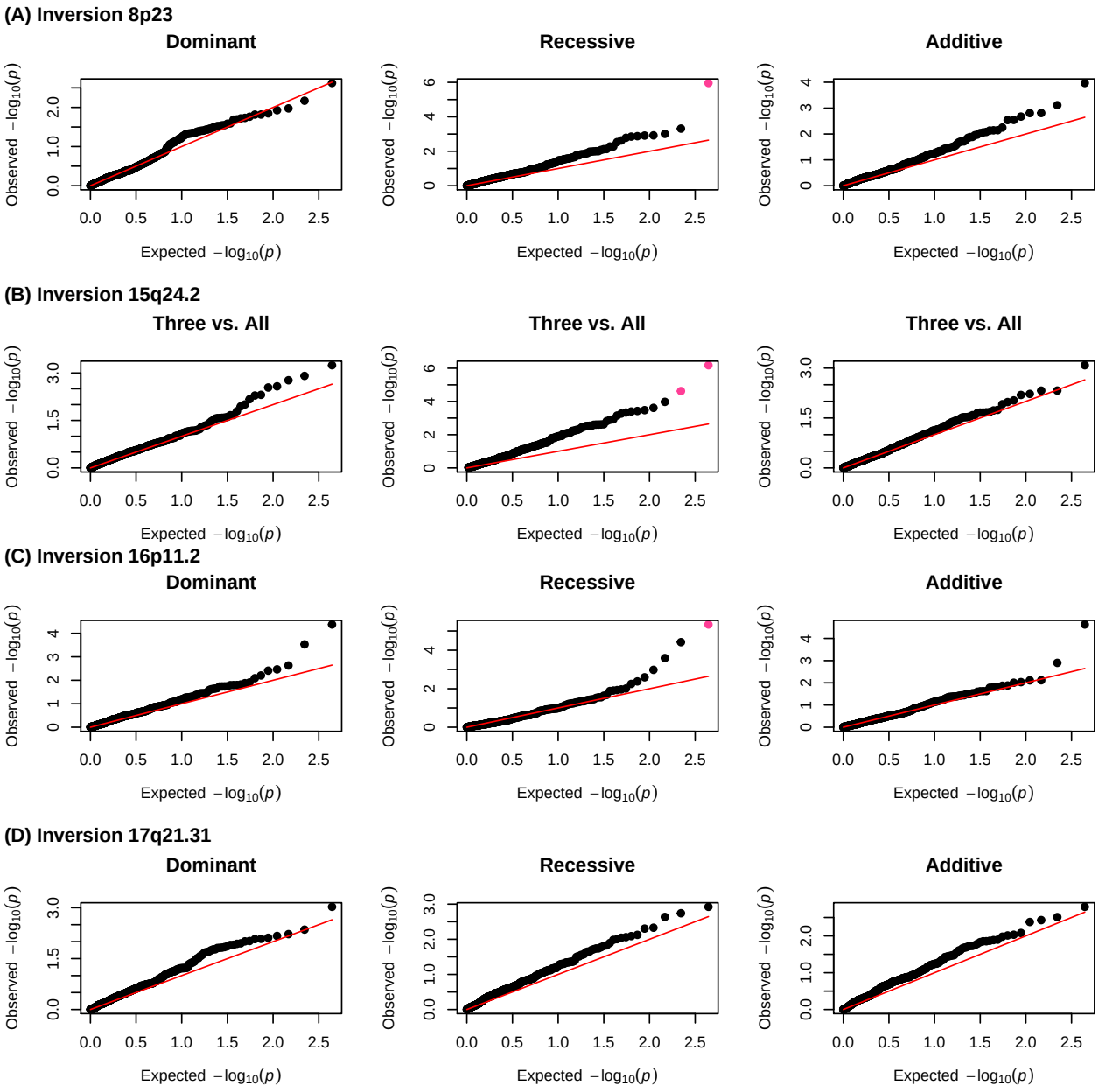

Figure 7. Quantile-Quantile (QQ) plot of observed vs. expected P-values of LGG samples. The QQ plot of observed P-values shows whether they follow the expected null distribution (red line) apart from significant miRNA with an Adjusted P-value lower than 0.05 (colored points).

1.1.8. LIHC

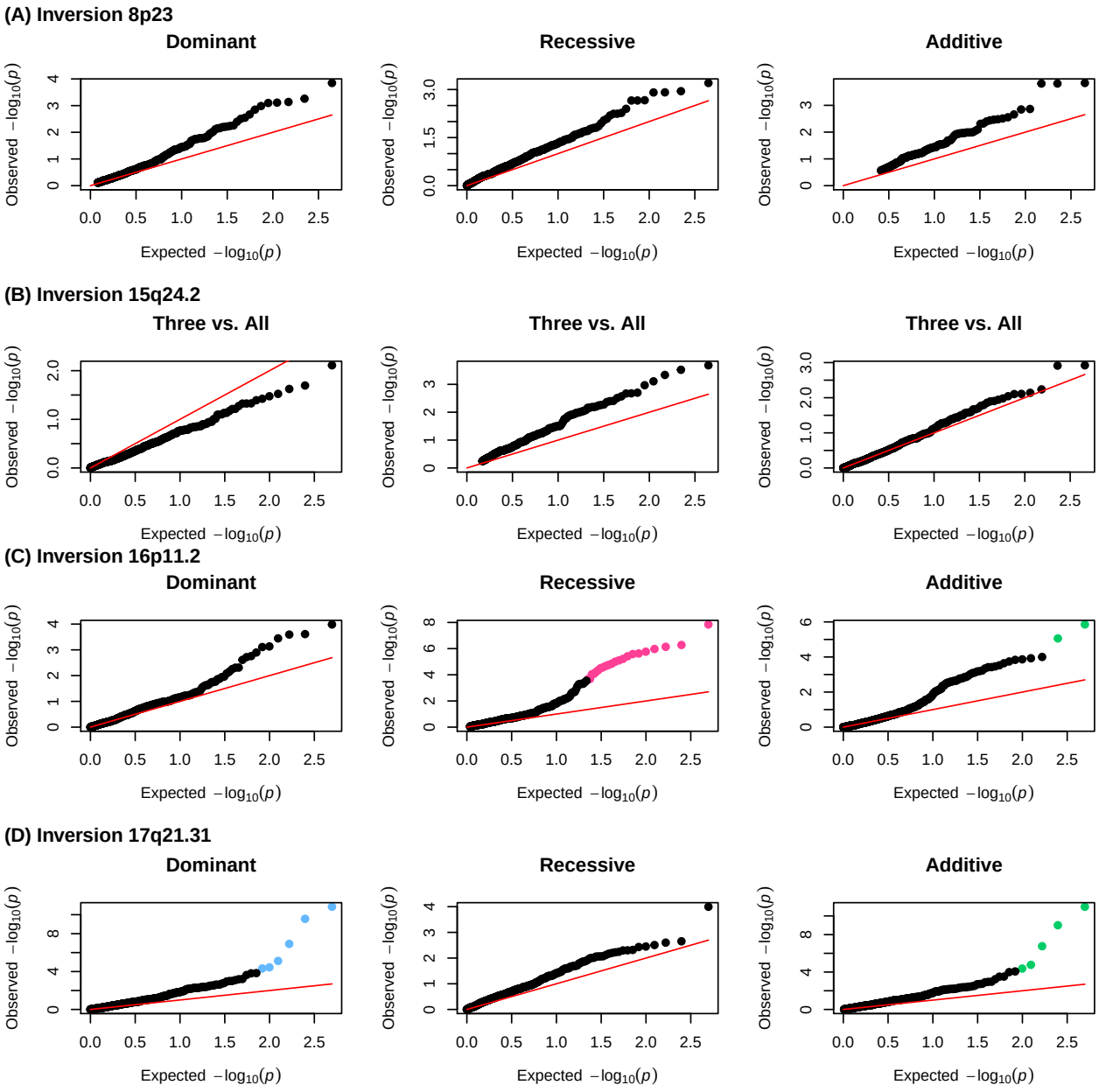

Figure 8. Quantile-Quantile (QQ) plot of observed vs. expected P-values of LIHC samples. The QQ plot of observed P-values shows whether they follow the expected null distribution (red line) apart from significant miRNA with an Adjusted P-value lower than 0.05 (colored points).

1.1.9. LUAD

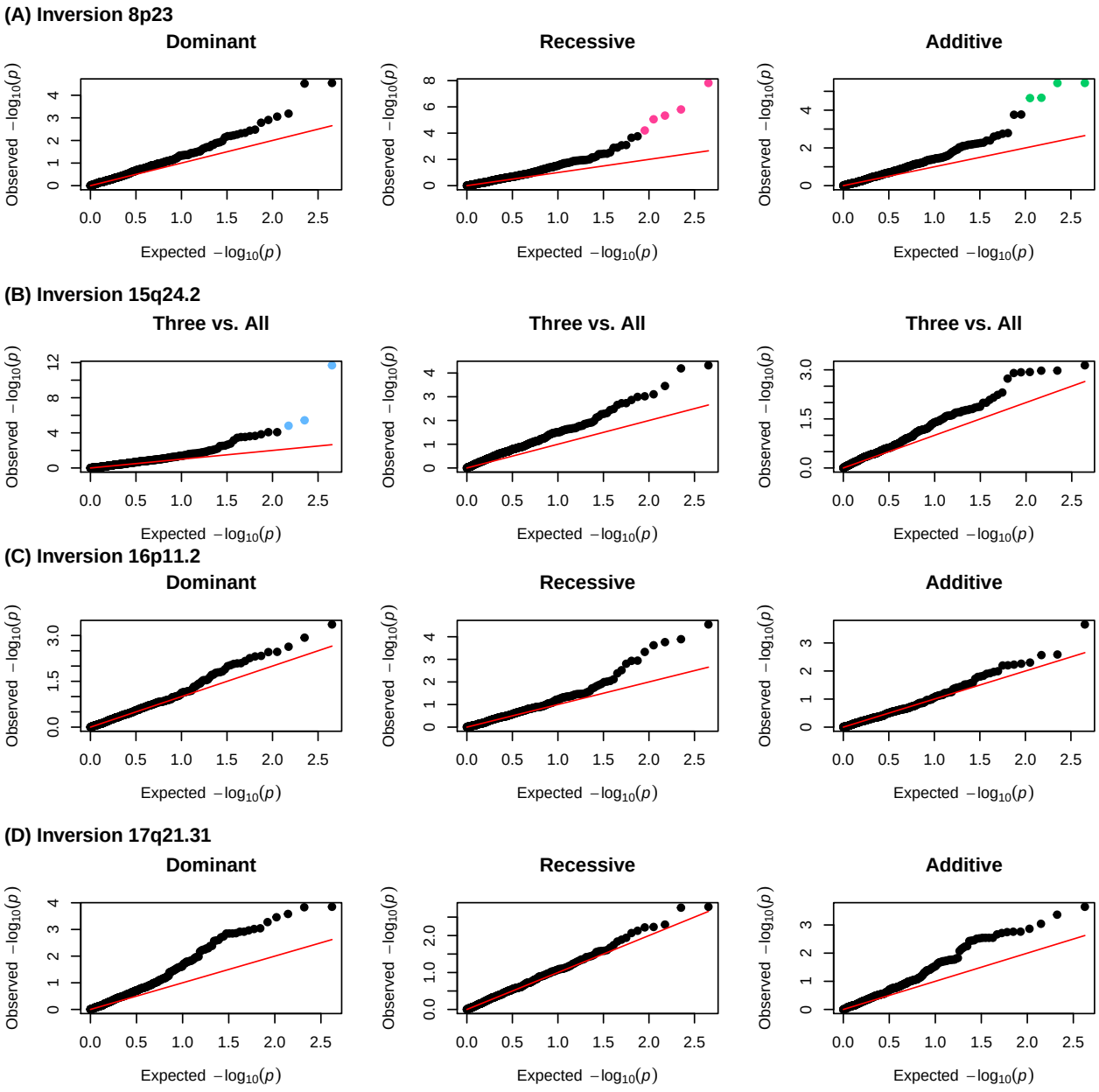

Figure 9. Quantile-Quantile (QQ) plot of observed vs. expected P-values of LUAD samples. The QQ plot of observed P-values shows whether they follow the expected null distribution (red line) apart from significant miRNA with an Adjusted P-value lower than 0.05 (colored points).

1.1.10. PRAD

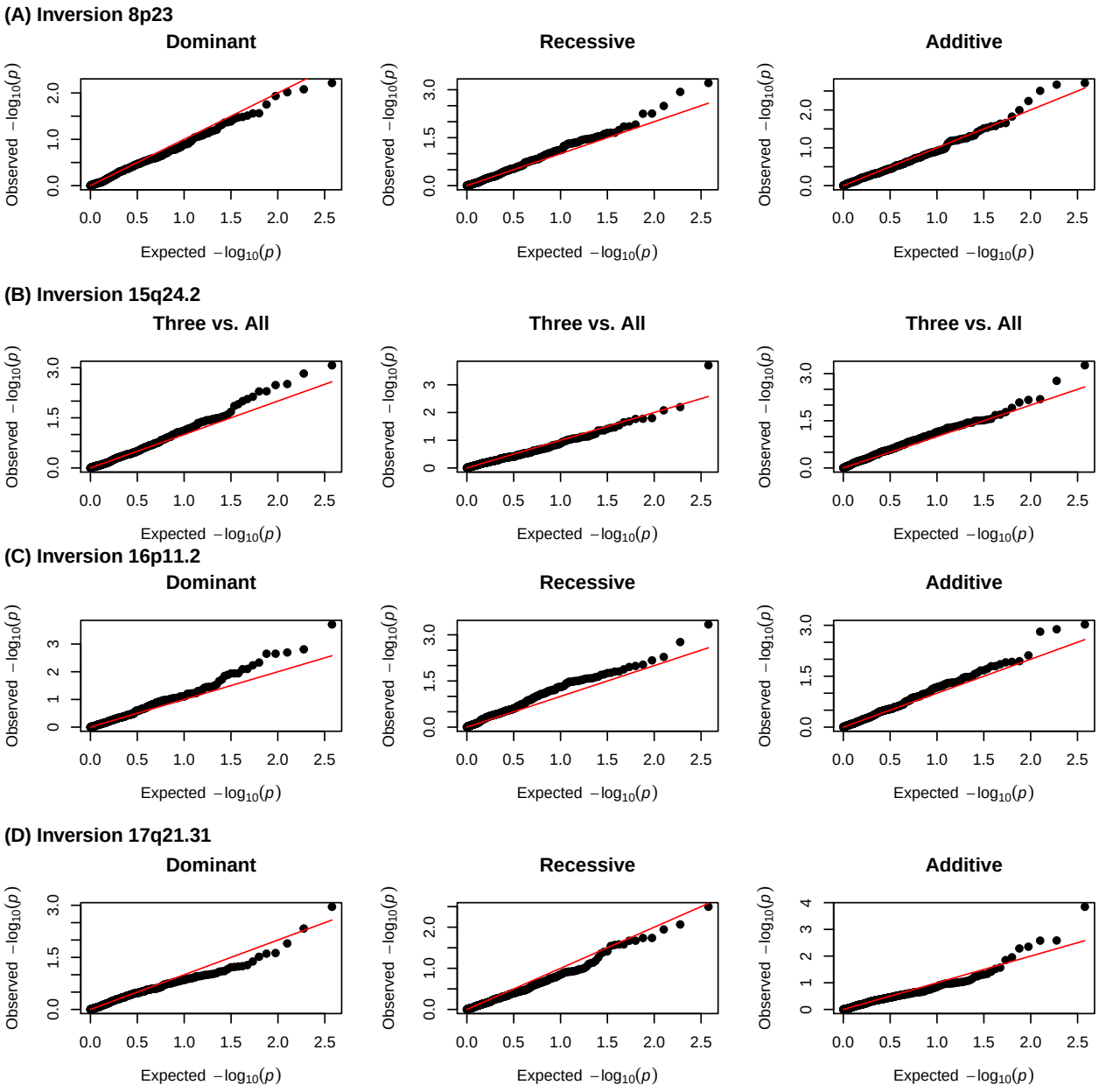

Figure 10. Quantile-Quantile (QQ) plot of observed vs. expected P-values of PRAD samples. The QQ plot of observed P-values shows whether they follow the expected null distribution (red line) apart from significant miRNA with an Adjusted P-value lower than 0.05 (colored points).

1.1.11. READ

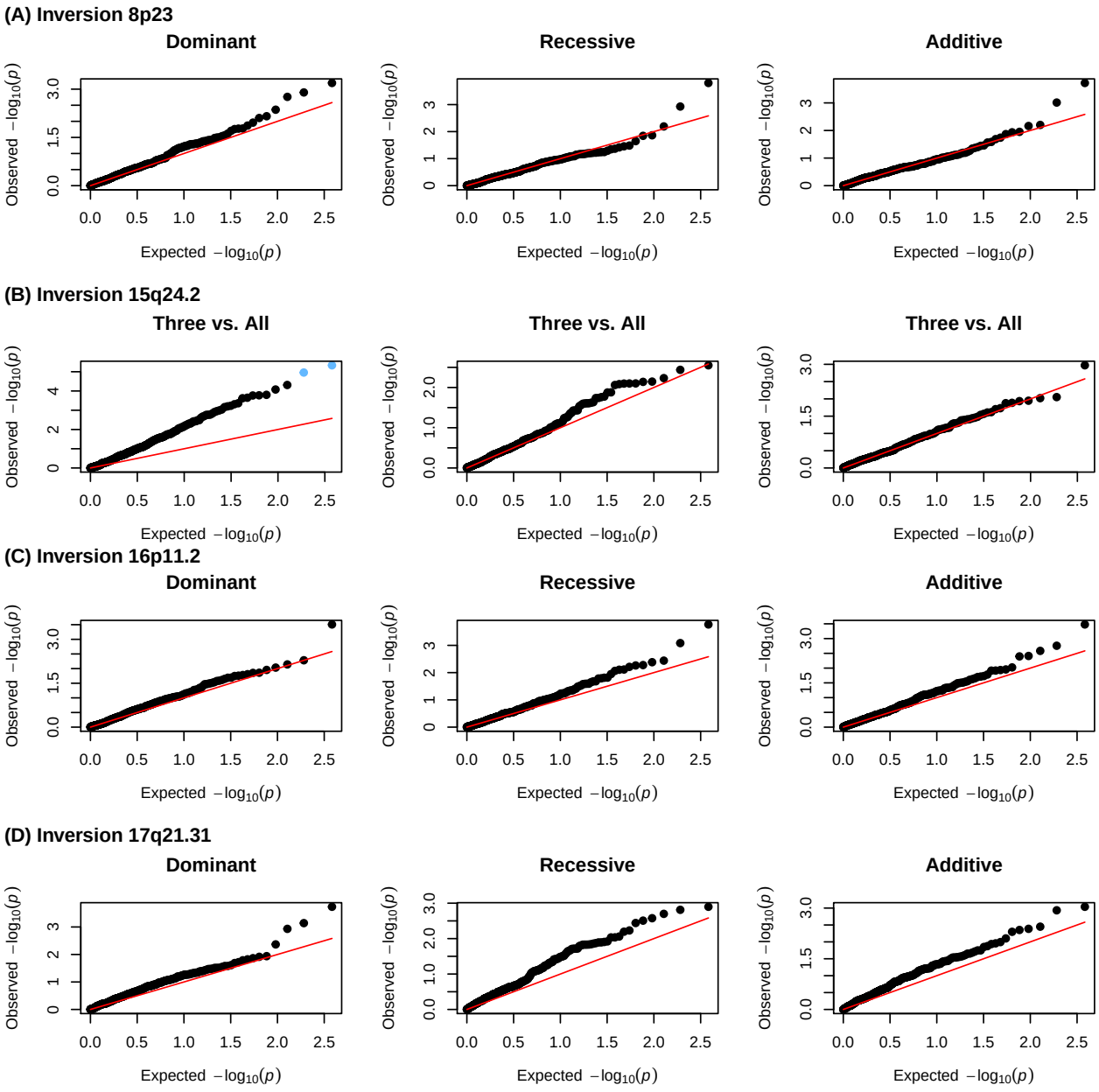

Figure 11. Quantile-Quantile (QQ) plot of observed vs. expected P-values of READ samples. The QQ plot of observed P-values shows whether they follow the expected null distribution (red line) apart from significant miRNA with an Adjusted P-value lower than 0.05 (colored points).

1.1.12. SKCM

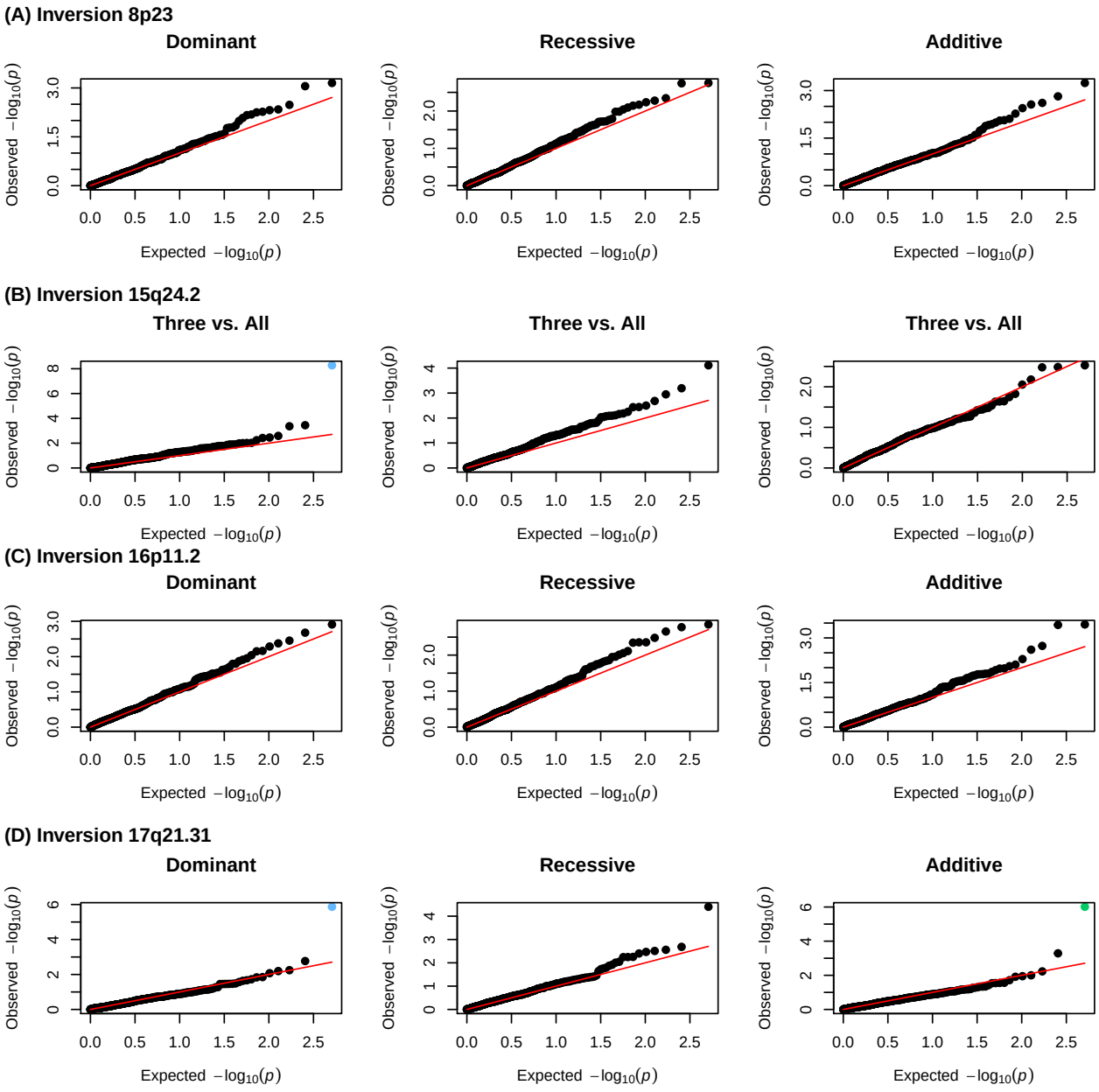

Figure 12. Quantile-Quantile (QQ) plot of observed vs. expected P-values of SKCM samples. The QQ plot of observed P-values shows whether they follow the expected null distribution (red line) apart from significant miRNA with an Adjusted P-value lower than 0.05 (colored points).

1.1.13. STAD

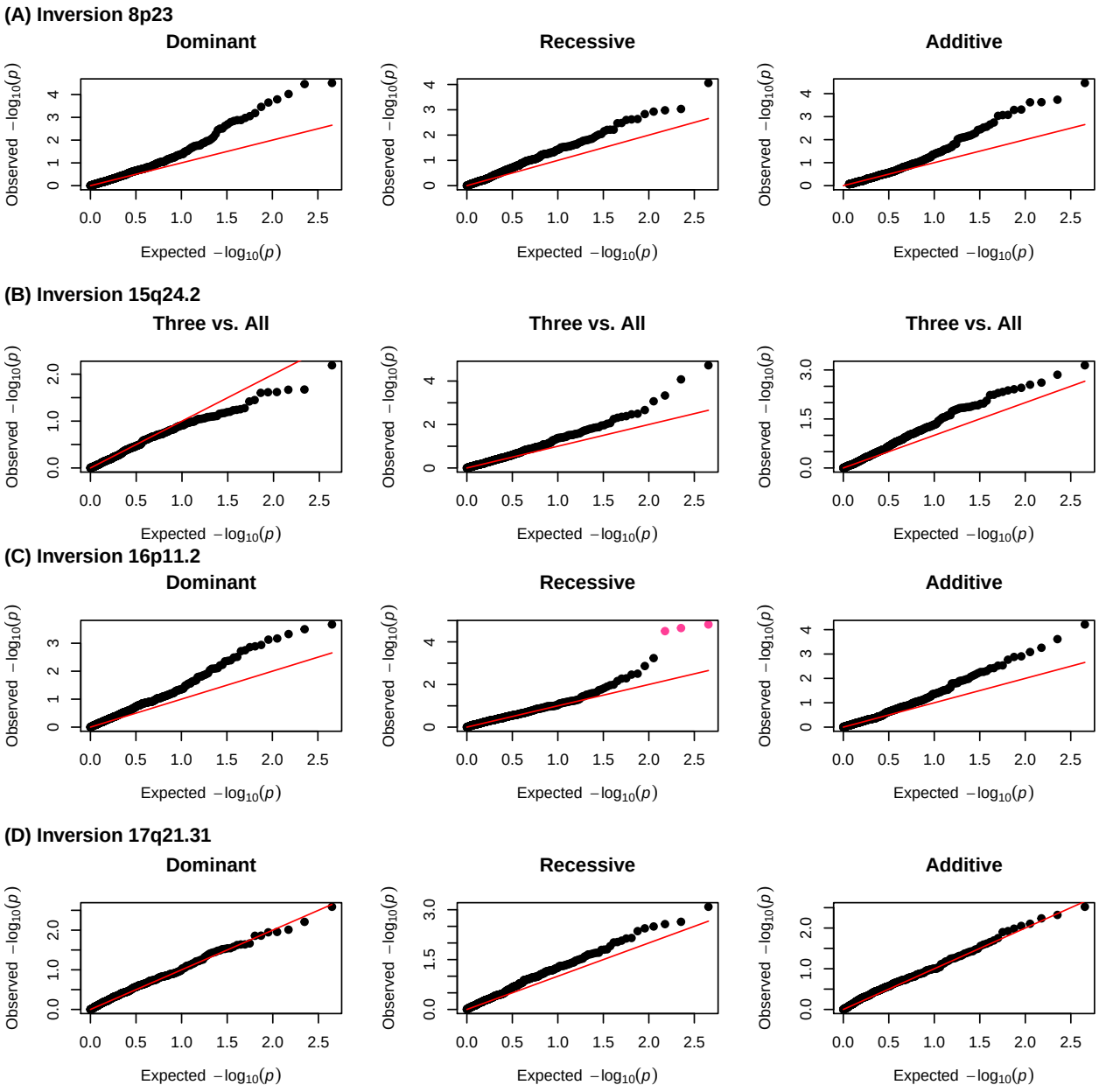

Figure 13. Quantile-Quantile (QQ) plot of observed vs. expected P-values of STAD samples. The QQ plot of observed P-values shows whether they follow the expected null distribution (red line) apart from significant miRNA with an Adjusted P-value lower than 0.05 (colored points).

1.1.14. THCA

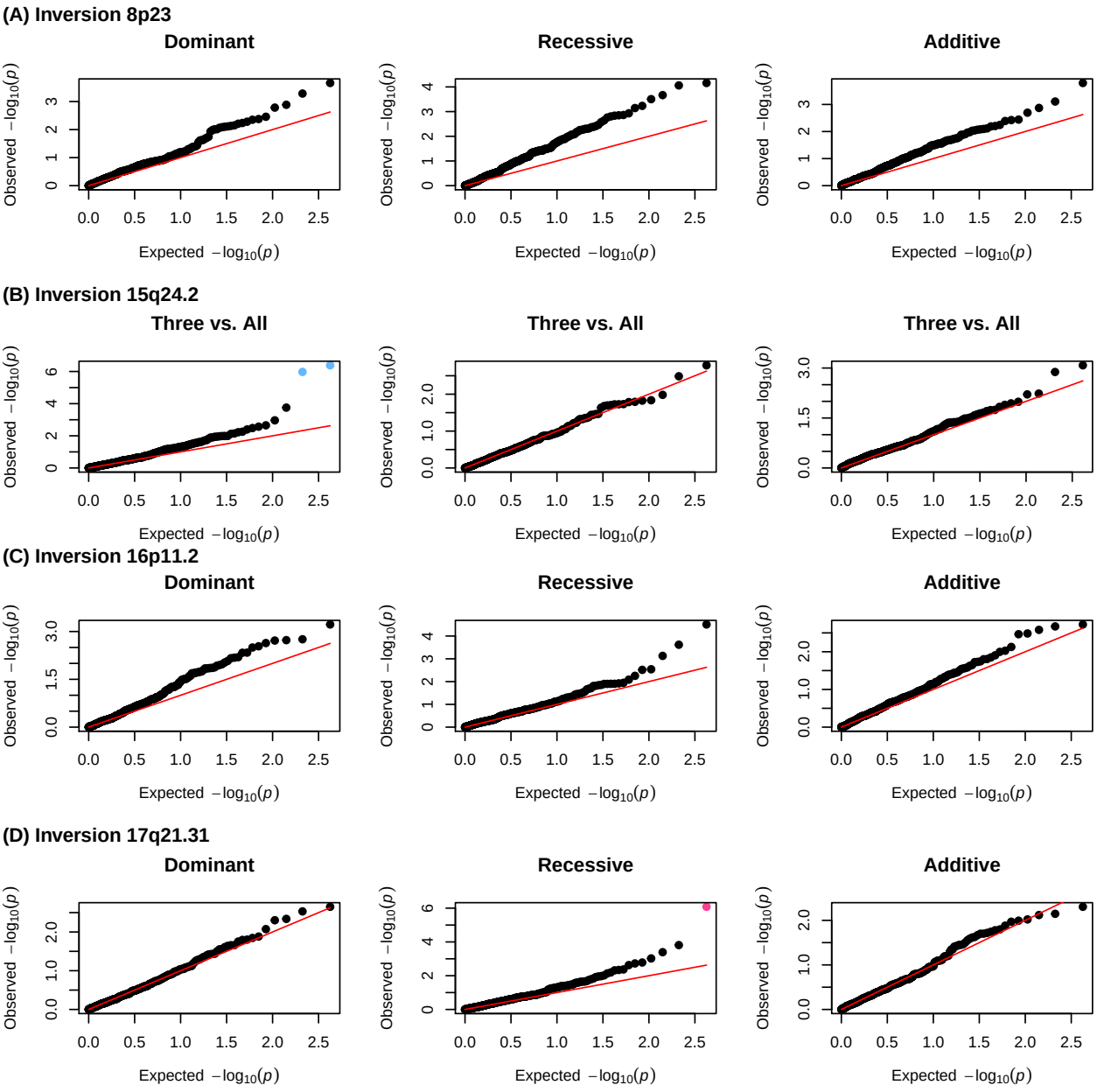

Figure 14. Quantile-Quantile (QQ) plot of observed vs. expected P-values of THCA samples. The QQ plot of observed P-values shows whether they follow the expected null distribution (red line) apart from significant miRNA with an Adjusted P-value lower than 0.05 (colored points).

1.1.15. UCEC

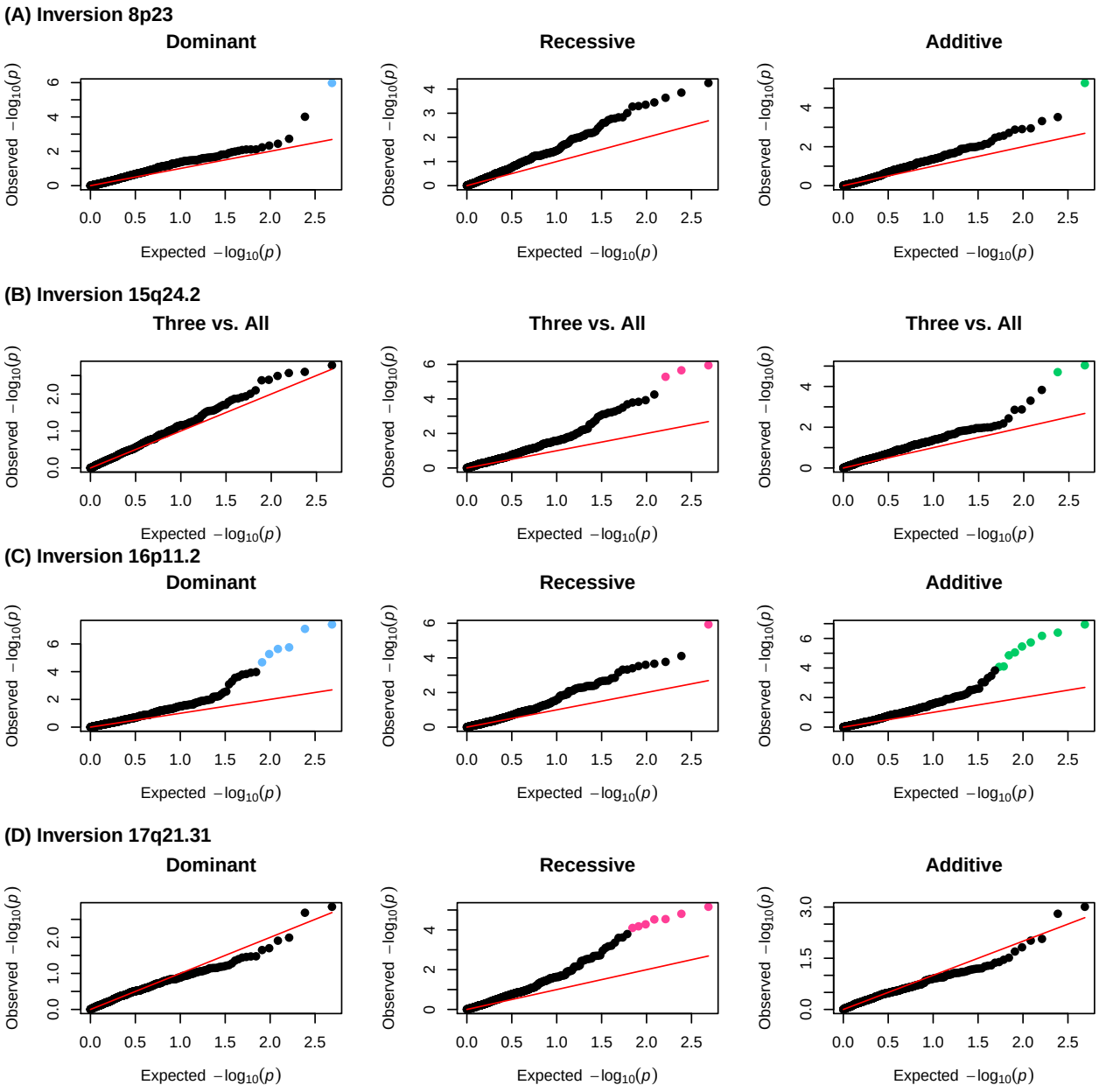

Figure 15. Quantile-Quantile (QQ) plot of observed vs. expected P-values of UCEC samples. The QQ plot of observed P-values shows whether they follow the expected null distribution (red line) apart from significant miRNA with an Adjusted P-value lower than 0.05 (colored points).

1.2. Significative miRNA (Tables)

1.2.1. BLCA

Table 1: Significant miRNA in BLCA cancer in chromosomal inversion 15q24.2

	Cis	Adj. P-value One vs. all	Adj. P-value Three vs. all	Adj. P-value Six vs. all
hsa-miR-1269	Yes	3.693e-05	1	1

Table 2: Significant miRNA in BLCA cancer in chromosomal inversion 16p11.2

	Cis	Adj. P-value Dominant	Adj. P-value Recessive	Adj. P-value Additive
hsa-miR-1226	Yes	2.687e-06	0.001071	2.578e-06
hsa-miR-1269	No	3.530e-04	1.000000	1.542e-03
hsa-miR-652	No	3.721e-04	1.000000	4.313e-02
hsa-miR-324	Yes	1.679e-02	1.000000	4.313e-02
hsa-miR-483	No	3.753e-02	1.000000	4.313e-02
hsa-miR-3620	Yes	9.331e-02	1.000000	1.041e-01

Table 3: Significant miRNA in BLCA cancer in chromosomal inversion 17q21.31

	Cis	Adj. P-value Dominant	Adj. P-value Recessive	Adj. P-value Additive
hsa-miR-522	No	0.5029307257505	0.0005329	1
hsa-miR-518e	Yes	0.715733533704758	0.0005893	1
hsa-miR-520f	Yes	0.870038998771372	0.0005893	1
hsa-miR-527	No	1	0.0005893	1
hsa-miR-518a-1	No	1	0.0043315	1
hsa-miR-3074	Yes	1	0.0304626	1
hsa-miR-345	Yes	-	0.0440697	1

Table 4: Significant miRNA in BLCA cancer in chromosomal inversion 8p23

	Cis	Adj. P-value Dominant	Adj. P-value Recessive	Adj. P-value Additive
hsa-miR-548f-1	No	0.3742	4.680e-05	3.179e-08
hsa-miR-512-2	No	1.0000	8.235e-05	4.012e-03
hsa-miR-873	Yes	1.0000	1.635e-04	1.141e-02
hsa-miR-372	Yes	1.0000	1.635e-04	2.042e-02
hsa-miR-520c	Yes	1.0000	2.060e-04	2.261e-02
hsa-miR-512-1	No	1.0000	2.060e-04	2.261e-02
hsa-miR-517a	No	1.0000	2.166e-04	2.766e-02
hsa-miR-517b	No	1.0000	3.089e-04	2.766e-02
hsa-miR-520a	Yes	1.0000	9.221e-04	2.766e-02
hsa-miR-520f	No	1.0000	1.197e-03	2.826e-02
hsa-miR-624	Yes	1.0000	1.197e-03	8.851e-02
hsa-miR-517c	No	1.0000	1.359e-03	1.067e-01
hsa-miR-518c	No	1.0000	1.808e-03	1.087e-01
hsa-miR-3691	Yes	1.0000	2.515e-03	1.249e-01
hsa-miR-129-1	No	1.0000	2.950e-03	1.337e-01
hsa-miR-345	No	1.0000	3.185e-03	1.365e-01
hsa-miR-526b	Yes	1.0000	3.185e-03	1.423e-01
hsa-miR-525	No	1.0000	3.185e-03	1.425e-01
hsa-miR-518b	No	1.0000	3.724e-03	1.549e-01
hsa-miR-1323	Yes	1.0000	3.724e-03	1.549e-01
hsa-miR-1274b	No	1.0000	3.724e-03	1.558e-01
hsa-miR-1301	No	1.0000	4.593e-03	1.586e-01
hsa-miR-3676	No	1.0000	4.689e-03	1.811e-01
hsa-miR-518a-1	No	1.0000	7.375e-03	1.811e-01
hsa-miR-519c	Yes	1.0000	7.993e-03	1.877e-01
hsa-miR-519d	Yes	1.0000	7.993e-03	1.905e-01
hsa-miR-520d	Yes	1.0000	7.993e-03	1.946e-01
hsa-miR-520g	No	1.0000	8.153e-03	1.946e-01
hsa-miR-615	Yes	1.0000	8.153e-03	1.946e-01
hsa-miR-196a-1	No	1.0000	8.153e-03	1.946e-01
hsa-miR-451	No	1.0000	8.153e-03	1.970e-01
hsa-miR-498	No	1.0000	8.153e-03	2.628e-01
hsa-miR-515-2	No	1.0000	8.153e-03	2.628e-01
hsa-miR-518f	No	1.0000	1.031e-02	2.628e-01
hsa-miR-520b	Yes	1.0000	1.079e-02	4.799e-01
hsa-miR-3200	Yes	1.0000	1.118e-02	8.266e-01
hsa-miR-522	No	1.0000	1.297e-02	1.000e+00
hsa-miR-223	No	1.0000	1.297e-02	1.000e+00
hsa-miR-363	Yes	1.0000	1.297e-02	1.000e+00
hsa-miR-518e	No	1.0000	2.104e-02	1.000e+00
hsa-miR-449a	Yes	1.0000	2.284e-02	1.000e+00
hsa-miR-215	Yes	1.0000	3.885e-02	1.000e+00
hsa-let-7f-1	Yes	1.0000	4.261e-02	1.000e+00
hsa-miR-129-2	No	1.0000	4.329e-02	1.000e+00
hsa-miR-521-1	No	1.0000	4.426e-02	1.000e+00
hsa-miR-1180	Yes	1.0000	4.649e-02	1.000e+00
hsa-miR-375	No	1.0000	4.784e-02	1.000e+00

1.2.2. BRCA

Table 5: Significant miRNA in BRCA cancer in chromosomal inversion 8p23

	Cis	Adj. P-value Dominant	Adj. P-value Recessive	Adj. P-value Additive
hsa-miR-577	Yes	0.002012	1.773e-05	0.0002454
hsa-miR-885	Yes	0.002012	3.609e-03	0.0002454
hsa-miR-224	Yes	0.013639	3.872e-03	0.0041067
hsa-miR-509-3	No	0.027756	1.595e-02	0.0041067
hsa-miR-519a-1	No	0.027756	2.690e-02	0.0120450
hsa-miR-508	No	0.032450	3.569e-02	0.0779833
hsa-miR-509-2	No	0.034757	6.050e-02	0.6854359
hsa-miR-514-1	No	0.195039	7.100e-02	1.0000000
hsa-miR-514-2	No	0.215575	3.057e-01	1.0000000
hsa-miR-184	No	1.000000	6.276e-01	1.0000000
hsa-miR-495	No	1.000000	6.304e-01	1.0000000
hsa-miR-487b	Yes	1.000000	1.000e+00	1.0000000

1.2.3. COAD

Table 6: Significant miRNA in COAD cancer in chromosomal inversion 15q24.2

	Cis	Adj. P-value One vs. all	Adj. P-value Three vs. all	Adj. P-value Six vs. all
hsa-miR-133a-1	No	0.3988	4.871e-05	0.009833
hsa-miR-133b	No	0.7058	1.000e+00	0.028664

Table 7: Significant miRNA in COAD cancer in chromosomal inversion 16p11.2

	Cis	Adj. P-value Dominant	Adj. P-value Recessive	Adj. P-value Additive
hsa-miR-150	Yes	0.3427	0.01213	0.02452

Table 8: Significant miRNA in COAD cancer in chromosomal inversion 17q21.31

	Cis	Adj. P-value Dominant	Adj. P-value Recessive	Adj. P-value Additive
hsa-miR-151	No	0.03465	1	0.01897232
hsa-miR-219-1	No	0.03465	1	0.01897232
hsa-miR-874	Yes	0.04288	1	0.03656698
hsa-miR-193b	Yes	0.04787	1	0.03656698
hsa-miR-501	Yes	0.04787	1	0.04136907
hsa-miR-106b	Yes	0.05805	1	0.04693777

1.2.4. KICH

Table 9: Significant miRNA in KICH cancer in chromosomal inversion 15q24.2

	Cis	Adj. P-value One vs. all
hsa-miR-9-1	No	1.187e-17
hsa-miR-9-2	No	1.187e-17

1.2.5. KIRC

Table 10: Significant miRNA in KIRC cancer in chromosomal inversion 8p23

	Cis	Adj. P-value Dominant	Adj. P-value Recessive	Adj. P-value Additive
hsa-miR-9-1	No	1	3.937e-08	0.0414
hsa-miR-9-2	No	1	3.937e-08	0.0414

Table 11: Significant miRNA in KIRC cancer in chromosomal inversion 16p11.2

	Cis	Adj. P-value Dominant	Adj. P-value Recessive	Adj. P-value Additive
hsa-miR-9-1	No	1	0.002944	0.02127
hsa-miR-9-2	No	1	0.002944	0.02127

1.2.6. KIRP

Table 12: Significant miRNA in KIRP cancer in chromosomal inversion 8p23

	Cis	Adj. P-value Dominant	Adj. P-value Recessive	Adj. P-value Additive
hsa-miR-187	No	1	3.591e-06	8.975e-05
hsa-miR-205	Yes	1	1.540e-02	5.963e-03

Table 13: Significant miRNA in KIRP cancer in chromosomal inversion 15q24.2

	Cis	Adj. P-value One vs. all	Adj. P-value Three vs. all	Adj. P-value Six vs. all
hsa-miR-508	Yes	1	1	8.647e-06
hsa-miR-509-1	No	1	1	9.202e-05
hsa-miR-509-2	No	1	1	1.556e-03
hsa-miR-509-3	Yes	1	1	3.043e-03

Table 14: Significant miRNA in KIRP cancer in chromosomal inversion 17q21.31

	Cis	Adj. P-value Dominant	Adj. P-value Recessive	Adj. P-value Additive
hsa-miR-592	Yes	1	0.01646	1
hsa-miR-215	No	1	0.01646	1

1.2.7. LGG

Table 15: Significant miRNA in LGG cancer in chromosomal inversion 8p23

	Cis	Adj. P-value Dominant	Adj. P-value Recessive	Adj. P-value Additive
hsa-miR-34c	Yes	1	0.004252	0.4167

Table 16: Significant miRNA in LGG cancer in chromosomal inversion 15q24.2

	Cis	Adj. P-value One vs. all	Adj. P-value Three vs. all	Adj. P-value Six vs. all
hsa-miR-184	No	1	0.002462	1
hsa-miR-196b	No	1	0.044362	1

Table 17: Significant miRNA in LGG cancer in chromosomal inversion 16p11.2

	Cis	Adj. P-value Dominant	Adj. P-value Recessive	Adj. P-value Additive
hsa-miR-891b	No	1	0.018	1

1.2.8. LIHC

Table 18: Significant miRNA in LIHC cancer in chromosomal inversion 17q21.31

	Cis	Adj. P-value Dominant	Adj. P-value Recessive	Adj. P-value Additive
hsa-miR-200c	Yes	6.400e-08	0.4432	4.544e-08
hsa-miR-141	Yes	6.002e-07	1.0000	2.132e-06
hsa-miR-891a	Yes	1.754e-04	1.0000	2.469e-04
hsa-miR-431	No	8.316e-03	1.0000	1.830e-02
hsa-miR-432	Yes	3.144e-02	1.0000	3.675e-02
hsa-miR-889	Yes	3.446e-02	1.0000	6.240e-02

Table 19: Significant miRNA in LIHC cancer in chromosomal inversion 16p11.2

	Cis	Adj. P-value Dominant	Adj. P-value Recessive	Adj. P-value Additive
hsa-miR-493	Yes	1	5.756e-05	0.006122
hsa-miR-432	Yes	1	9.801e-04	0.019140
hsa-miR-329-2	No	1	9.801e-04	0.106617
hsa-miR-337	No	1	1.072e-03	0.106617
hsa-miR-376c	No	1	1.382e-03	0.106617
hsa-miR-411	No	1	1.505e-03	0.106617
hsa-miR-494	Yes	1	1.505e-03	0.124006
hsa-miR-758	No	1	1.944e-03	0.139268
hsa-miR-127	No	1	2.740e-03	0.139268
hsa-miR-431	No	1	3.219e-03	0.139268
hsa-miR-370	Yes	1	3.666e-03	0.151483
hsa-miR-654	Yes	1	4.789e-03	0.184287
hsa-miR-539	Yes	1	5.482e-03	0.184287
hsa-miR-380	Yes	1	6.082e-03	0.202144
hsa-miR-487b	No	1	7.201e-03	0.297911
hsa-miR-379	No	1	7.949e-03	0.297911
hsa-miR-382	Yes	1	1.056e-02	0.297911
hsa-miR-655	Yes	1	1.349e-02	0.352365
hsa-miR-410	No	1	1.807e-02	0.361442
hsa-miR-541	Yes	1	1.823e-02	0.485960
hsa-miR-381	No	1	3.834e-02	0.485960
hsa-miR-134	Yes	1	3.834e-02	0.691793
hsa-miR-495	Yes	1	7.625e-02	0.775808

1.2.9. LUAD

Table 20: Significant miRNA in LUAD cancer in chromosomal inversion 8p23

	Cis	Adj. P-value Dominant	Adj. P-value Recessive	Adj. P-value Additive
hsa-miR-9-1	No	0.06028	6.013e-05	0.007241
hsa-miR-9-2	No	0.06028	3.118e-03	0.007241
hsa-miR-582	Yes	1.00000	6.100e-03	0.022644
hsa-miR-215	Yes	1.00000	8.727e-03	0.022644
hsa-miR-149	Yes	1.00000	4.943e-02	0.997545

Table 21: Significant miRNA in LUAD cancer in chromosomal inversion 15q24.2

	Cis	Adj. P-value One vs. all	Adj. P-value Three vs. all	Adj. P-value Six vs. all
hsa-miR-216a	Yes	8.045e-09	0.6691	1
hsa-miR-217	No	7.339e-03	1.0000	1
hsa-miR-483	No	2.041e-02	1.0000	1

1.2.10. READ

Table 22: Significant miRNA in READ cancer in chromosomal inversion 15q24.2

	Cis	Adj. P-value One vs. all	Adj. P-value Three vs. all	Adj. P-value Six vs. all
hsa-miR-134	No	0.01536	1	1
hsa-miR-379	Yes	0.01824	1	1

1.2.11. SKCM

Table 23: Significant miRNA in SKCM cancer in chromosomal inversion 15q24.2

	Cis	Adj. P-value One vs. all	Adj. P-value Three vs. all	Adj. P-value Six vs. all
hsa-miR-206	No	2.379e-05	1	1

Table 24: Significant miRNA in SKCM cancer in chromosomal inversion 17q21.31

	Cis	Adj. P-value Dominant	Adj. P-value Recessive	Adj. P-value Additive
hsa-miR-1247	Yes	0.00606	1	0.004354

1.2.12. STAD

Table 25: Significant miRNA in STAD cancer in chromosomal inversion 16p11.2

	Cis	Adj. P-value Dominant	Adj. P-value Recessive	Adj. P-value Additive
hsa-miR-514-3	No	1	0.04161	1
hsa-miR-598	No	1	0.04161	1
hsa-miR-135a-1	No	1	0.04161	1

1.2.13. THCA

Table 26: Significant miRNA in THCA cancer in chromosomal inversion 15q24.2

	Cis	Adj. P-value One vs. all	Adj. P-value Three vs. all	Adj. P-value Six vs. all
hsa-miR-34c	No	0.001532	1	1
hsa-miR-34b	No	0.001979	1	1

Table 27: Significant miRNA in THCA cancer in chromosomal inversion 17q21.31

	Cis	Adj. P-value Dominant	Adj. P-value Recessive	Adj. P-value Additive
hsa-miR-210	Yes	1	0.003085	1

1.2.14. UCEC

Table 28: Significant miRNA in UCEC cancer in chromosomal inversion 8p23

	Cis	Adj. P-value Dominant	Adj. P-value Recessive	Adj. P-value Additive
hsa-miR-138-1	No	0.004515	1	0.02287

Table 29: Significant miRNA in UCEC cancer in chromosomal inversion 15q24.2

	Cis	Adj. P-value One vs. all	Adj. P-value Three vs. all	Adj. P-value Six vs. all
hsa-miR-433	Yes	1	0.004708	0.03833
hsa-miR-370	Yes	1	0.004708	0.04139
hsa-miR-320b-2	No	1	0.007480	1.00000

Table 30: Significant miRNA in UCEC cancer in chromosomal inversion 16p11.2

	Cis	Adj. P-value Dominant	Adj. P-value Recessive	Adj. P-value Additive
hsa-miR-1269	No	0.0001691	0.005049	0.0004866
hsa-miR-196a-2	No	0.0001759	0.167449	0.0008687
hsa-miR-196a-1	No	0.0024704	0.213976	0.0009550
hsa-miR-323b	Yes	0.0024704	0.213976	0.0019969
hsa-miR-374a	No	0.0045957	0.544131	0.0030150
hsa-miR-514-1	No	0.0150616	0.835820	0.0063276
hsa-miR-514-2	No	0.0631131	1.000000	0.0085138
hsa-miR-514-3	No	0.0631131	1.000000	0.0400296
hsa-miR-582	No	0.0700082	1.000000	0.0400296

Table 31: Significant miRNA in UCEC cancer in chromosomal inversion 17q21.31

	Cis	Adj. P-value Dominant	Adj. P-value Recessive	Adj. P-value Additive
hsa-miR-138-2	Yes	1	0.02959	1
hsa-miR-181d	Yes	1	0.03203	1
hsa-miR-194-1	No	1	0.03203	1
hsa-miR-551b	No	1	0.03203	1
hsa-miR-194-2	No	1	0.04515	1
hsa-miR-192	Yes	1	0.04738	1
hsa-miR-324	Yes	1	0.04879	1

1.3. Boxplots

1.3.1. BLCA

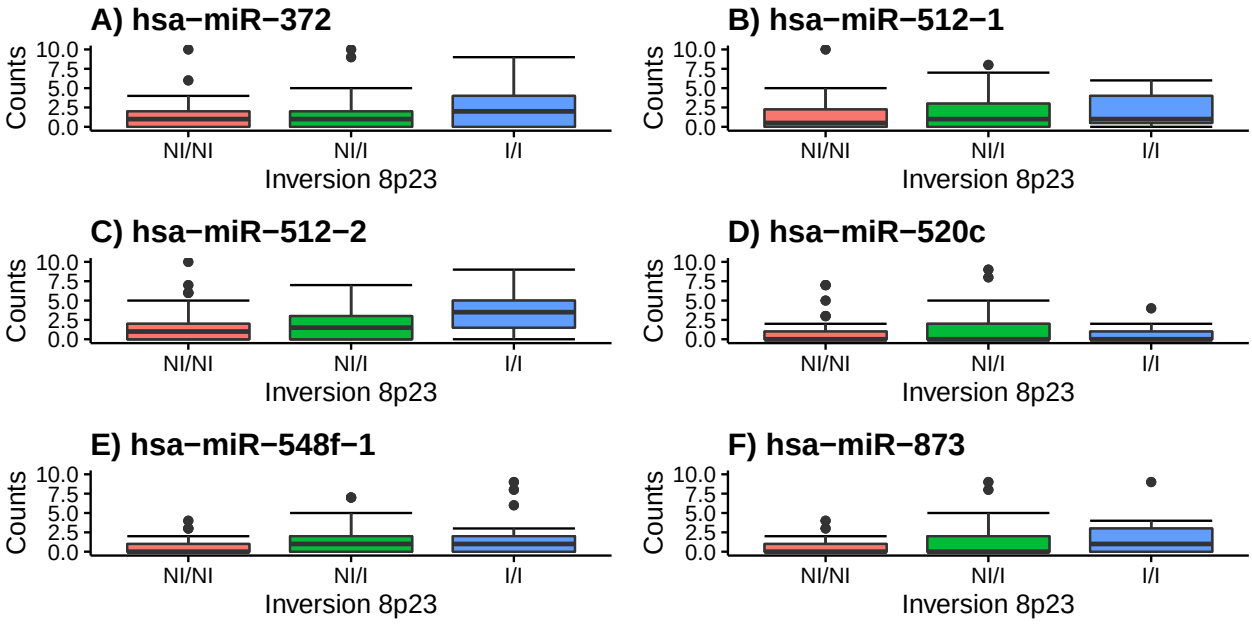

Figure 16. Association between inversion 8p23 genotypes and miRNA expression in BLCA samples. Boxplots for miRNA expression with respect to inversion 8p23, interquartile (box) and median (line). Genotype names are coded as: N (noninverted) refers to the orientation represented in the human genome reference (hg19) and I, to the inverted state.

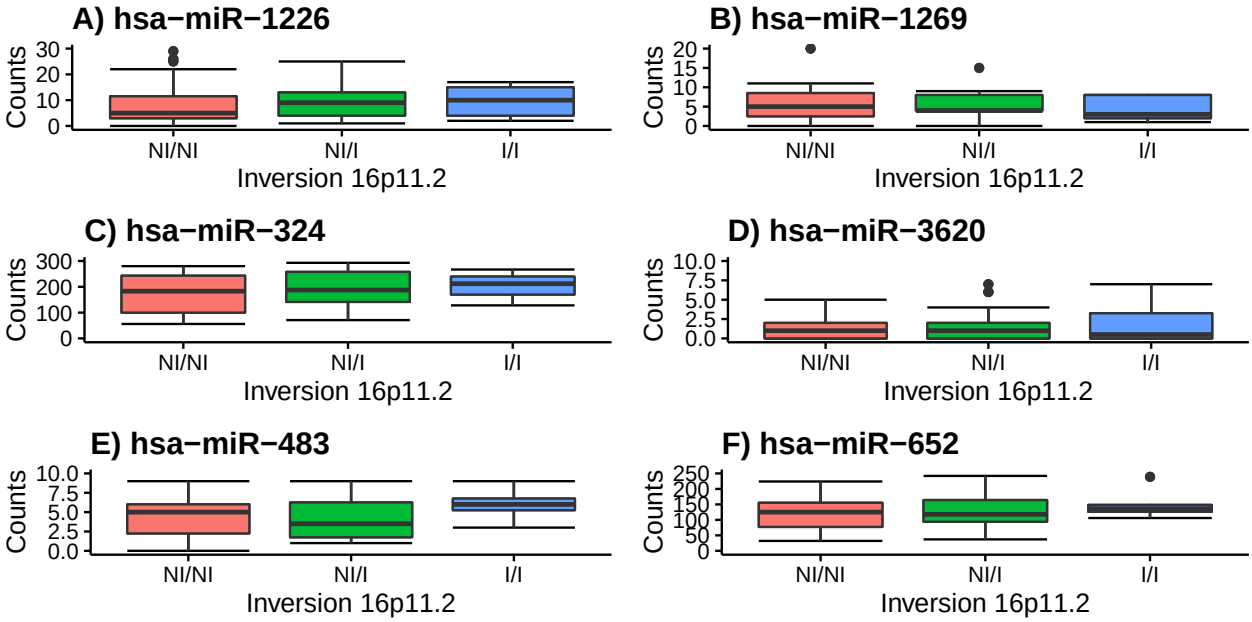

Figure 17. Association between inversion 16p11.2 genotypes and miRNA expression in BLCA samples. Boxplots for miRNA expression with respect to inversion 16p11.2, interquartile (box) and median (line). Genotype names are coded as: N (noninverted) refers to the orientation represented in the human genome reference (hg19) and I, to the inverted state.

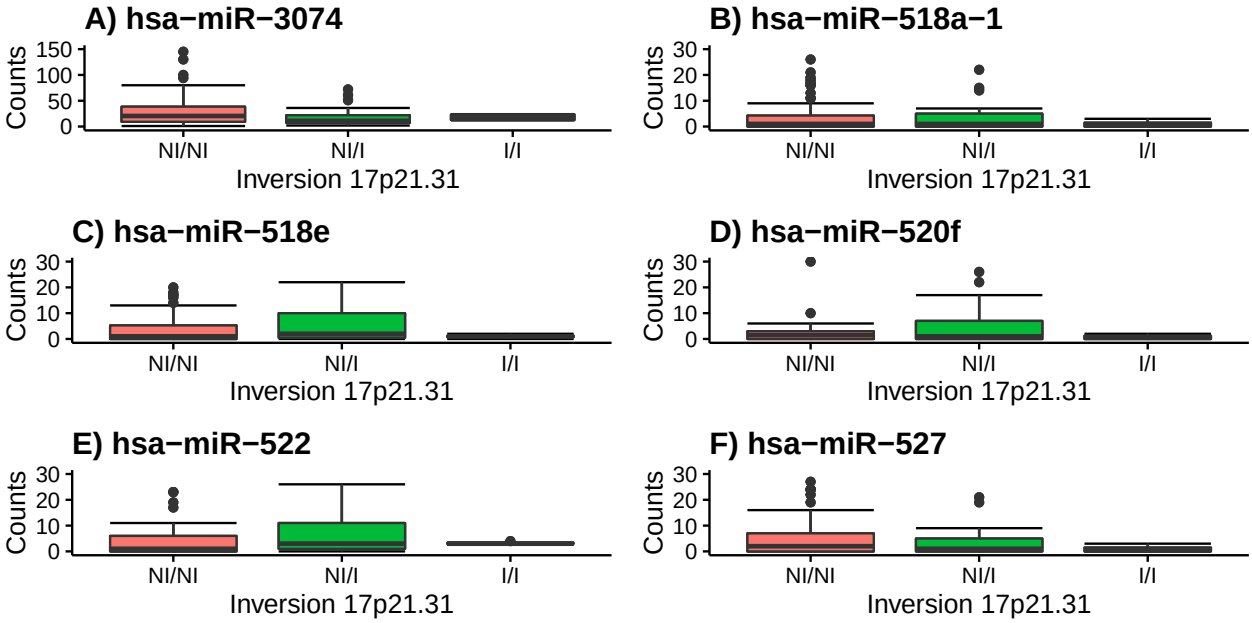

Figure 18. Association between inversion 17p21.31 genotypes and miRNA expression in BLCA samples. Boxplots for miRNA expression with respect to inversion 17p21.31, interquartile (box) and median (line). Genotype names are coded as: N (noninverted) refers to the orientation represented in the human genome reference (hg19) and I, to the inverted state.

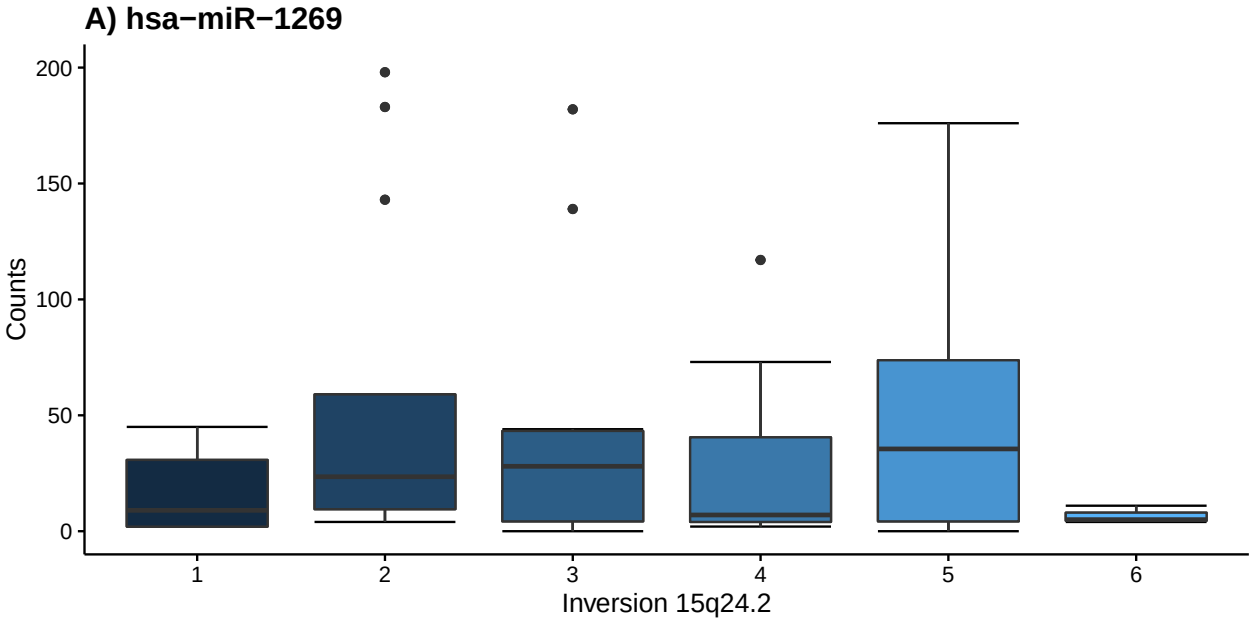

Figure 19. Association between inversion 15q24.2 genotypes and miRNA expression in BLCA samples. Boxplots for miRNA expression with respect to inversion 15q24.2, interquartile (box) and median (line). Genotype names are coded by six inverted haplotypes.

1.3.2. BRCA

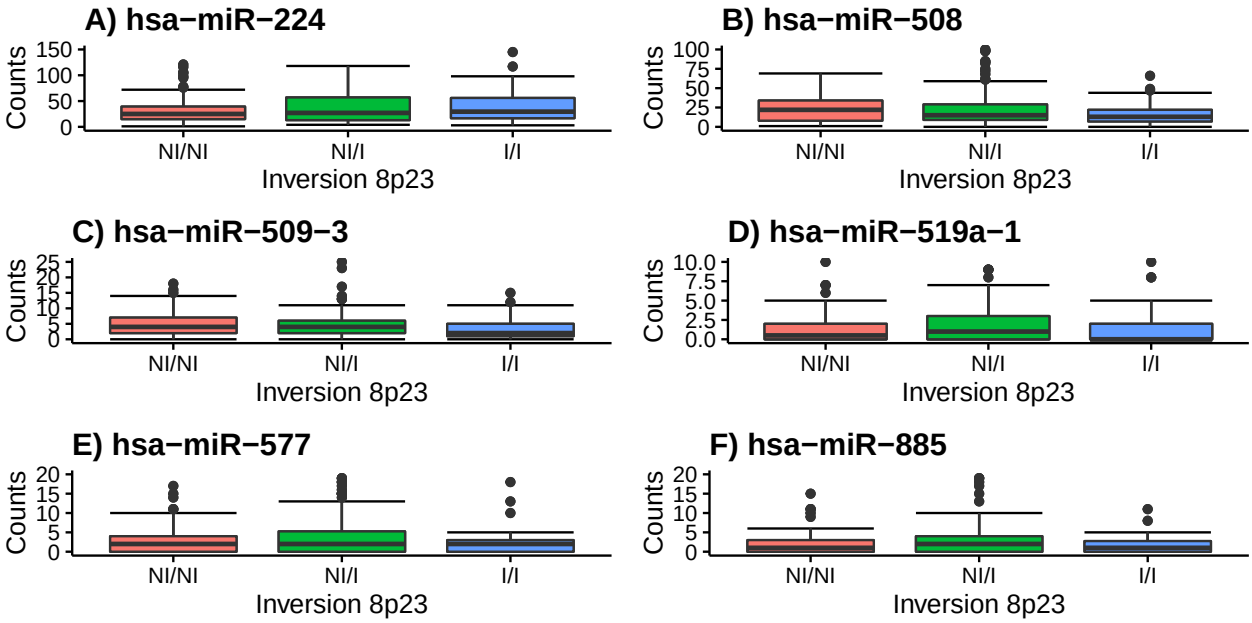

Figure 20. Association between inversion 8p23 genotypes and miRNA expression in BRCA samples. Boxplots for miRNA expression with respect to inversion 8p23, interquartile (box) and median (line). Genotype names are coded as: N (noninverted) refers to the orientation represented in the human genome reference (hg19) and I, to the inverted state.

1.3.3. COAD

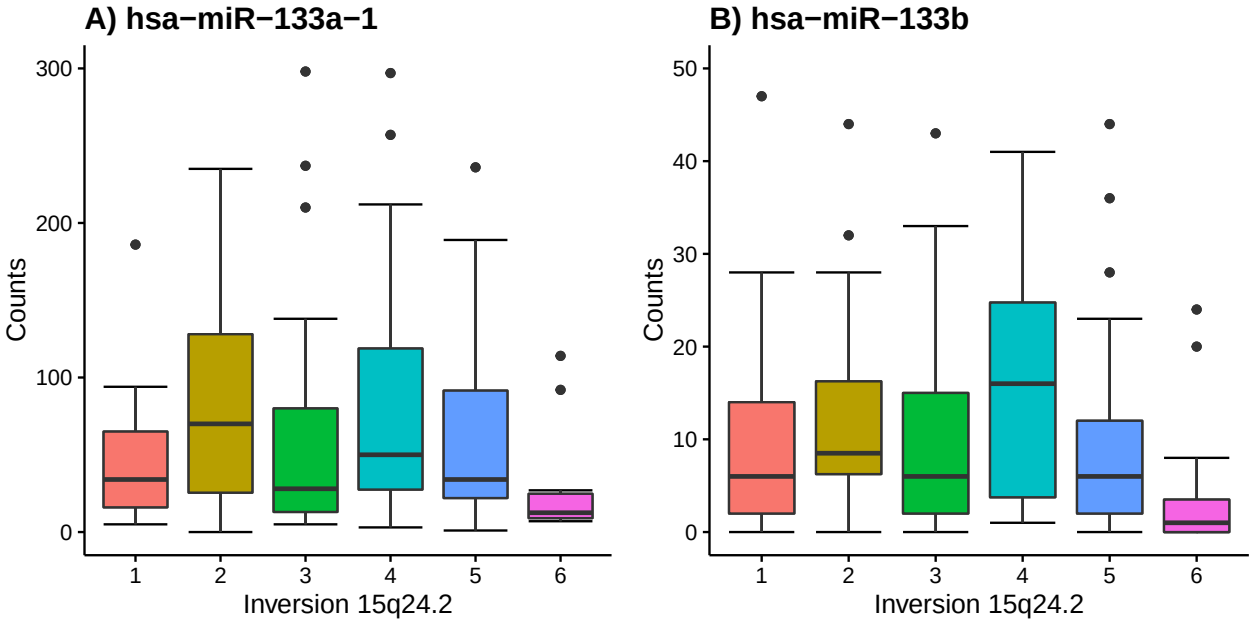

Figure 21. Association between inversion 15q24.2 genotypes and miRNA expression in COAD samples. Boxplots for miRNA expression with respect to inversion 15q24.2, interquartile (box) and median (line). Genotype names are coded by six inverted haplotypes.

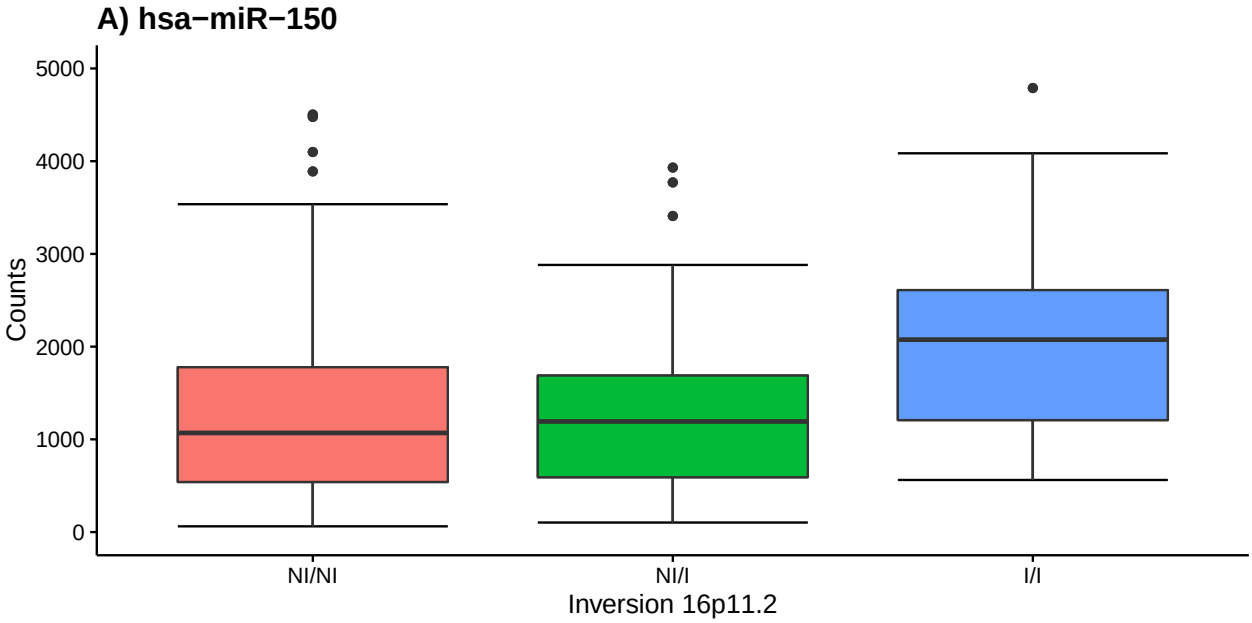

Figure 22. Association between inversion 16p11.2 genotypes and miRNA expression in COAD samples. Boxplots for miRNA expression with respect to inversion 16p11.2, interquartile (box) and median (line). Genotype names are coded as: N (noninverted) refers to the orientation represented in the human genome reference (hg19) and I, to the inverted state.

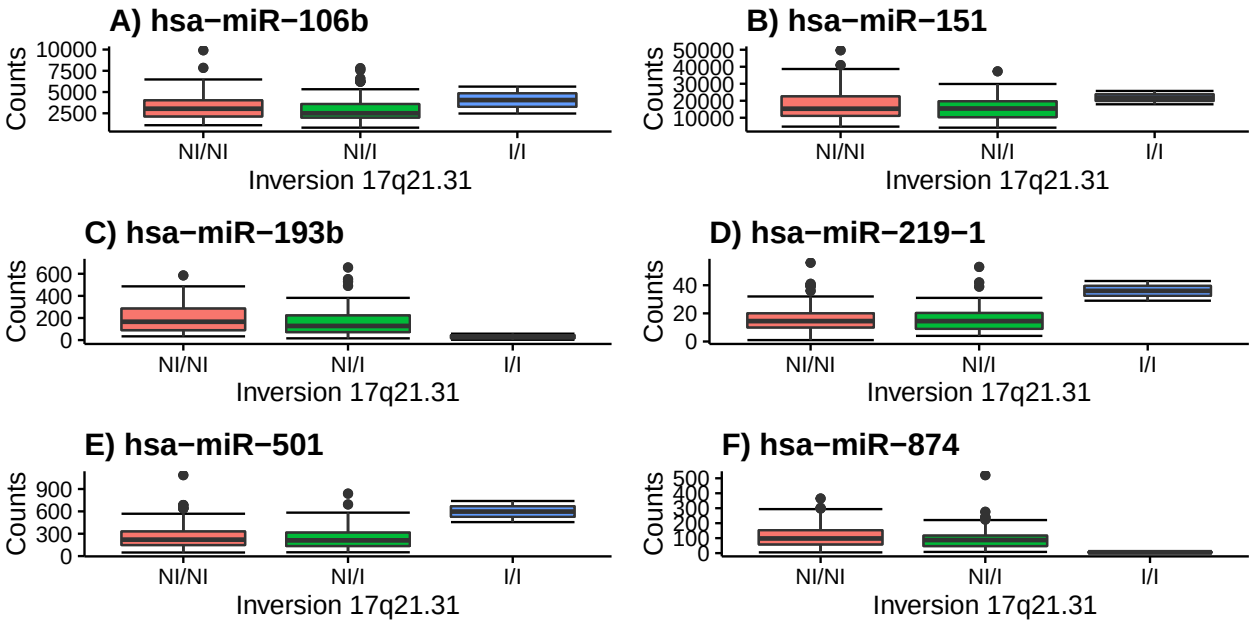

Figure 23. Association between inversion 17p21.31 genotypes and miRNA expression in COAD samples. Boxplots for miRNA expression with respect to inversion 17p21.31, interquartile (box) and median (line). Genotype names are coded as: N (noninverted) refers to the orientation represented in the human genome reference (hg19) and I, to the inverted state.

1.3.4. KICH

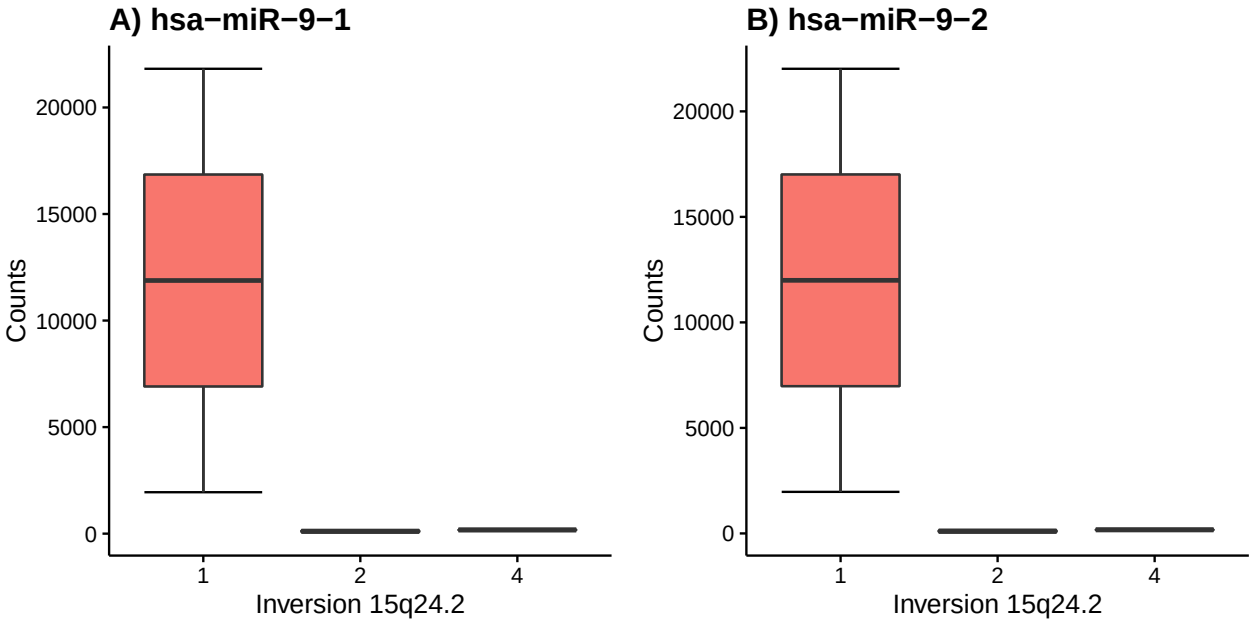

Figure 24. Association between inversion 15q24.2 genotypes and miRNA expression in KICH samples. Boxplots for miRNA expression with respect to inversion 15q24.2, interquartile (box) and median (line). Genotype names are coded by six inverted haplotypes.

1.3.5. KIRC

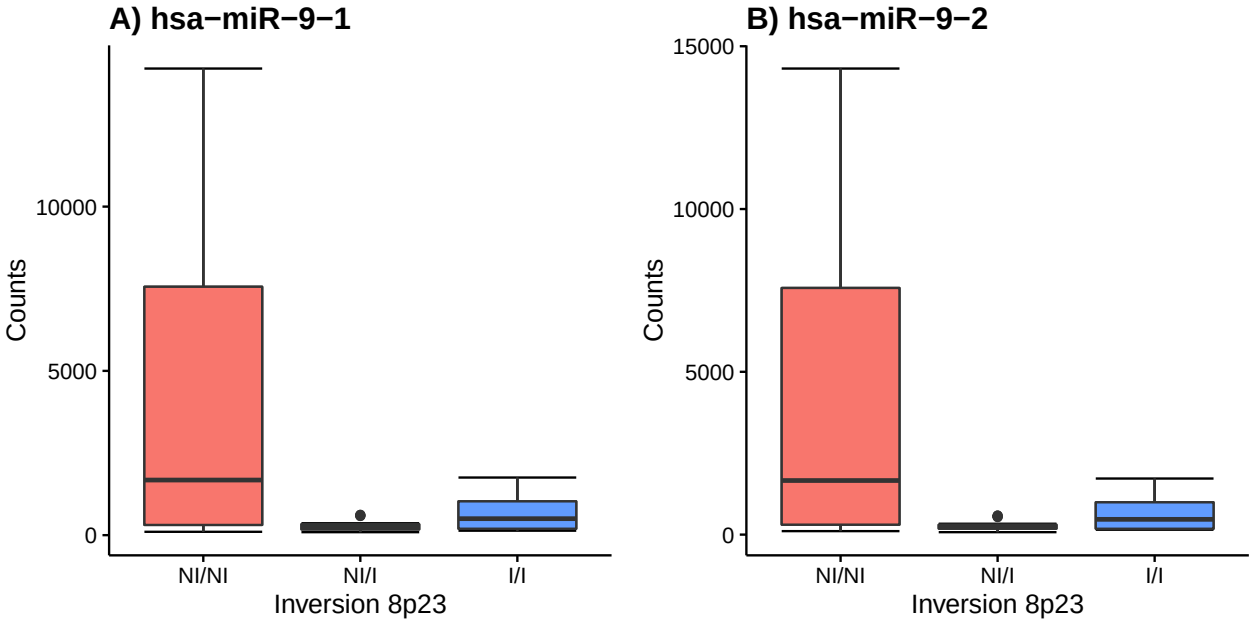

Figure 25. Association between inversion 8p23 genotypes and miRNA expression in KIRC samples. Boxplots for miRNA expression with respect to inversion 8p23, interquartile (box) and median (line). Genotype names are coded as: N (noninverted) refers to the orientation represented in the human genome reference (hg19) and I, to the inverted state.

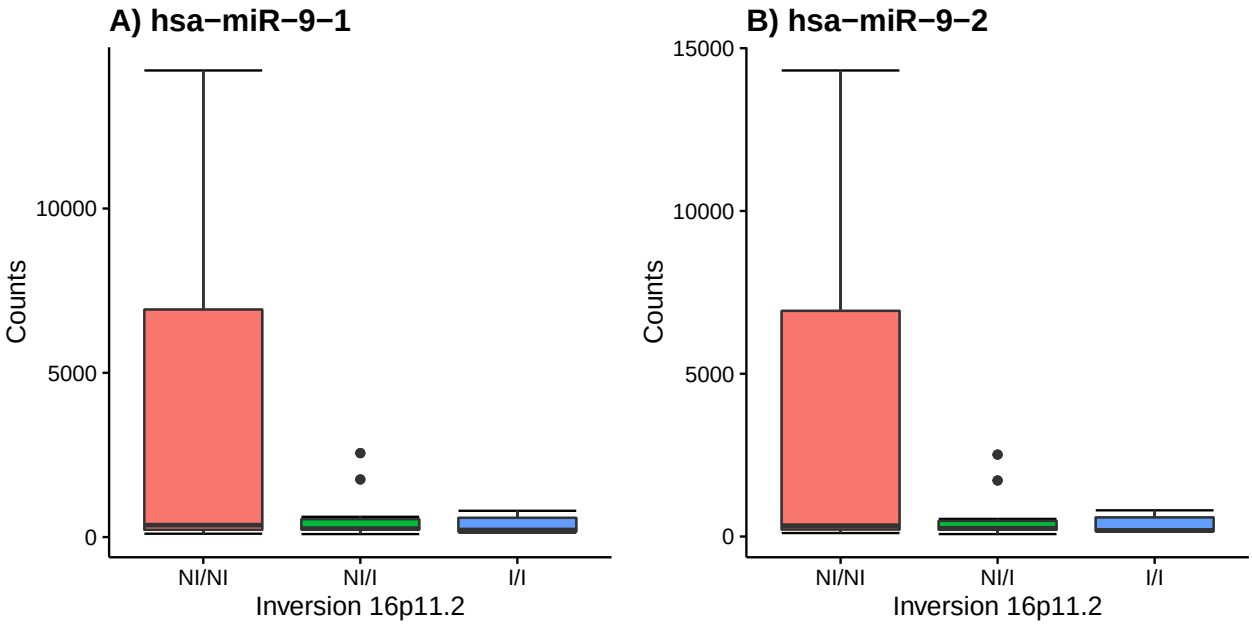

Figure 26. Association between inversion 16p11.2 genotypes and miRNA expression in KIRC samples. Boxplots for miRNA expression with respect to inversion 16p11.2, interquartile (box) and median (line). Genotype names are coded as: N (noninverted) refers to the orientation represented in the human genome reference (hg19) and I, to the inverted state.

1.3.6. KIRP

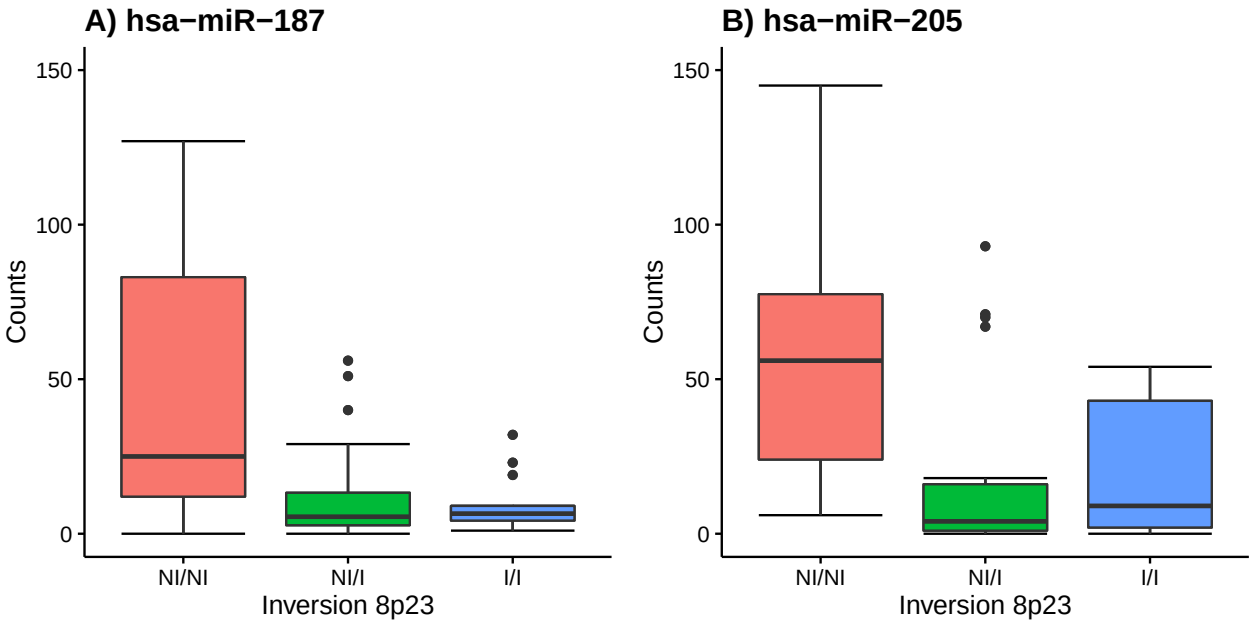

Figure 27. Association between inversion 8p23 genotypes and miRNA expression in KIRP samples. Boxplots for miRNA expression with respect to inversion 8p23, interquartile (box) and median (line). Genotype names are coded as: N (noninverted) refers to the orientation represented in the human genome reference (hg19) and I, to the inverted state.

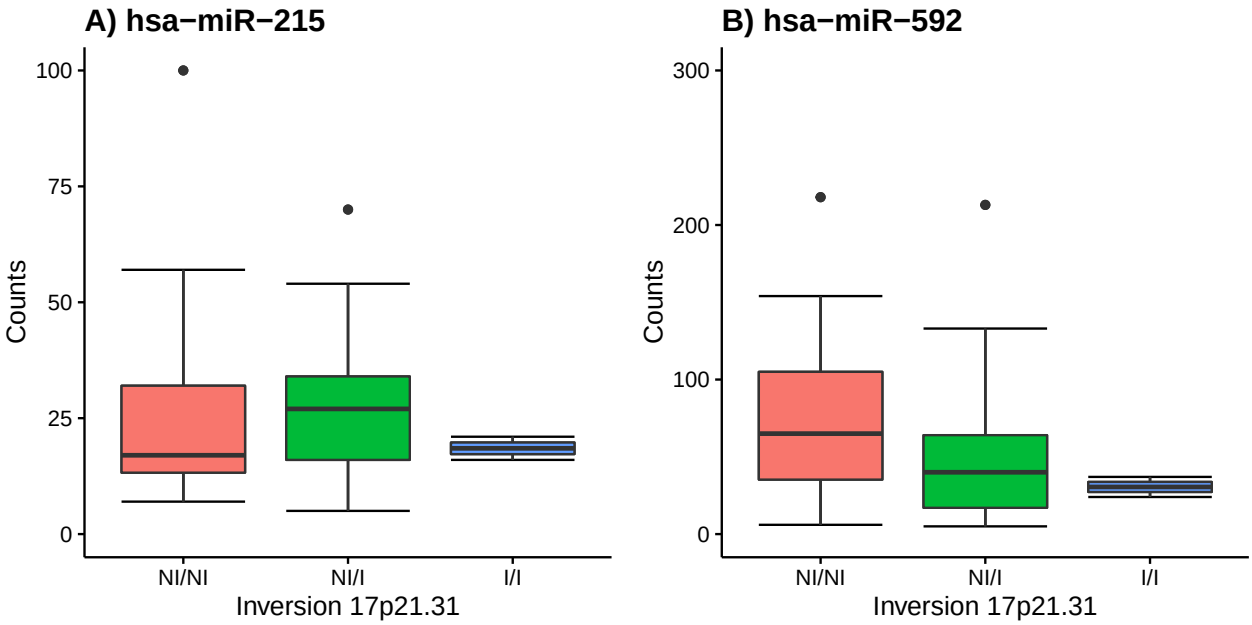

Figure 28. Association between inversion 17p21.31 genotypes and miRNA expression in KIRP samples. Boxplots for miRNA expression with respect to inversion 17p21.31, interquartile (box) and median (line). Genotype names are coded as: N (noninverted) refers to the orientation represented in the human genome reference (hg19) and I, to the inverted state.

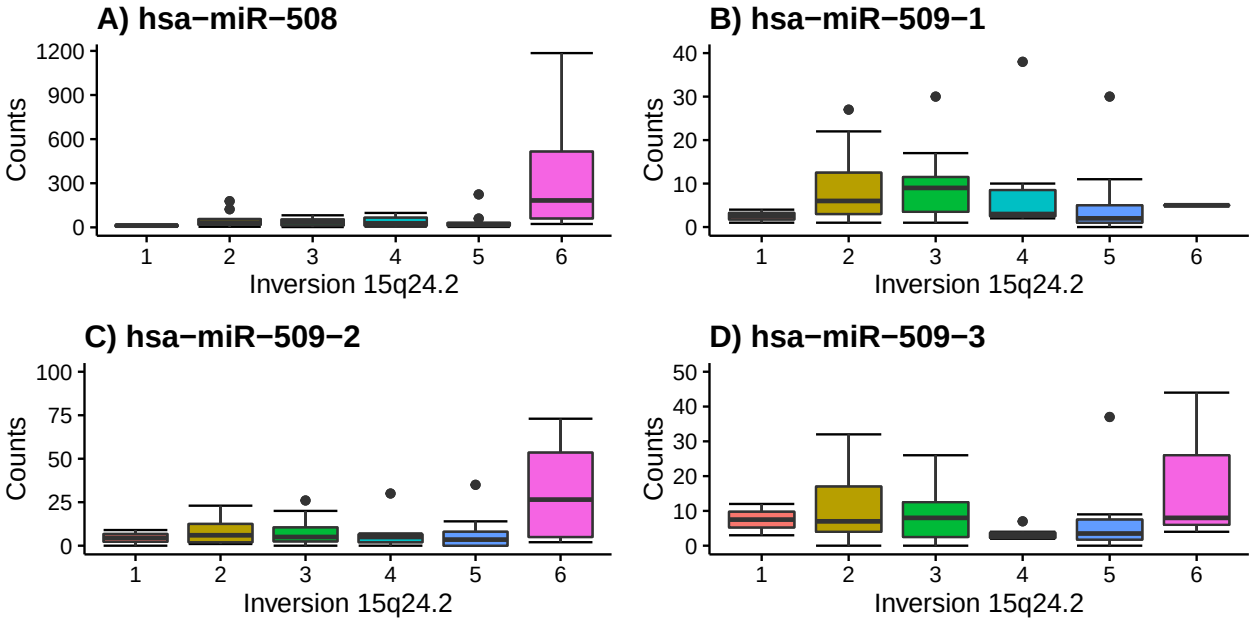

Figure 29. Association between inversion 15q24.2 genotypes and miRNA expression in KIRP samples. Boxplots for miRNA expression with respect to inversion 15q24.2, interquartile (box) and median (line). Genotype names are coded by six inverted haplotypes.

1.3.7. LGG

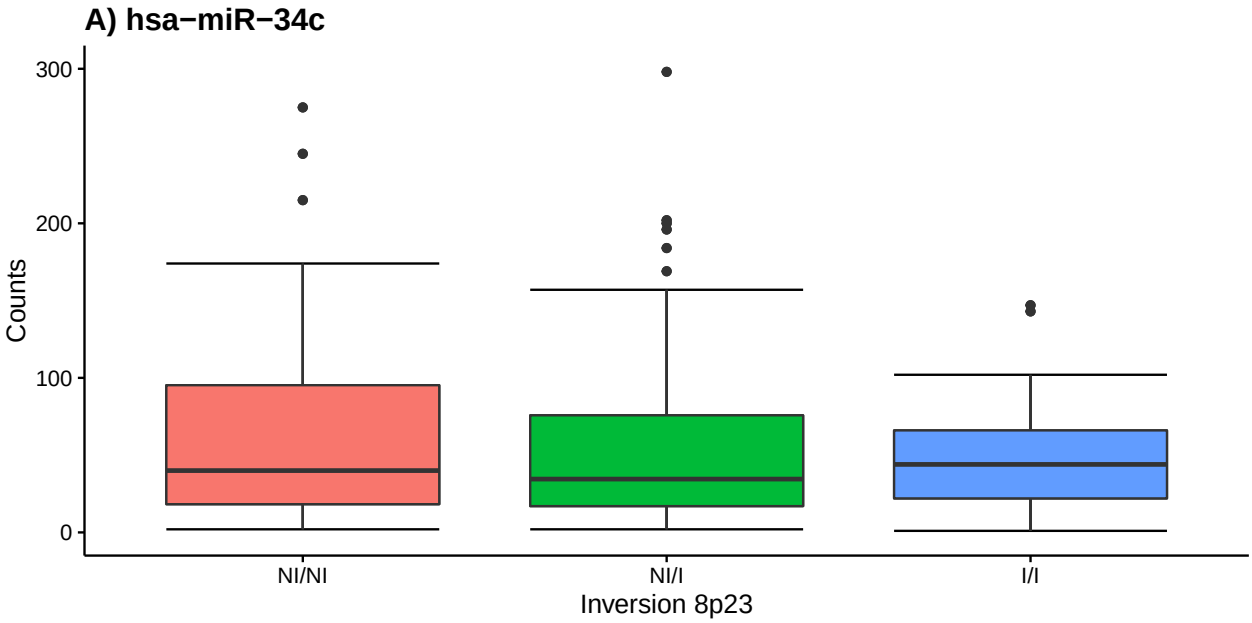

Figure 30. Association between inversion 8p23 genotypes and miRNA expression in LGG samples. Boxplots for miRNA expression with respect to inversion 8p23, interquartile (box) and median (line). Genotype names are coded as: N (noninverted) refers to the orientation represented in the human genome reference (hg19) and I, to the inverted state.

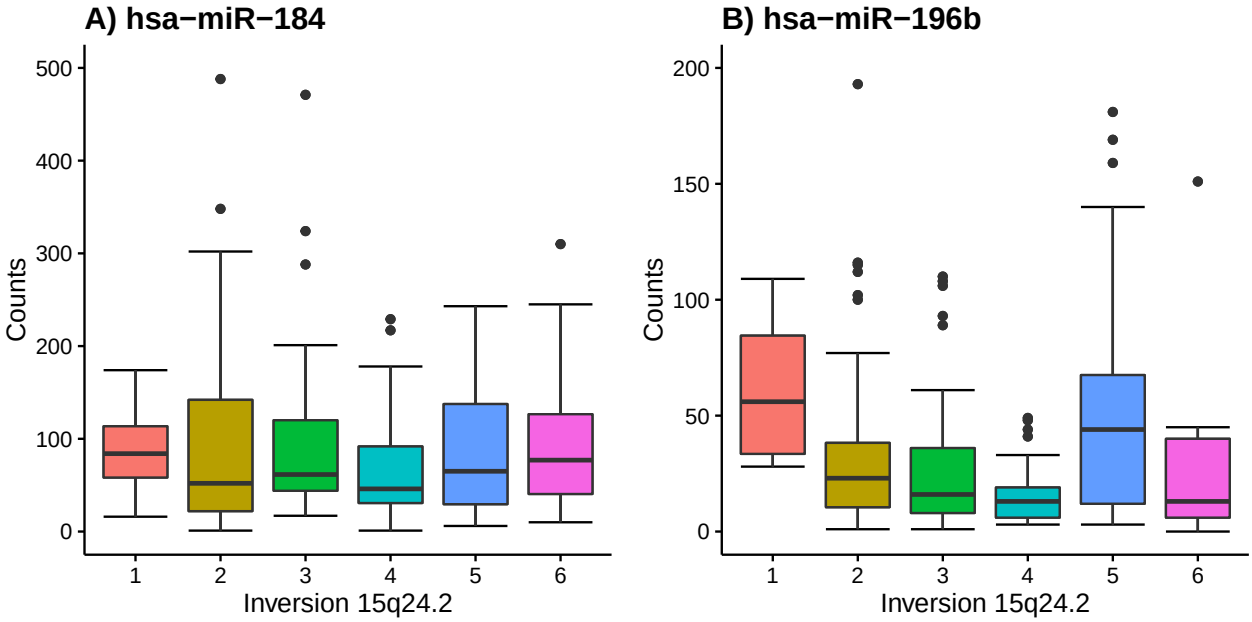

Figure 31. Association between inversion 15q24.2 genotypes and miRNA expression in LGG samples. Boxplots for miRNA expression with respect to inversion 15q24.2, interquartile (box) and median (line). Genotype names are coded by six inverted haplotypes.

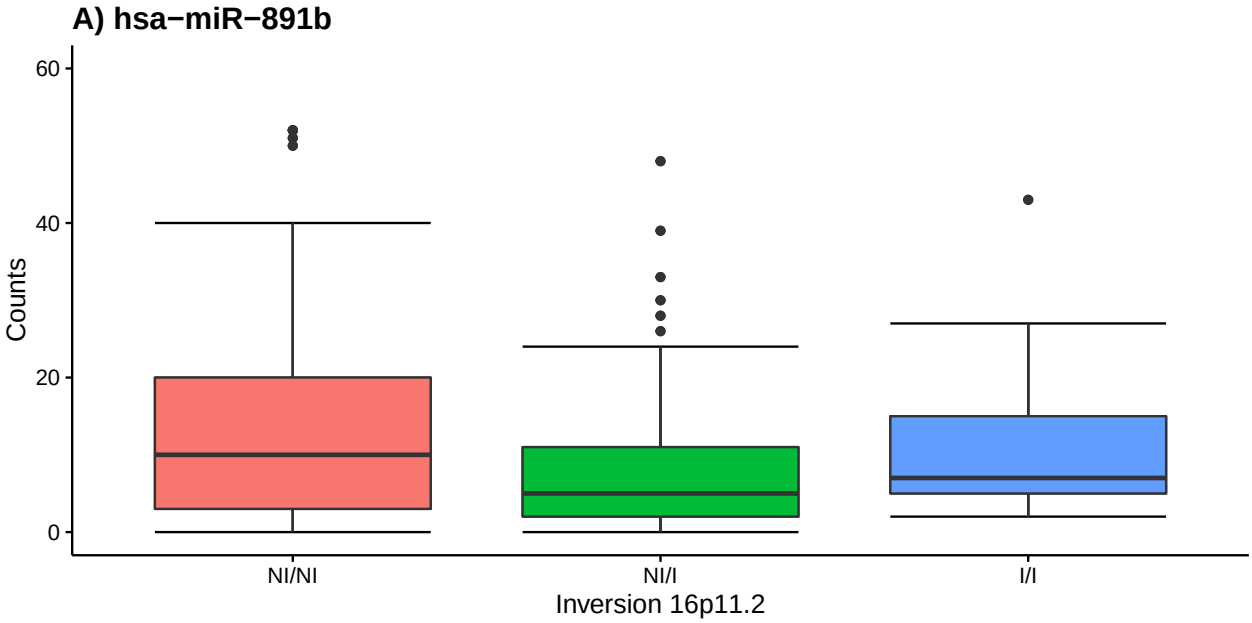

Figure 32. Association between inversion 16p11.2 genotypes and miRNA expression in LGG samples. Boxplots for miRNA expression with respect to inversion 16p11.2, interquartile (box) and median (line). Genotype names are coded as: N (noninverted) refers to the orientation represented in the human genome reference (hg19) and I, to the inverted state.

1.3.8. LIHC

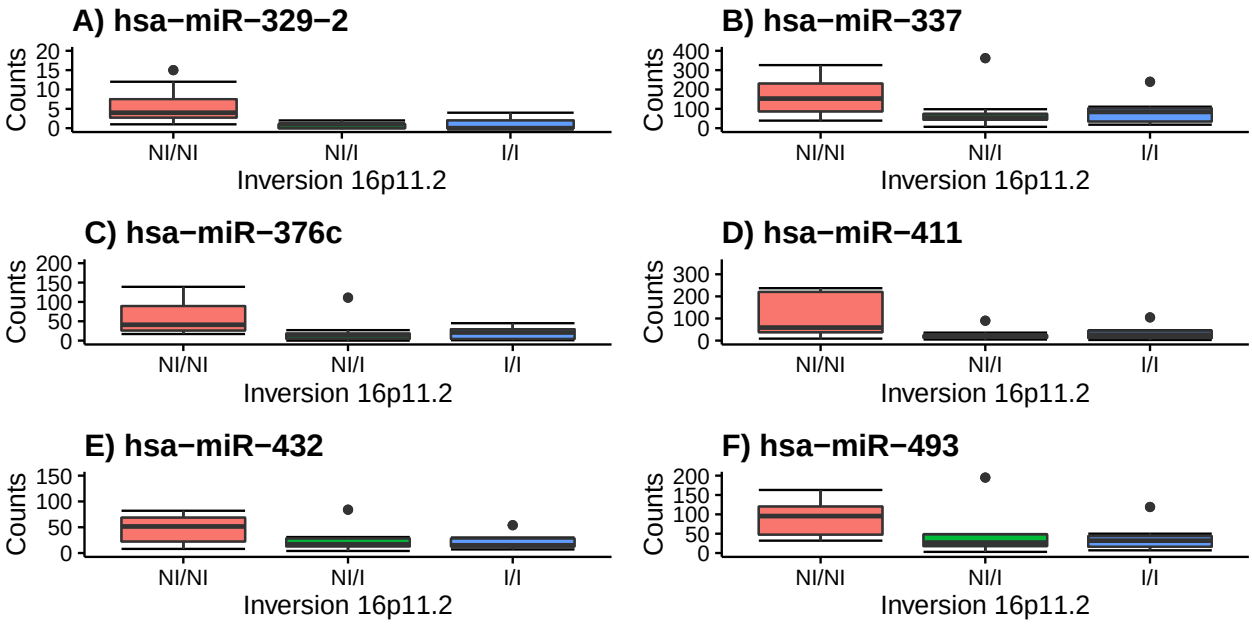

Figure 33. Association between inversion 16p11.2 genotypes and miRNA expression in LIHC samples. Boxplots for miRNA expression with respect to inversion 16p11.2, interquartile (box) and median (line). Genotype names are coded as: N (noninverted) refers to the orientation represented in the human genome reference (hg19) and I, to the inverted state.

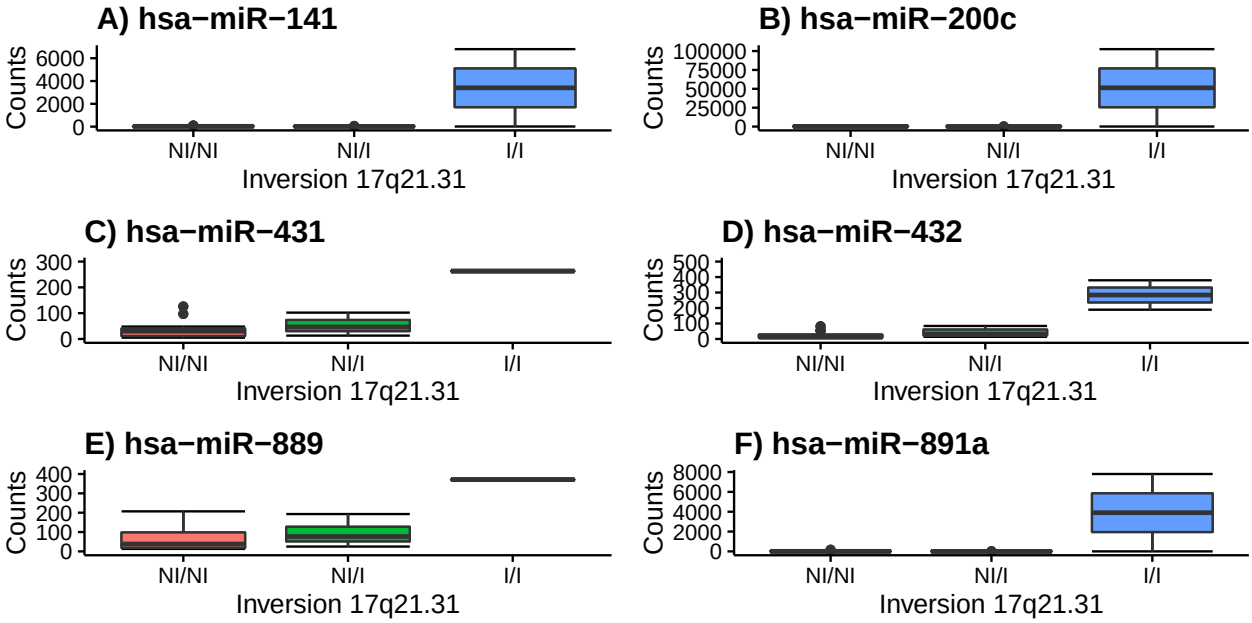

Figure 34. Association between inversion 17p21.31 genotypes and miRNA expression in LIHC samples. Boxplots for miRNA expression with respect to inversion 17p21.31, interquartile (box) and median (line). Genotype names are coded as: N (noninverted) refers to the orientation represented in the human genome reference (hg19) and I, to the inverted state.

1.3.9. LUAD

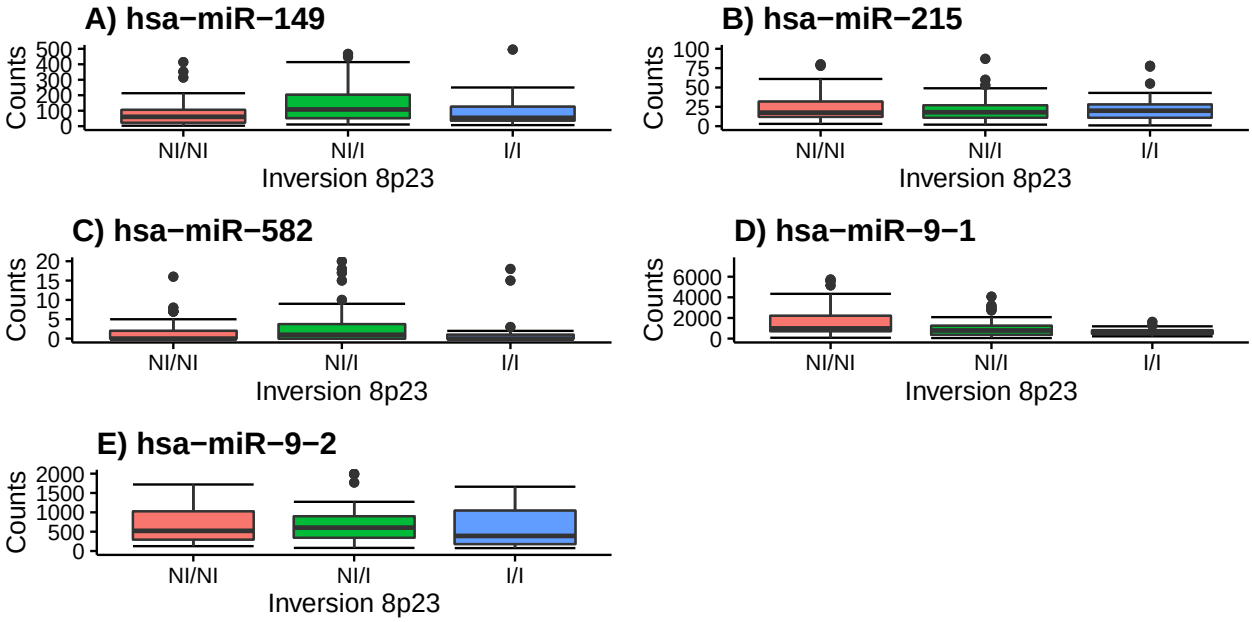

Figure 35. Association between inversion 8p23 genotypes and miRNA expression in LUAD samples. Boxplots for miRNA expression with respect to inversion 8p23, interquartile (box) and median (line). Genotype names are coded as: N (noninverted) refers to the orientation represented in the human genome reference (hg19) and I, to the inverted state.

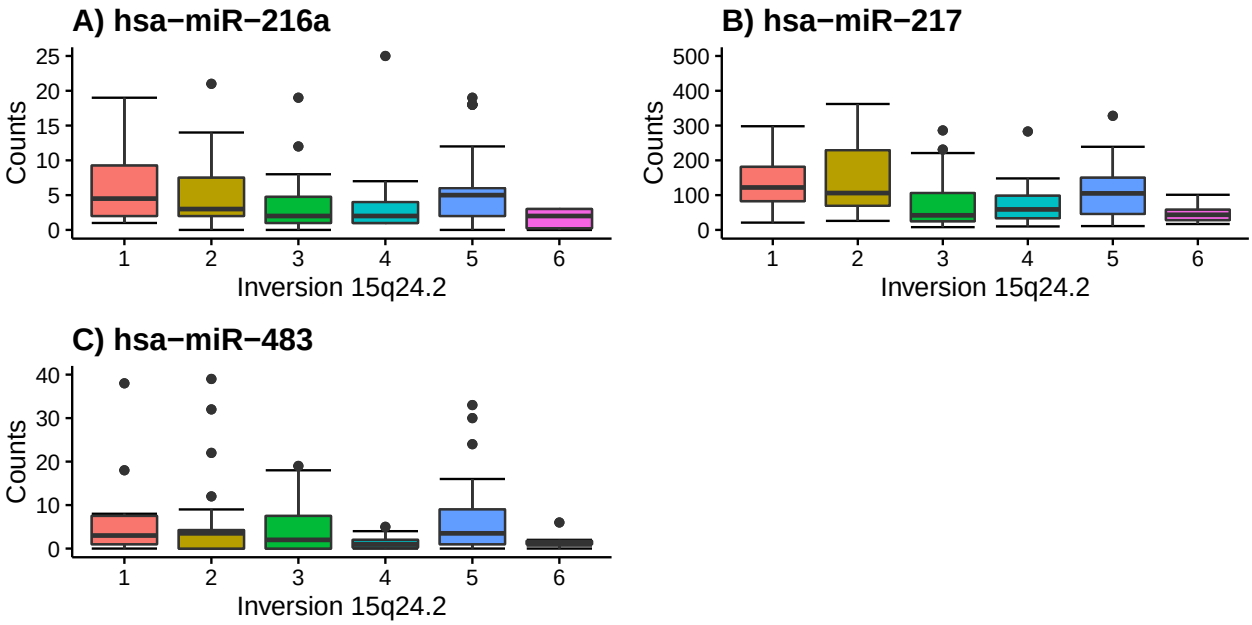

Figure 36. Association between inversion 15q24.2 genotypes and miRNA expression in LUAD samples. Boxplots for miRNA expression with respect to inversion 15q24.2, interquartile (box) and median (line). Genotype names are coded by six inverted haplotypes.

1.3.10. READ

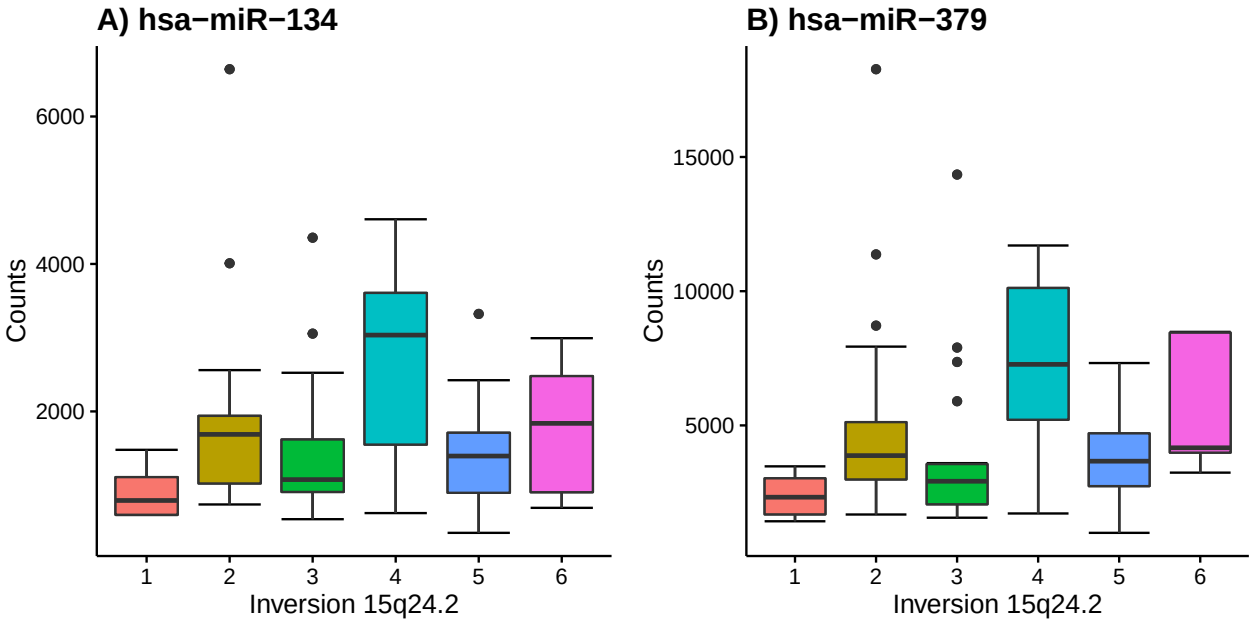

Figure 37. Association between inversion 15q24.2 genotypes and miRNA expression in READ samples. Boxplots for miRNA expression with respect to inversion 15q24.2, interquartile (box) and median (line). Genotype names are coded by six inverted haplotypes.

1.3.11. SKCM

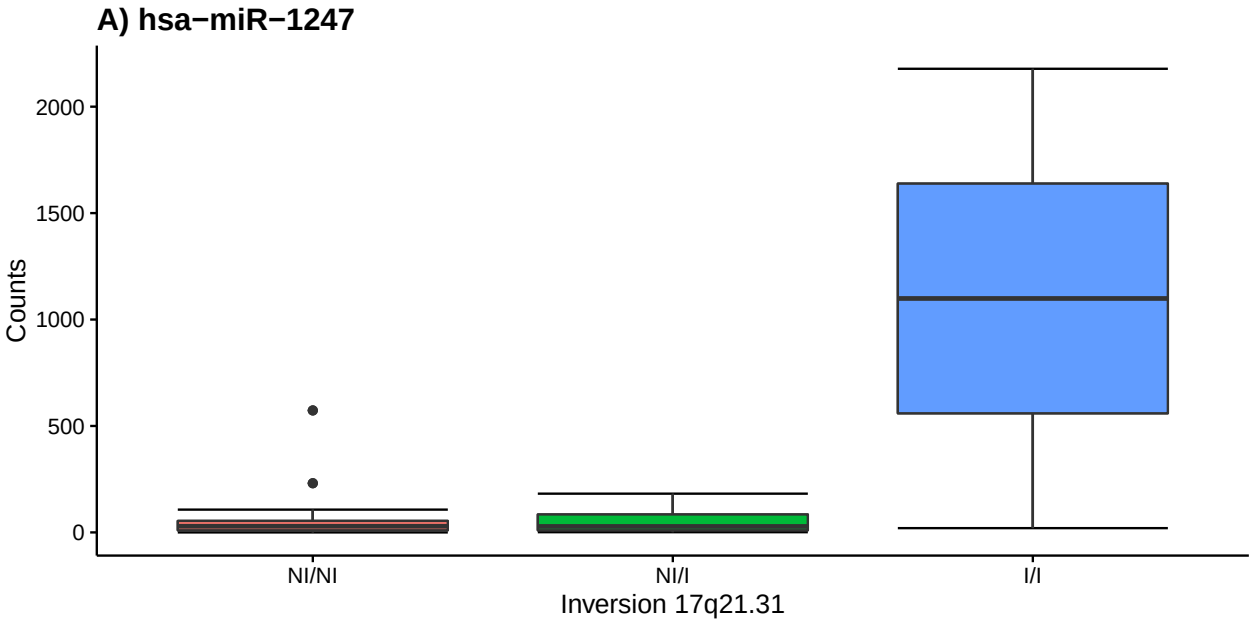

Figure 38. Association between inversion 17p21.31 genotypes and miRNA expression in READ samples. Boxplots for miRNA expression with respect to inversion 17p21.31, interquartile (box) and median (line). Genotype names are coded as: N (noninverted) refers to the orientation represented in the human genome reference (hg19) and I, to the inverted state.

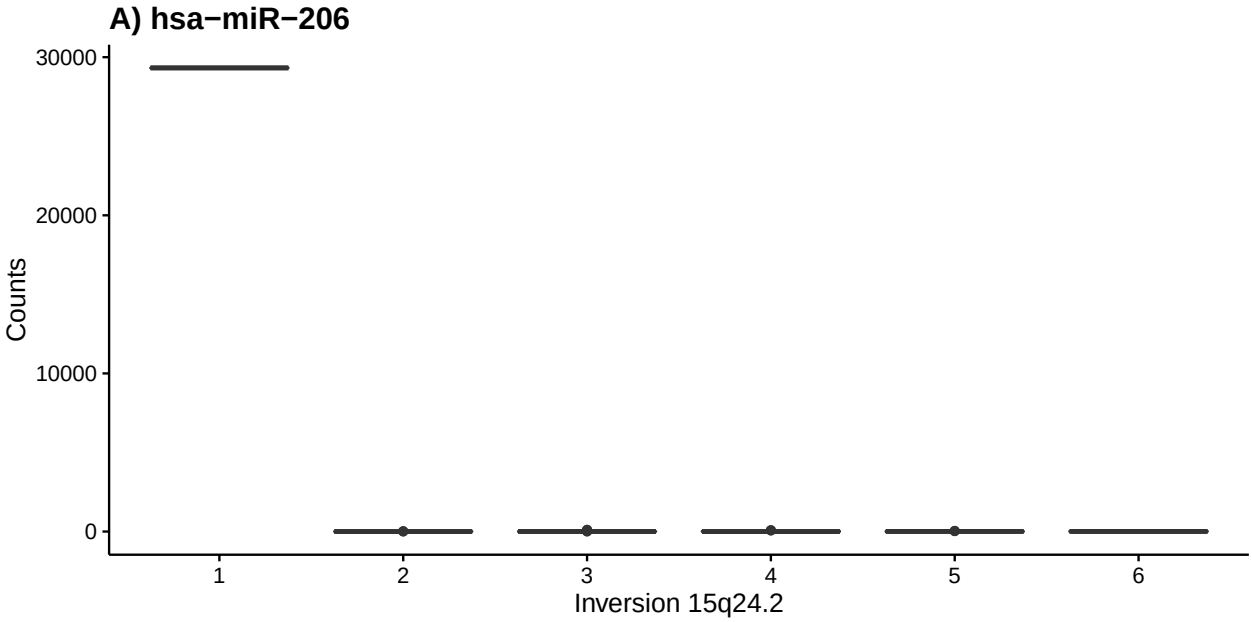

Figure 39. Association between inversion 15q24.2 genotypes and miRNA expression in READ samples. Boxplots for miRNA expression with respect to inversion 15q24.2, interquartile (box) and median (line). Genotype names are coded by six inverted haplotypes.

1.3.12. STAD

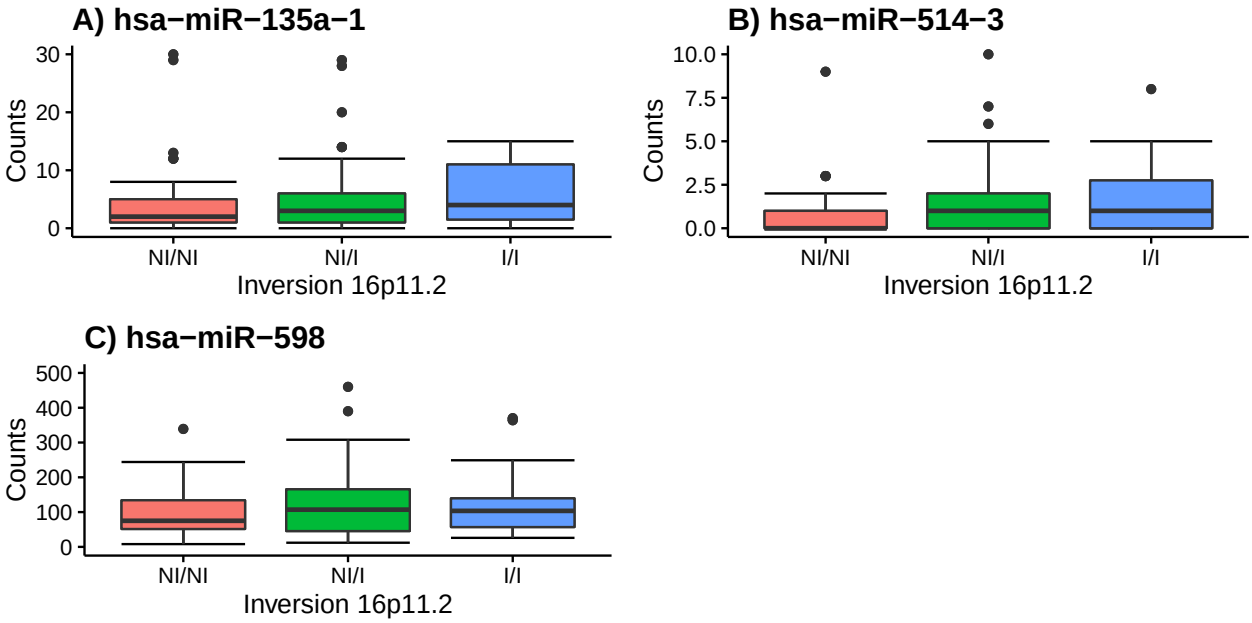

Figure 40. Association between inversion 16p11.2 genotypes and miRNA expression in STAD samples. Boxplots for miRNA expression with respect to inversion 16p11.2, interquartile (box) and median (line). Genotype names are coded as: N (noninverted) refers to the orientation represented in the human genome reference (hg19) and I, to the inverted state.

1.3.13. THCA

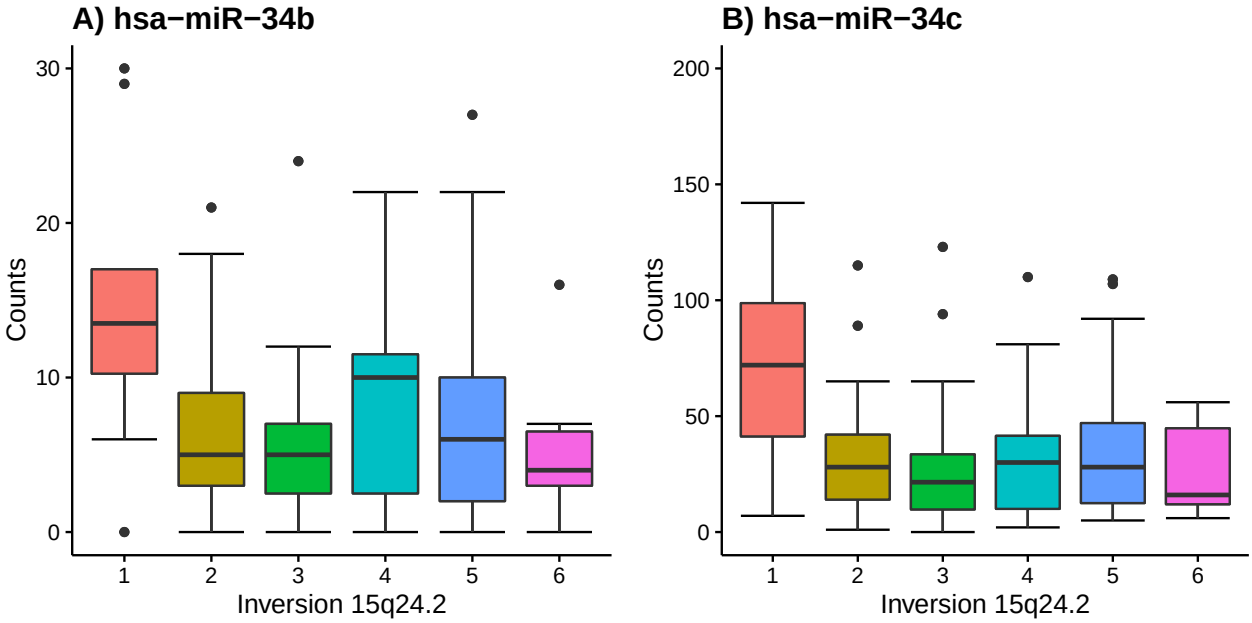

Figure 41. Association between inversion 15q24.2 genotypes and miRNA expression in THCA samples. Boxplots for miRNA expression with respect to inversion 15q24.2, interquartile (box) and median (line). Genotype names are coded by six inverted haplotypes.

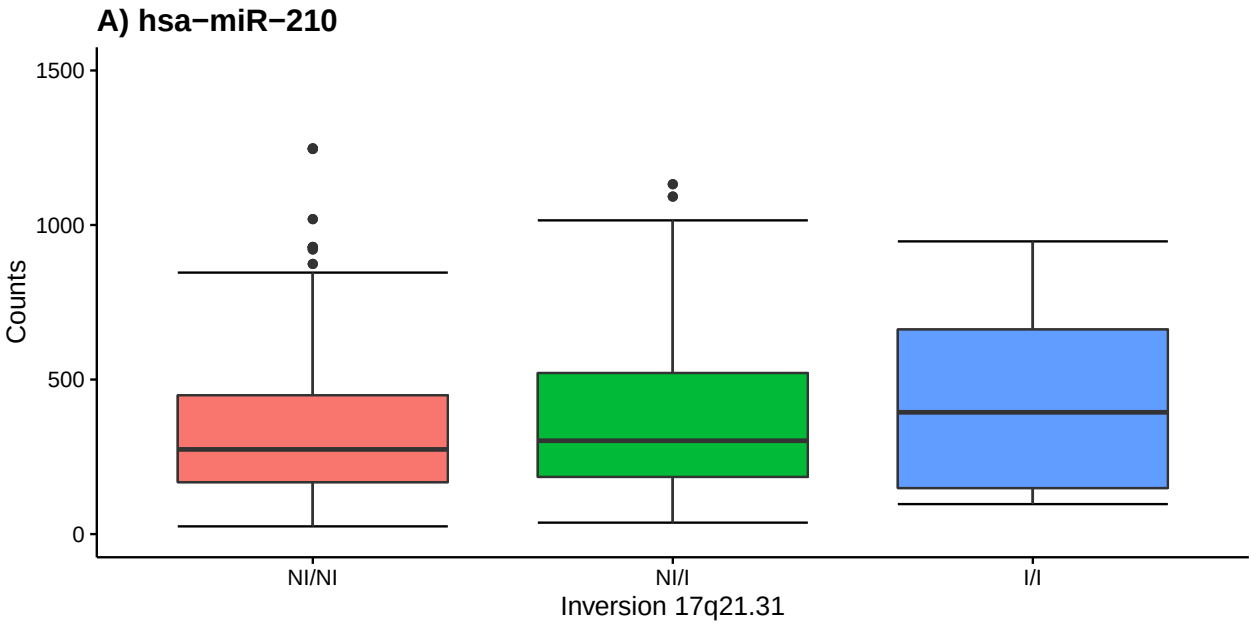

Figure 42. Association between inversion 17p21.31 genotypes and miRNA expression in THCA samples. Boxplots for miRNA expression with respect to inversion 17p21.31, interquartile (box) and median (line). Genotype names are coded as: N (noninverted) refers to the orientation represented in the human genome reference (hg19) and I, to the inverted state.

1.3.14. UCEC

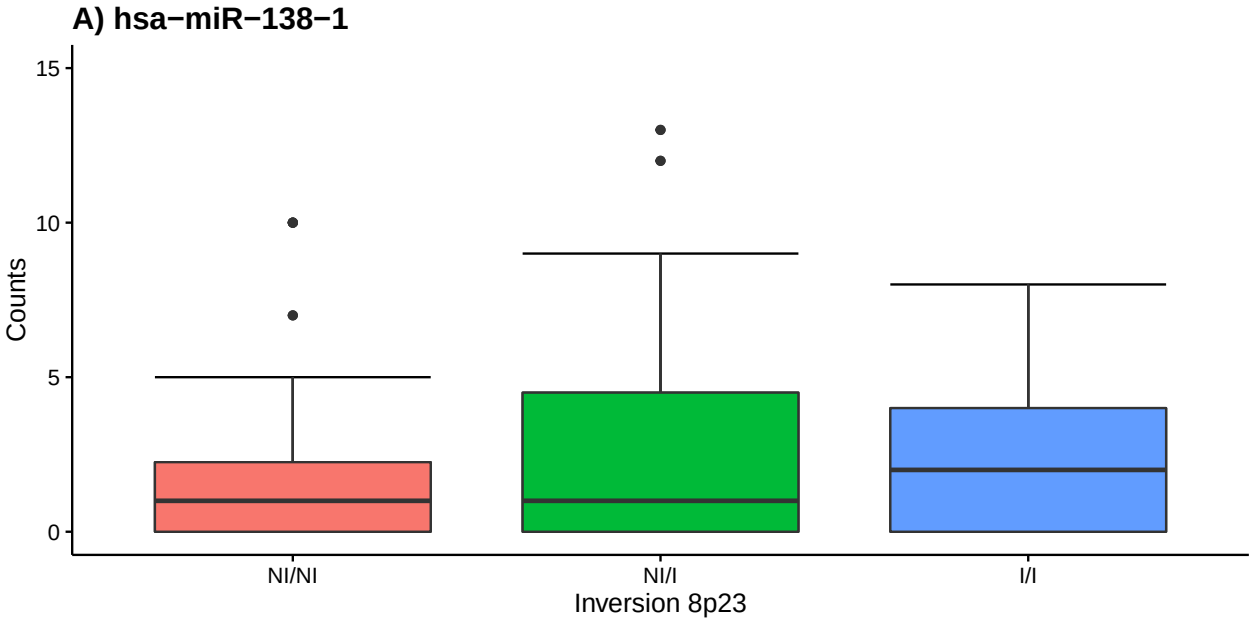

Figure 43. Association between inversion 8p23 genotypes and miRNA expression in UCEC samples. Boxplots for miRNA expression with respect to inversion 8p23, interquartile (box) and median (line). Genotype names are coded as: N (noninverted) refers to the orientation represented in the human genome reference (hg19) and I, to the inverted state.

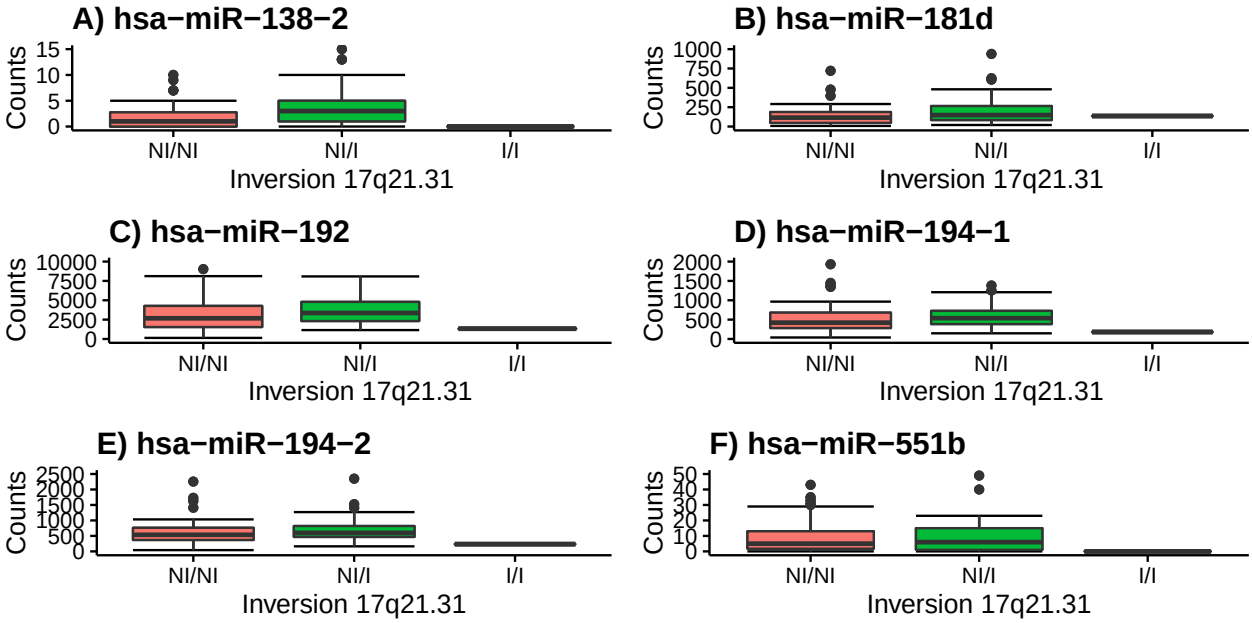

Figure 44. Association between inversion 17p21.31 genotypes and miRNA expression in UCEC samples. Boxplots for miRNA expression with respect to inversion 17p21.31, interquartile (box) and median (line). Genotype names are coded as: N (noninverted) refers to the orientation represented in the human genome reference (hg19) and I, to the inverted state.

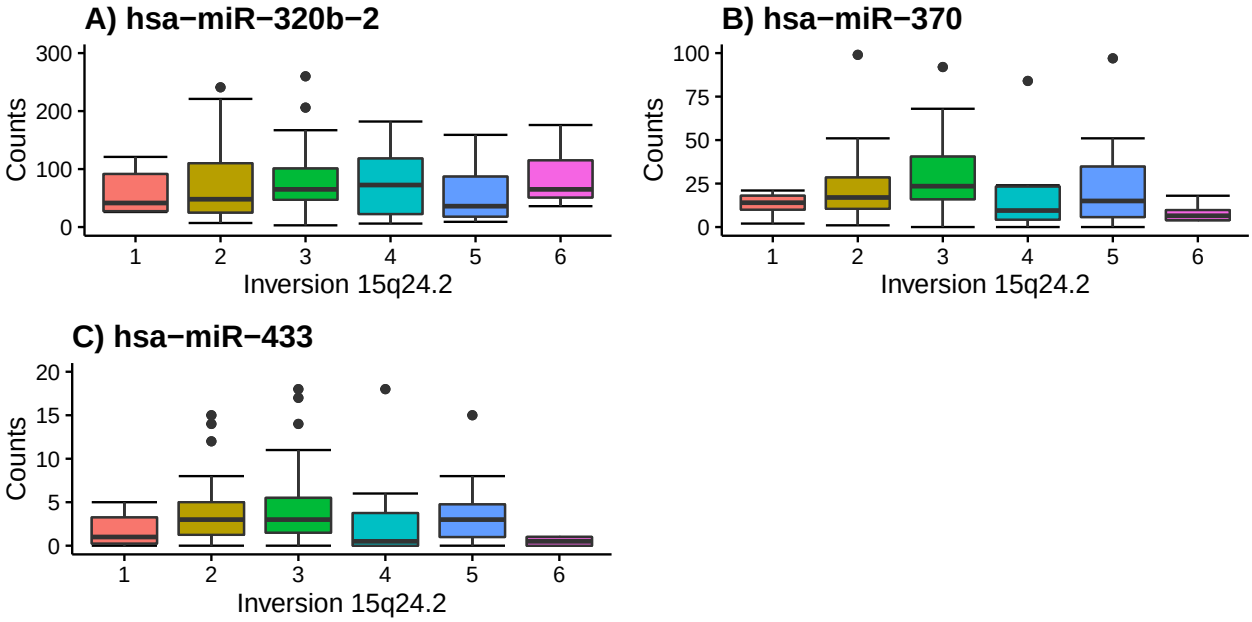

Figure 45. Association between inversion 15q24.2 genotypes and miRNA expression in UCEC samples. Boxplots for miRNA expression with respect to inversion 15q24.2, interquartile (box) and median (line). Genotype names are coded by six inverted haplotypes.

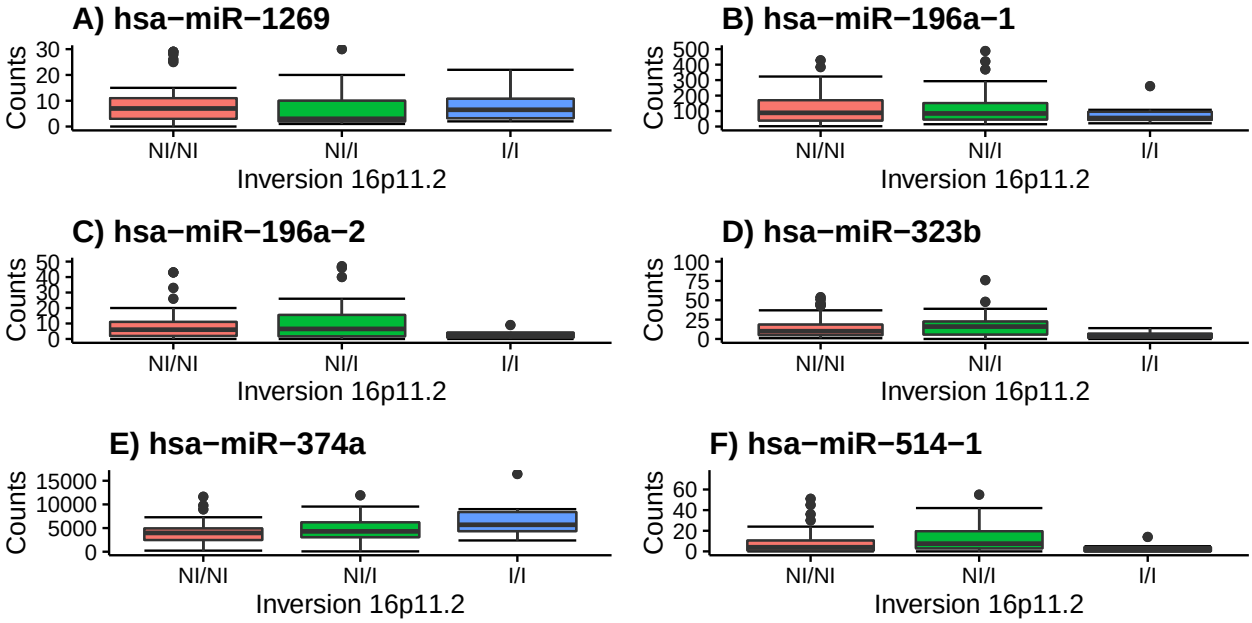

Figure 46. Association between inversion 16p11.2 genotypes and miRNA expression in UCEC samples. Boxplots for miRNA expression with respect to inversion 16p11.2, interquartile (box) and median (line). Genotype names are coded as: N (noninverted) refers to the orientation represented in the human genome reference (hg19) and I, to the inverted state.